Supporting Information:

Fast, selective and scalable flow ammonolysis of oxiranes accessible from glycerol toward bio-based amines

Florian Barbaz,[a] Hubert Hellwig,[a] Diana V. Silva-Brenes,[a,b] and Jean-Christophe M. Monbaliu[a,c]*

[a] Center for Integrated Technology and Organic Synthesis (CiTOS), MolSys Research Unit, University of Liège, B-4000 Liège (Sart-Tilman), Belgium.

Email: jc.monbaliu@uliege.be

[b] FloW4all Flow Technology Resource Center, MolSys Research Unit, University of Liège, B-4000 Liège (Sart-Tilman), Belgium.

[c] WEL Research Institute, Avenue Pasteur 6, 1300 Wavre, Belgium.

Table of content

1. Table of reagents

Chemicals, purities, CAS numbers and suppliers are provided in Table S1. Chemicals were purchased from commercial sources and used as received.

Table S1. List of reagents. [a] https://bluebearchemicals.com/products/

Solvent	**CAS number**	**Purity (%)**	**Supplier**
Methanol (MeOH)	67-56-1	99.8% HPLC grade	Fisher
Chemicals	**CAS number**	**Purity** (%)	**Supplier**
Epichlorohydrin (**1b**)	106-89-8	>99	Merck
Glycidol (**1a, bio-based**)[a]	556-52-5	>99	BlueBear Chemicals
Glycidol (**1a**)	556-52-5	96	Merck
Dimethyl carbonate (**DMC**)	616-38-6	99	Thermo scientific
3-Amino-1,2-propanediol (**2a**)	616-30-8	>98	TCI
1,3-Diamino-2-propanol (**2c**)	616-29-5	95	Sigma Aldrich
2-Amino-1,3-propanediol	534-03-2	97	ABCR
Azetidin-3-ol-hydrochloride	18621-18-6		Enamine
1,3,4,6,7,8,9,10-Octahydropyrimido[1,2-a]azepine (DBU)	6674-22-2	99.47	BLDpharm
1,5-Diazabicyclo[4.3.0]-5-nonene (DBN)	3001-72-7	>98	TCI
Ammonia solution-32% (NH_4OH)	1336-21-6	/	Merck
Ammonia solution-28-30% (NH_4OH)	1336-21-6	/	Fisher
Ethyl chloroformate	541-41-3	>98	Fluka
Methyl chloroformate	79-22-1	99	Acros Organics
Benzaldehyde	100-25-7	98%	Merck
Pyridine	110-86-1	>99.8	Fluka Chemika

2. Analytical methods

NMR

The ^{1}H and ^{13}C NMR spectra were recorded with a Bruker Avance III 400 MHz NMR spectrometer. Chemical shifts (δ) were reported in ppm and coupling constants (J) were reported in Hertz (Hz). Multiplicities were reported as singlet (s), doublet (d), triplet (t), dd (doublet of doublet) and multiplet (m).

GC

Quantification of yields and conversions were carried out through GC-FID analyses on a Shimadzu-GC-2030 system equipped with a Flame Ionization Detector (FID).

Column: Shimadzu SH-RTX-1701 (Mid-polariry phase: Crossbond™ 14% cyanopropyl|phenyl/86% dimethyl polysiloxane, Length: 30.0 m, ID: 0.25 mm).
Injection Temp: 250.00 °C
Injection Mode: Split
Injection volume: 1 µL
Purge Flow: 3.0 mL/min
Flow Control Mode: Linear Velocity
Linear Velocity: 40 cm/sec
Method 1:
Column Oven Temp: 40.0 °C

Split Ratio: 100.0
Pressure: 132.0 kPa
Total Flow: 198.9 mL/min
Column Flow: 1.94 mL/min
The temperature gradient program is described in Table S2.

Table S2. Temperature gradient program of Method 1

Rate ($°C \cdot min^{-1}$)	Temperature (°C)	Hold Time (min)
-	40	1
20	100	3
40	220	1
50	270	3

Method 2:
Column Oven Temp: 40.0 °C
Split Ratio: 50.0
Pressure: 134.8 kPa
Total Flow: 99.9 mL/min
Column Flow: 1.9 mL/min
The temperature gradient program is described in Table S3.

Table S3. Temperature gradient program of Method 2

Rate ($°C \cdot min^{-1}$)	Temperature (°C)	Hold Time (min)
-	50	3
20	153	0
1	164	0
20	270	5

FID
Detector SFID1
Temp: 280 °C

GC-MS
Product identification was supported with GC-MS analyses on a Shimadzu-GCMS-QP2020 NX.

Ion Source Temp: 200.00 °C
Interface Temp: 250.00 °C
Solvent Cut Time: 2.00 min
Detector Gain Mode: Relative to the Tuning Result
Detector Gain: +0.00 kV
Threshold: 0
[MS Table]
Start Time: 2.00 min
ACQ Mode: Scan
Event Time: 0.30 s
Scan Speed: 1666
Start m/z: 35.00
End m/z: 500.00

In-line IR

IR spectra were recorded on a Mettler Toledo ReactIR 700 spectrometer, with TEMCT detector and Norton-Beer medium apodization.

A DiComp (Diamond) with DS Micro Flow Cell ATR probe was used for the measurements. IR spectra were measured between 4000 to 650 cm^{-1} with a resolution 4 cm^{-1}. For each sample 128 scans were accumulated, with a low gain. Mettler Toledo iC IR 7.1.91.0 and iC Quant 7.1.91.0 were used to record and process the spectra.

3. Ammonolysis of oxiranes 1a,b

3.1 Ammonolysis with aqueous ammonia

3.1.1 Lab-scale microfluidic experiments

3.1.1.1 Microfluidic setup

Knauer pumps were used to deliver the two feed solutions (feed 1: oxiranes **1a,b** in methanol, 1-4 M; feed 2: aqueous ammonia, 32 wt.-%). Both feeds were preheated through 1 mL coils (SS for aqueous ammonia, PFA for **1a,b**) then mixed though a high-performance arrowhead mixer, and then reacted in a 1/16" SS coil reactor (various internal volume). A pressure sensor and a thermocouple were added downstream the reactor, before the back-pressure regulator (BPR, 250 psi). Details of the setup are presented in Figure S1, and parts are listed in Table S4.

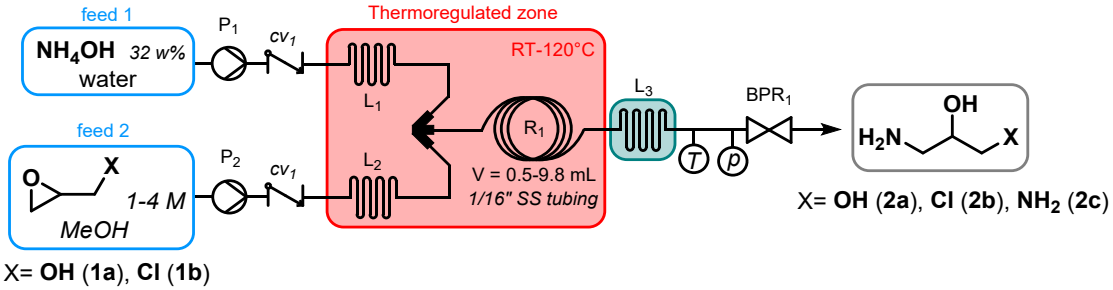

Figure S1. Detailed microfluidic setup for the ammonolysis of glycidol (**1a**) with aqueous NH_3 toward the formation of 3-amino-1,2-propandiol (**2a**).

Table S4. List of parts of the continuous microfluidic system for the ammonolysis of **1a** with aqueous NH_3 toward **2a**.

Symbol	Name, description	Reference number / product name	Manufacturer
Pumps			
P_1, P_2	HPLC-type pump (plunger) 10 mL stainless steel head	Azura P4.1S	KNAUER GmbH
Back pressure regulators and check valves			
BPR_1	Back pressure regulator, spring-loaded, 250 psi	P-764	IDEX corporation
cv_1, cv_2	Check-valve, spring loaded	CV-300NF	IDEX corporation
Tubing, pre-heating loop, reactor			
L_1	Pre-heating loop, 1/16" PFA tubing coil, i.d. = 0.75 mm, V = 1 mL	1502XL	IDEX corporation
L_2	Pre-heating loop, 1/16" SS tubing coil, i.d. = 0.75 mm, V = 1 mL	U-190	IDEX corporation
L_3	Pre-heating loop, 1/16" SS tubing coil, i.d. = 0.75 mm, V = 1 mL	U-190	IDEX corporation

R_1	Reactor, 1/16” SS? tubing coil, i.d. = 0.75 mm, V = 0.5-9.8 mL	U-190	IDEX corporation
Mixers			
Mixer	High pressure static mixing arrow-head	U-466	IDEX corporation
Sensors			
P	Chemically resistant pressure transducer (0-50 bars) [S1]	-	Developed internally
T	K-type thermocouple o.d. 0.5 mm with 310SS sheathinstalled in a PEEK Tee	Thermocouple: 444-1275 Tee: P-716	RS RPO (thermocouple) IDEX (Union Tee)

3.1.1.2 Ammonolysis of glycidol with aqueous ammonia

All experiments were carried out with the setup described in section S3.1.1.1. Samples were collected over one residence time and thermally quenched (the efficacy of the thermal quench was validated beforehand: the same sample was analyzed after 1 h and led to identical results). Samples were diluted in isopropanol before GC analysis with duplicates. The conversion and the selectivity were calculated by GC-FID %area comparison (GC-FID method 1, Figure S2,3).

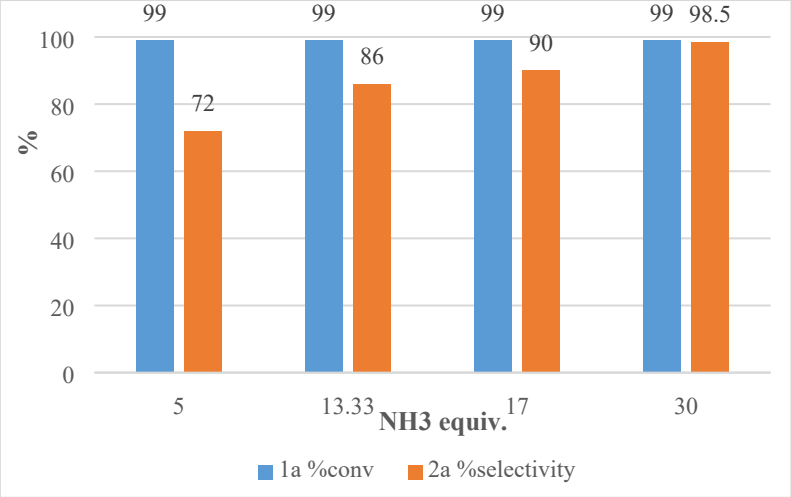

Figure S2. Influence of the excess NH_3 on the aqueous ammonolysis of **1a** (all samples were obtained after a residence time of 2 min at 120 °C).

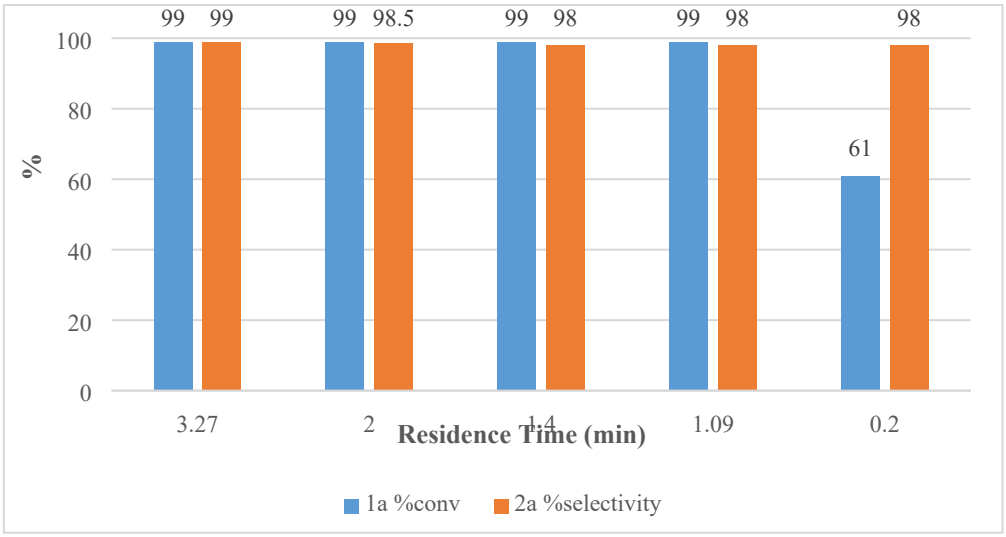

Figure S3. Influence of the residence time on the aqueous ammonolysis of **1a** (all sample were obtained at 120 °C with 30 equivalents of NH_3).

3.1.1.3 Ammonolysis of epichlorohydrin with aqueous ammonia

All experiments were carried out with the setup described in section S3.1.1.1. The collection, quench and analytical protocols were identical to those reported in S3.1.1.2. The results are presented in Figure S4.

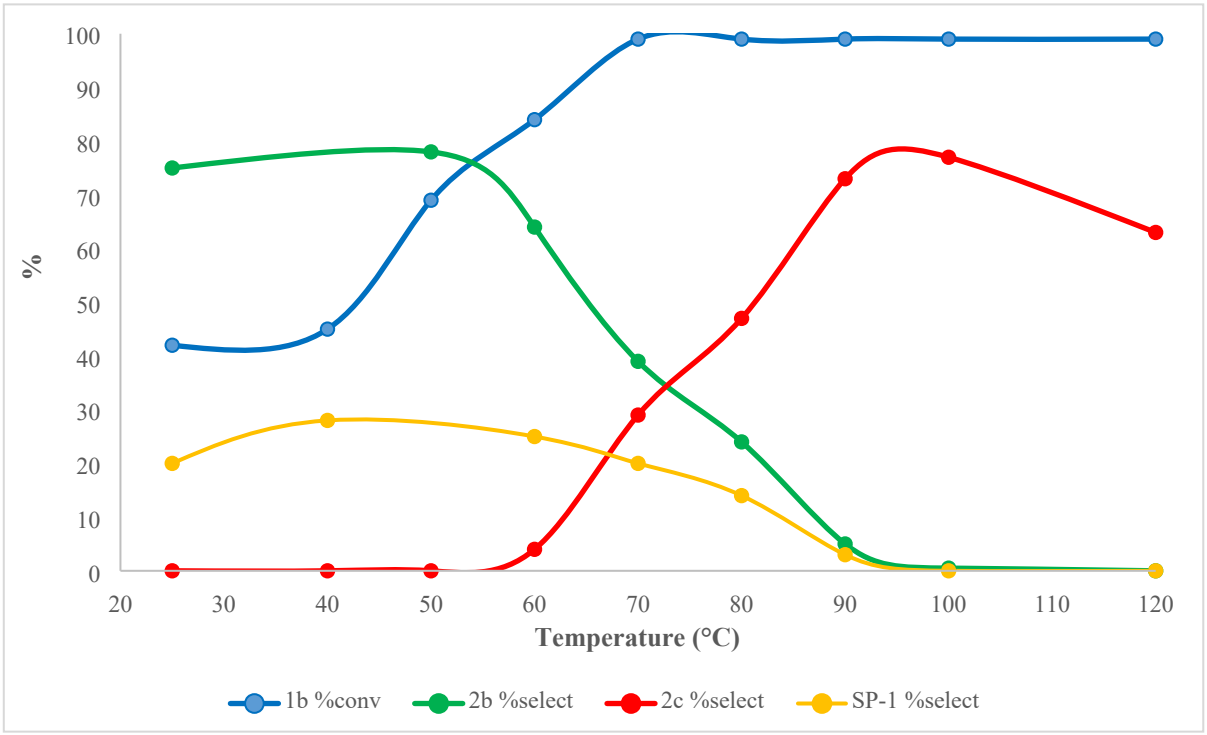

Figure S4. Influence of the temperature on the aqueous ammonolysis of **1b** (all samples were obtained after a residence time of 1 min with 30 equivalents of NH_3 at various temperatures).

The structure of side product **SP-1** could not be established with high confidence (Figure S5). Its instability in the crude mixture and sensitivity to water prevented isolation. GC-MS data are consistent with a three-membered ring (epoxide **SP-1a** or aziridine **SP-1b**) formed via intramolecular cyclization with loss of chloride. An azetidine (**SP-1c**) has the same molar mass and a compatible MS fragmentation

pattern, but comparison with an authentic standard (commercial **SP-1c**) by GC did not match, ruling out **SP-1c**.

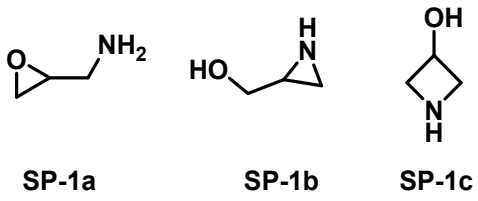

Figure S5. Potential structures for impurity **SP-1**.

3.1.2 Pilot-scale mesofluidic experiments

3.1.2.1 Mesofluidic setup

A silicon carbide (SiC) reactor was selected from the Corning® Advanced-flow™ reactor portfolio (Corning® AFR™ G1 SiC) instead of glass reactors, because glass is not fully chemically compatible with strong aqueous bases. A 30% aq. ammonia feed was delivered continuously by a dual-piston (500 mL each) Teledyne® ISCO pump. The 4 M glycidol (**1a**) solution in MeOH was delivered by a Knauer BlueShadow® 80P HPLC pump coupled to a Bronkhorst® CoriFlow™ mass-flow meter. Both feeds were preheated in separate modules and then mixed at the set temperature in a third fluidic module (FM). Two additional modules increased the reactor volume to 24 mL. Temperature was monitored at the reactor outlet and pressure at the aqueous-feed inlet. The outlet was connected to a tube-in-tube cooling heat exchanger at 0 °C, to thermally quench the reactor effluent. System pressure was held at 13 bar using an Equilibar® BPR coupled with Bronkhorst® EL-PRESS pressure controller. Collection flasks were sealed and vented to an acidic neutralization tank to prevent ammonia release. Process temperature reported herein was measured by a thermocouple placed in the heat-transfer fluid line immediately upstream of the reactor module: the thermostat was set to 120 °C, while the measured temperature was 110 °C. Details of the reactor setup are given in Figure S6; parts and auxiliaries are listed in Table S5. A photograph of the reactor is given in Figure S7.

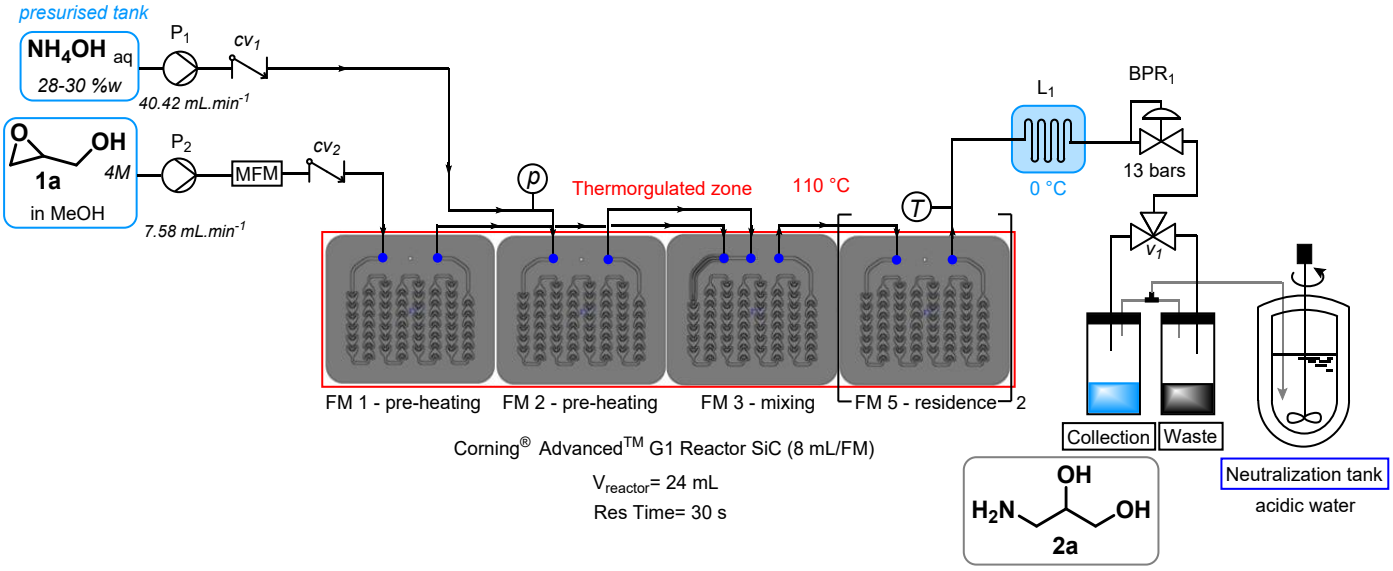

Figure S6. Details of the mesofluidic setup for the aqueous ammonolysis of glycidol (**1a**) toward the formation of 3-amino-1,2-propandiol (**2a**).

Table S5. List of parts of the continuous mesofluidic setup for the **1a** aqueous ammonolysis toward **2a**.

Symbol	Name, description	Reference number / product name	Manufacturer
Pumps			
P_1	Dual piston (500 mL/each) ISCO Pump	SyriXus A500	Teledyne
P_2	HPLC-type pump (plunger) 500 mL Titanium head	BlueShadow® 80P	KNAUER GmbH
Back pressure regulators, check valves and valves			
BPR_1	Equilibar® Back Pressure Regulator coupled with a Bronkhorst El-Press Pressure Controller	BPR: H3P1SNN8-NSBP1500T100S4KKB-G Pressure Controller: M23211621B; PCS-DV-B-100-PG	Pressure Control Solution (BPR) Bronkhorst (Pressure Controller)
cv	Poppet Check Valve 316SS (1/4")	SS-4C-1	Swagelok
v_1	4-way valve PEEK Bulkhead "L" flow	V-101-L	IDEX corporation
Tubing, pre-heating loop, reactor			
L_1	Cooling loop, 1/4 SS tubing inside, 2x tee 1/2" and bored through reductions from 1/4" to 1/2" (tube in tube with cryofluid passing in the outer shell)	2x tee: SS-810-3 2x reducer: SS-400-R-8BT 1 m 1/4" SS316L tube: SS-T4-S-049-20 80 cm 1/2" SS316L tube: SS-T8-S-049-20	IDEX corporation
FM	Silicon carbide (SiC) plates (8 mL/flow module)	G1 reactor	Corning® Advanced-Flow™
Sensors			
P	Chemically resistant pressure transducer (0-50 bars)[S1]	-	Developed internally
T	K-type thermocouple with 310SS sheath 1.5 mm diameter installed in a 316SS Tee (1/4" ID) using 1/16" – 1/4" reducing adapter	Thermocouple: RS Pro 228-7445 Tee: SS-400-3 Reducer: SS-100-R-4BT	RS RPO (thermocouple) Swagelok (fittings)
MFM	Coriolis Mass Flow Meter (mini CORI-FLOW)	M14-RGD-11-0-S	Bronkhorst®

Figure S7. Photograph of the mesofluidic reactor setup for aqueous ammonolysis

3.1.2.2 Pilot-scale aqueous ammonolysis of glycidol

All experiments were carried out with the setup described in section S3.1.2.1. The collection, quench and analytical protocols were identical to those reported in S3.1.1.2. The results are summarized in Table S6. A typical GC-FID chromatogram of the crude reactor effluent is provided in Figure S8.

Table S6. Mesofluidic optimization for the aqueous ammonolysis of **1a** toward **2a**.

Entry	**Q_{1a}** ($mL \cdot min^{-1}$)	**Q_{NH4OH}** ($mL \cdot min^{-1}$)	**Res Time** (s)	**NH_3** (equiv.)	**Conv. 1a** (%)	**Select. 2a** (%)
a	2.67	21.33	60	30	>99	>99
b	3.56	28.44	45	30	>99	>99
c	5.33	42.62	30	30	>99	>99
d	7.58	40.42	30	20	>99	>99 (98*)
e	13.09	34.00	30	10	>99	97
f	15.16	80.80	12	20	94	>99

*The final selectivity of the crude obtained with the optimal reaction condition was calculated by NMR.

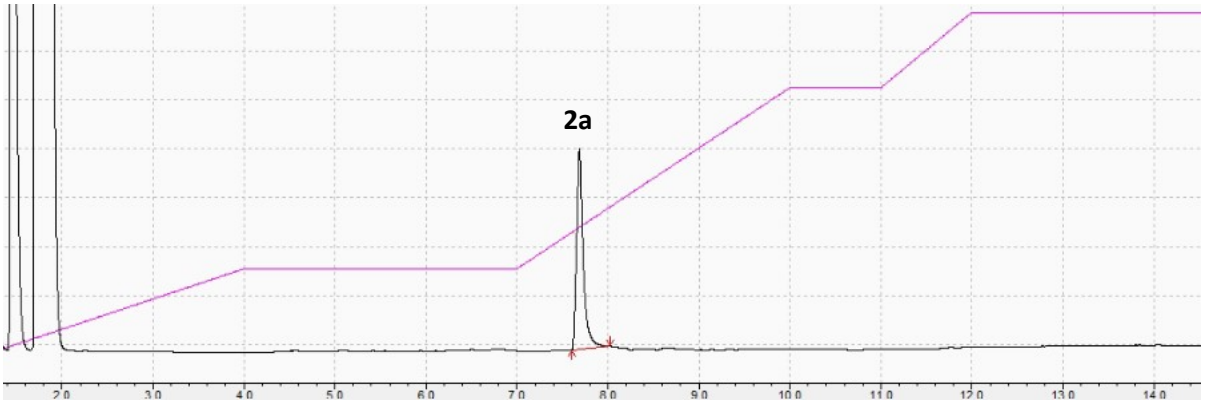

Figure S8. Typical GC-FID chromatogram of a crude reactor effluent (sample generated at 110 °C, 30 s of residence time with 30 equivalents of NH_3).

3.1.2.3 Process metrics

Process metrics were calculated according to ref.[S2]

E factor: 5.9 (based on optimal reaction condition: 20 equivalents of NH_3, 4 M glycidol (**1a**) solution in methanol, 98% yield in product **2a**). Water was not considered as waste according to the definition of classical E factor. Here, the easy water recovery (no metal and NH_3 easily distilled) justify this choice.

$$E = \frac{\sum waste}{\sum product} \rightarrow E = \frac{m(NH_3 excess) + m(MeOH) + m(sideproduct)}{m(2a)}$$

Table S7. Molar masses and density used for the calculation of the E factor

Compounds	Molar mass (g·mol^{-1})	Density (g·cm^{-3})
NH_3	17.031	-
1a	74.08	-
2a	91.11	-
MeOH	-	0.792

Output: 3.978 kg·day^{-1} (based on optimal reaction conditions mentioned above Table S6, entry d)

STY (Space Time Yield): 166 kg·day^{-1}·L^{-1} ($V_{reactor}$= 24 mL)

3.2 Ammonolysis with neat ammonia

3.2.1 Lab-scale microfluidic experiments

3.2.1.1 Microfluidic setup

Ammonia has a vapor pressure of ~9 - 10 bar at room temperature. According to the ammonia phase diagram, a back pressure of about 90 bar is required to keep neat ammonia liquid at 120 °C. To operate under these conditions, the microfluidic setup shown in Figure S9 was built. An ammonia cylinder was mounted upside down to pump liquid ammonia directly (avoiding gas-pressurization cycles). Neat liquid ammonia was delivered by a dual-piston Teledyne® ISCO pump (500 mL each) coupled with a Bronkhorst® CoriFlow™ M12 mass-flow meter was used to monitor ammonia density. A 4 M solution of oxirane **1a,b** in MeOH was delivered with a Knauer HPLC pump. Both dosing lines passed through a 1 mL preheating loops, after which the feeds were combined in an arrow-head PEEK static mixer and sent to a stainless-steel coil reactor (0.5 - 9.8 mL). The reaction effluent was then cooled in a 0.5 mL stainless-steel loop for thermal quench. System pressure was maintained at 90 bar using an Equilibar® BPR coupled with Bronkhorst EL-PRESS pilot pressure controller. Thermocouples and pressure sensors were placed at key locations. All sensors, pumps, the BPR, and the mass-flow meter were connected to a HITEC ZANG LabManager® for monitoring, data acquisition and control. Collection flasks were sealed and vented to an acidic neutralization tank to prevent ammonia release. Upon cooling the effluent to near-ambient temperature, its depressurization was highly endothermic (liquid-to-gas transition of ammonia), which caused icing of the BPR during long runs; this did not affect the process, but the BPR was immersed in a temperature-controlled water bath to prevent icing. After finishing the experiments, an argon flush with a purge valve, followed by a methanol wash, ensured safe cleaning of the ammonia feed line. All parts and auxiliaries are listed in Table S8.

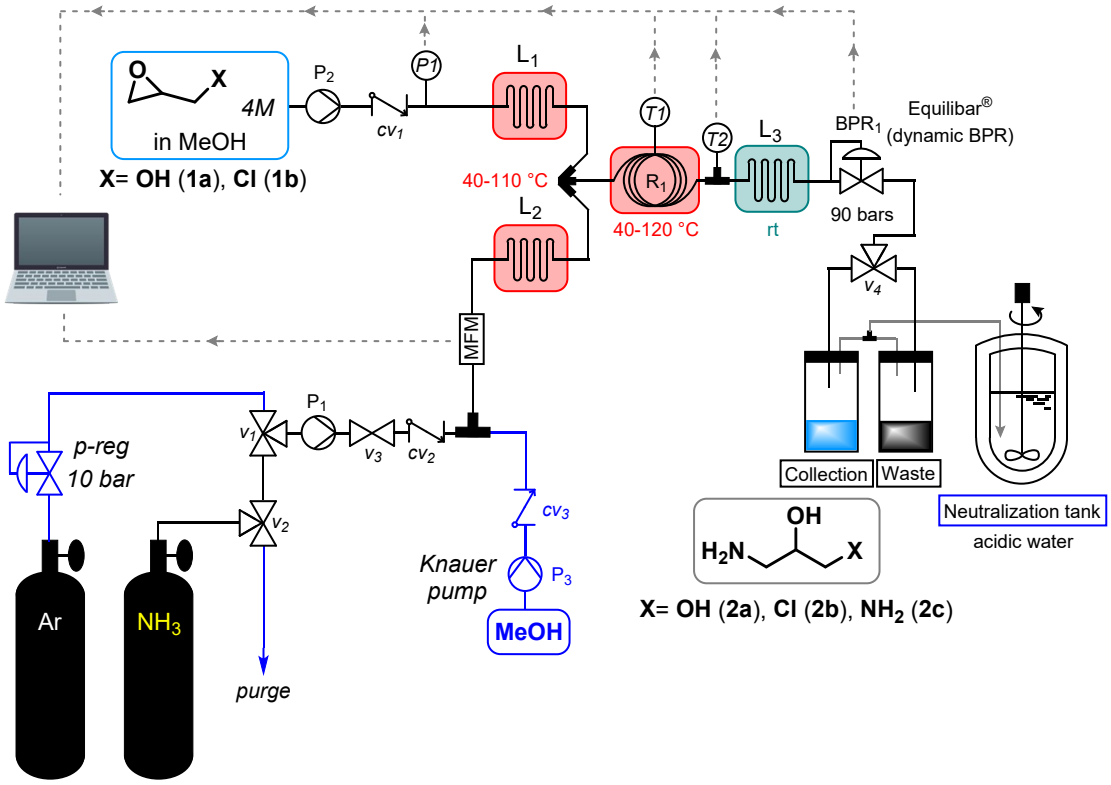

Figure S9. Complete scheme of the microfluidic setup for the ammonolysis with liquid NH_3 of oxiranes **1a**,**b** toward the formation of the corresponding amino-alcohol **2a,b,c**.

Table S8. List of parts of the continuous microfluidic setup for the ammonolysis with liquid NH_3 of **1b** toward **2b**.

Symbol	Name, description	Reference number / product name	Manufacturer
Pumps			
P_1	Dual piston (500 mL) ISCO Pump, pneumatic valves	SyriXus A500	Teledyne
P_2, P_3	HPLC-type pump (plunger) 10 mL stainless steel head	Azura P4.1S	KNAUER GmbH
Back pressure regulators, check valves and valves			
BPR_1	Equilibar® Back Pressure Regulator coupled with a Bronkhorst El-Press Pressure Controller	BPR: H3P1SNN8-NSBP1500T100S4KKB-G Pressure Controller: M23211621B; PCS-DV-B-100-PG	Pressure Control Solution (BPR) Bronkhorst (Pressure Controller)
cv_1	Check-valve, spring loaded	CV-300NF	IDEX corporation
cv_2	Poppet Check Valve 316SS (1/4")	SS-4C-1	Swagelok
v_1, v_2	3-ways ball valve 316SS, L flow path, (1/4" ID)	SS-43GXLS4	Swagelok
v_3	Quarter turn plug valve 316SS, (1/4" ID)	SS-4P4T	Swagelok
v_4	4-way valve PEEK Bulkhead "L"	V-101-L	IDEX corporation

	flow		
Tubing, pre-heating loop, reactor			
L_1, L_2	Pre-heating loops, 1/16” 316SS tubing coil, i.d = 0.75 mm, V= 1 mL	U-190	IDEX corporation
L_3	Cooling loop, 1/16” 316SS tubing coil, i.d = 0.75 mm, V= 0.5 mL	U-190	IDEX corporation
R_1	Reactor, 1/16” 316SS tubing coil, i.d = 0.75 mm, V= 0.5-9.8 mL	U-190	IDEX corporation
Mixers			
Mixer	High pressure static mixing arrow-head	U-466	IDEX corporation
Sensors			
P1	Flush diaphragm pressure transmitter (0-100 bars) 316TI/ 316L	Type S-11	WIKA
T1	K-type thermocouple o.d. 0.5 mm with 310SS sheath immerged in the oil bath, in contact with the reactor coil	Thermocouple: 444-1275	RS Group plc (thermocouple)
T2	K-type thermocouple o.d. 0.5 mm with 310SS sheath installed in a PEEK Tee[S1]	Thermocouple: 444-1275 Tee: P-716	RS Group plc(thermocouple) IDEX (Tee)
MFM	Coriolis Mass Flow Meter (mini CORI-FLOW)	M12-RGD-22-0-S	Bronkhorst®

3.2.1.2 Ammonolysis of glycidol with neat ammonia

All experiments were carried out with the setup described in section S3.2.1.1. Samples were collected over one residence time and thermally quenched (the efficacy of the thermal quench was validated beforehand: the same sample was analyzed after 1 h and led to identical results). Samples were diluted in isopropanol before GC analysis with duplicates. The conversion and the selectivity were calculated by GC-FID %area comparison (GC-FID method 1, Figures S10,11)

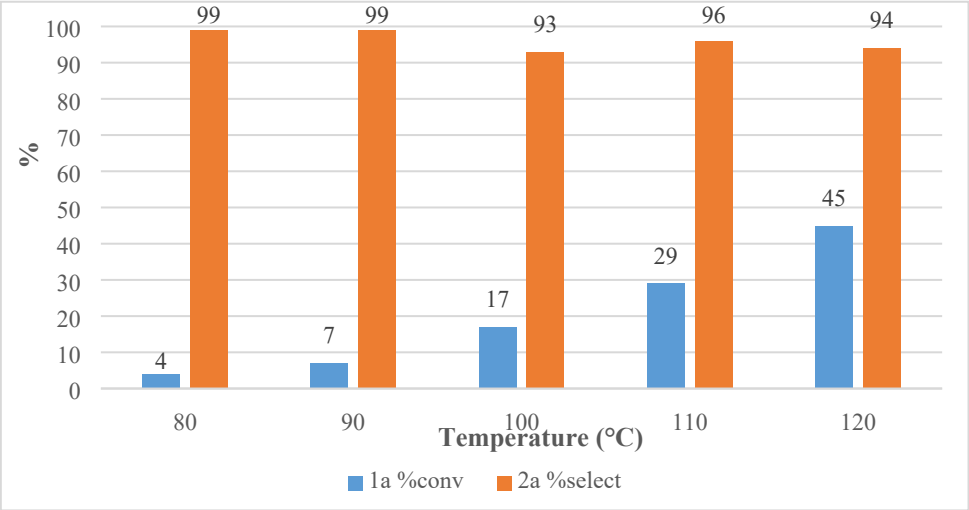

Figure S10. Influence of the temperature on the ammonolysis of **1a** with neat, liquified NH_3 (all samples were collected after 2 min of residence time with 30 equivalents of NH_3).

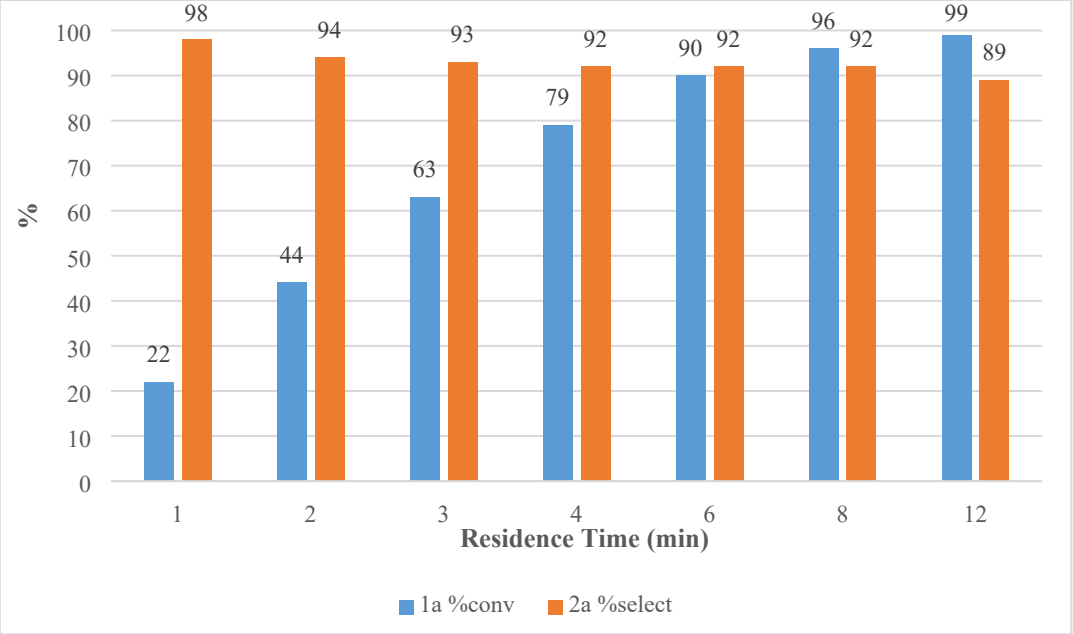

Figure S11. Influence of the residence time on the ammonolysis of **1a** with neat, liquified NH_3 (all samples were obtained from experiments varying the residence time under 120 °C with 30 equivalents of NH_3).

A modified setup was constructed for studying the influence of the addition of water on the ammonolysis of **1a** (Figure S12). A tee mixer was implemented on the ammonia feed line to inject the desired proportion of water. The results are presented in Figure S13.

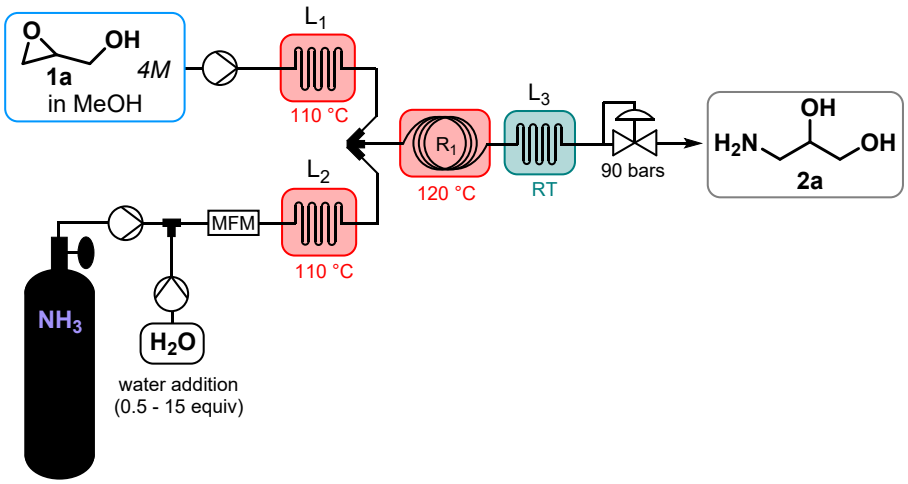

Figure S12. Simplified microfluidic flowchart for the ammonolysis of **1a** with liquid NH_3 with addition of water.

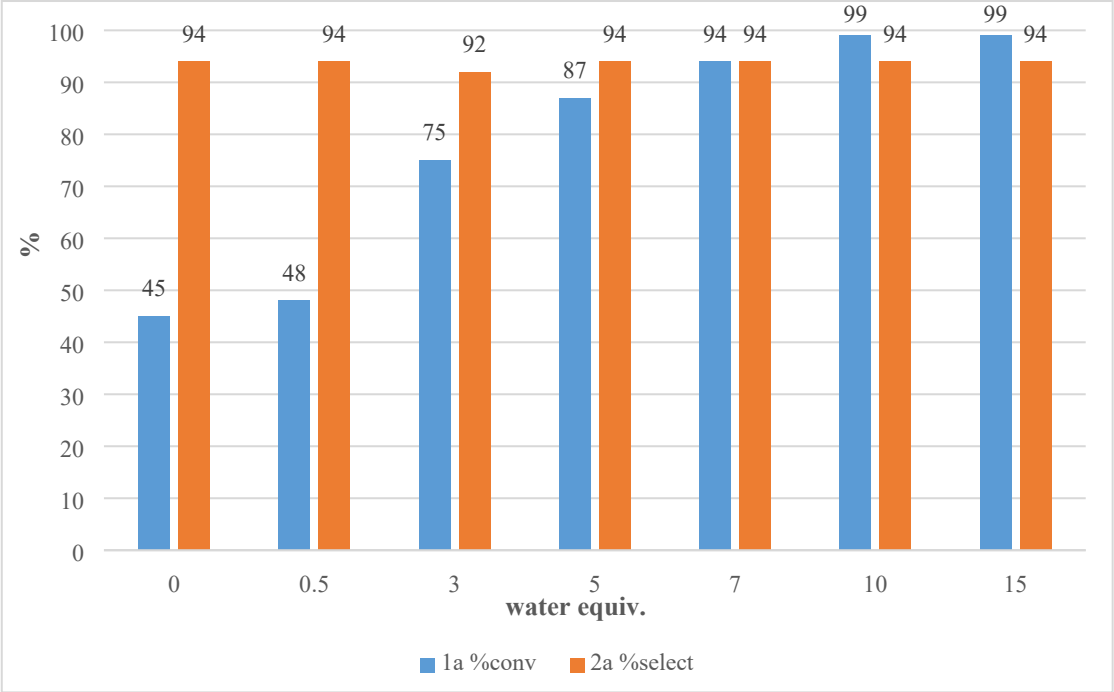

Figure S13. Influence of the addition of water for the ammonolysis of **1a** with liquid ammonia (all samples were obtained from experiments carried out with 2 min of residence time at 120 °C with 30 equivalents of NH_3).

3.2.1.3 Epichlorohydrin ammonolysis with neat ammonia

All experiments were carried out with the setup described in section S3.2.1.1. Sample collection, quench and preparation followed the same protocol as in S3.2.1.2. The conversion and the selectivity were calculated by GC-FID %area comparison (GC-FID method 1, Figures S14,15)

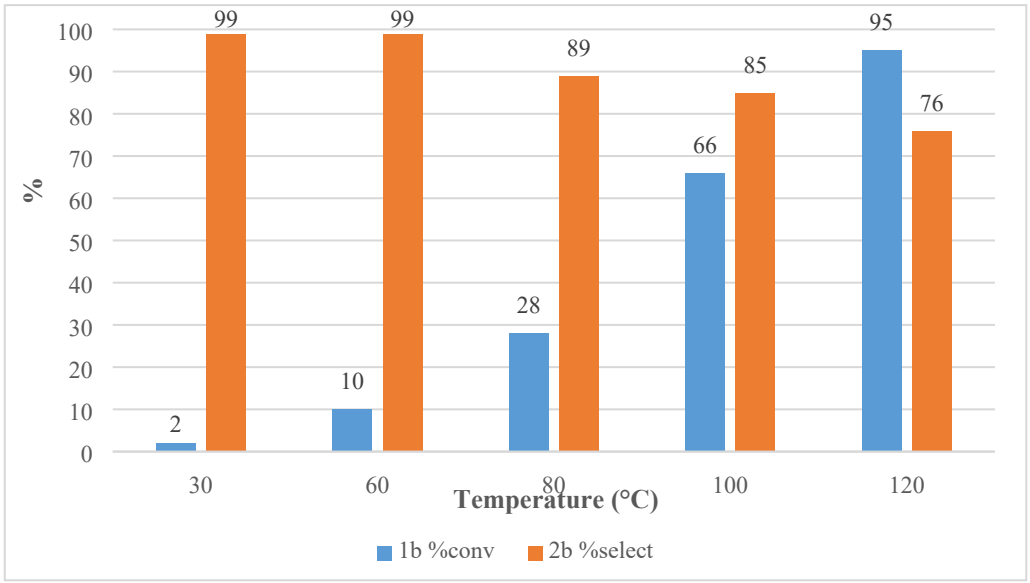

Figure S14. Influence of the temperature the ammonolysis of **1b** with neat, liquified ammonia (all samples were obtained from experiments carried out with 2 min of residence time with 30 equivalents of NH_3).

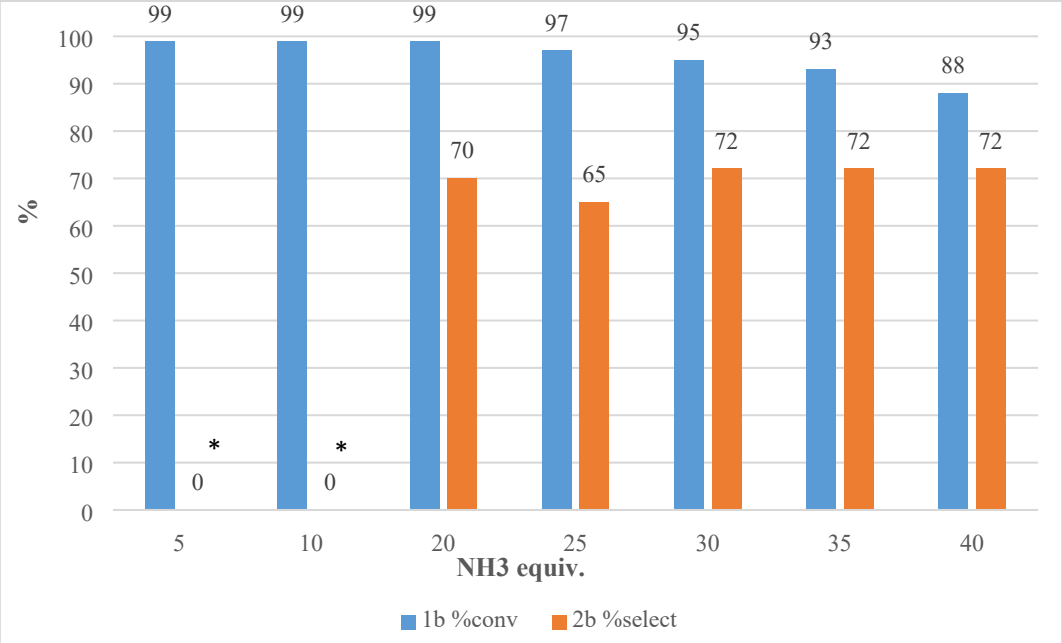

Figure S15. Influence of the excess NH_3 on the ammonolysis of **1b** with neat, liquified ammonia (all samples were obtained from experiments carried out with 2 min of residence time at 120 °C). *When less than 20 equivalents of NH_3 were used, a white solid precipitated in the collection flask (see Figure S16).

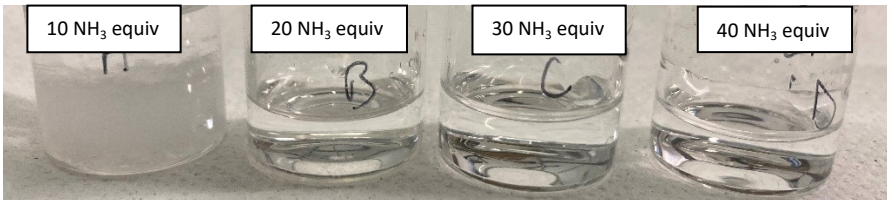

Figure S16. Appearance of a white precipitate for the samples generated with less than 20 equivalents of NH_3.

3.2.2 Pilot-scale mesofluidic experiments

3.2.2.1 Mesofluidic setup

The setup comprised two dosing lines delivering 4 M epichlorohydrin (**1b**) in MeOH and neat liquid ammonia to an Ehrfeld Mikrotechnik FlowPlate® A6 reactor. Both the organic feed and the ammonia were pumped by two dual-piston Teledyne® ISCO pumps (500 mL each). The ammonia line was identical to that described in section S3.2.1.1. Ammonia was preheated in a 5.6 mL plate; the **1b** feed was preheated in a heated stainless-steel line. The reagents were mixed in the 38.3 mL reactor. To keep ammonia liquid at a reactor temperature of 120 °C, the back pressure was set to 90 bar using an Equilibar® BPR coupled with Bronkhorst® EL-PRESS pressure controller. Temperature and pressure sensors were installed at key locations. The sensors, pumps, mass-flow meter (MFM), and BPR were monitored and controlled via a HITEC ZANG LabManager®. As section S3.2.1.1 for the microfluidic setup, flushing lines and purge valves were implemented. No post-reactor cooling loop was used to avoid clogging: the ammonolysis of **1b** can generate organic and/or inorganic chloride salts whose solubility is insufficient at room temperature, leading to precipitation, blockage, and overpressure. Although ammonia evaporation at the BPR outlet was vigorous due to the excess of liquid ammonia, all downstream tubing and connections remained tight, enabling safe neutralization. Neutralization with a dilute aqueous HCl solution was effective, and no ammonia release was detected. A detailed

flowchart of the mesofluidic setup is given in Figure S17. All parts and auxiliaries are listed in Table S9. A photograph of the mesofluidic setup is provided in Figure S18. The monitoring of process parameters with HITEC ZANG LabManager® is illustrated in Figure S19.

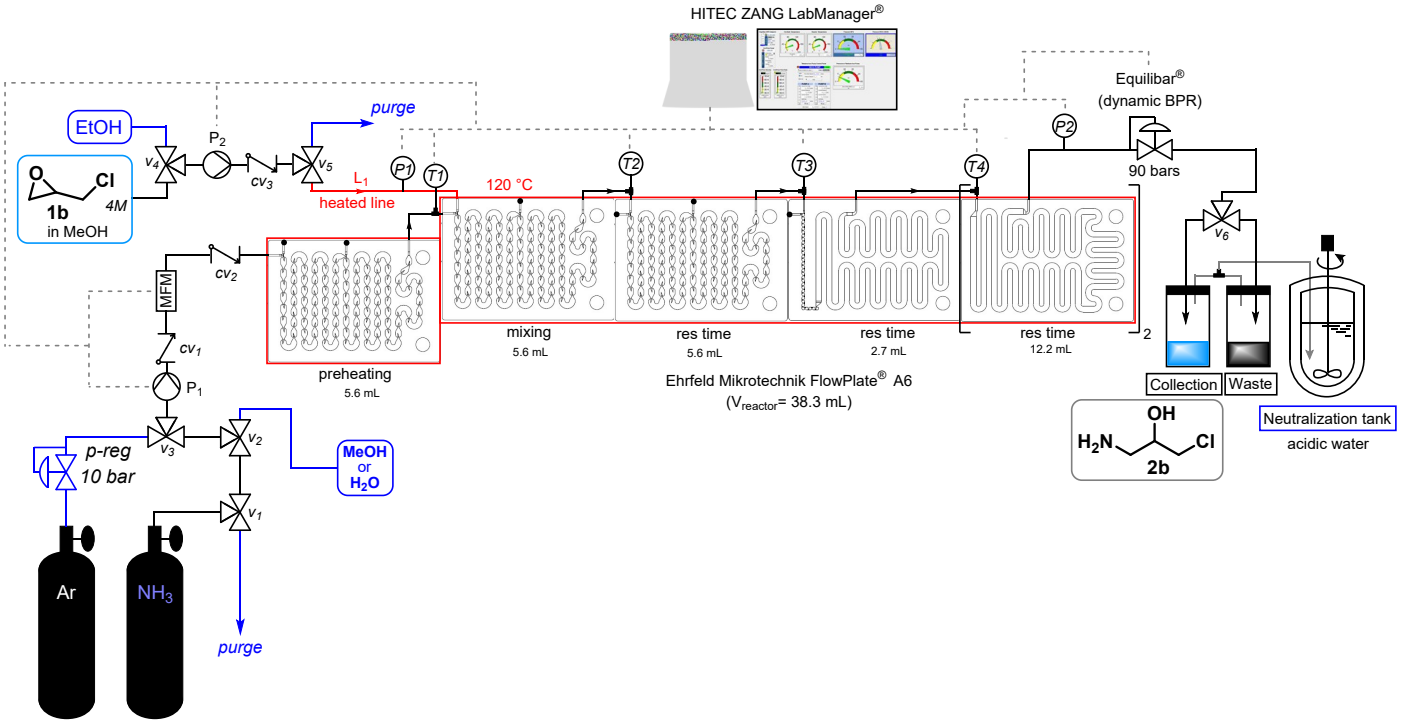

Figure S17. Complete scheme of the mesofluidic setup for the ammonolysis liquid NH_3 of epichlorohydrin (**1b**) toward the formation of 1-amino-3-chloro-2-propanol (**2b**).

Table S9. List of parts of the continuous mesofluidic system for the ammonolyis with liquid NH_3 of **1b** toward **2b**.

Symbol	Name, description	Reference number / product name	Manufacturer
Pumps			
P_1	Dual piston (500 mL) ISCO Pump, pneumatic valves	SyriXus A500	Teledyne
P_2	Dual piston (500 mL) ISCO Pump, electric valves	SyriXus E500	Teledyne
Back pressure regulators, check valves and valves			
BPR_1	Equilibar® Back Pressure Regulator coupled with a Bronkhorst El-Press Pressure Controller	BPR: H3P1SNN8-NSBP1500T100S4KKB-G Pressure Controller: M23211621B; PCS-DV-B-100-PG	Pressure Control Solution (BPR) Bronkhorst (Pressure Controller)
cv_1	Poppet Check Valve 316SS (1/4" ID)	SS-4C-1	Swagelok
cv_2, cv_3	Poppet Check Valve 316SS (1/8" ID)	SS-4C-1	Swagelok
v_1, v_2, v_3, v_4	3-ways ball valve 316SS, L flow path, (1/4" ID)	SS-43GXLS4	Swagelok
v_5	3-ways ball valve 316SS, L flow	SS-41GXHLS2	Swagelok

	path, (1/8” ID)		
v_6	4-way valve PEEK Bulkhead “L” flow	V-101-L	IDEX corporation
Tubing, pre-heating loop, reactor			
L_1	Pre-heating line, 1/8” 316SS tubing wrapped with resistive wire connected with an electric power supply	U-803	IDEX corporation In-house made
R_1	Hastelloy® C 22 flow plate ($V_{reactor}$= 38.3 mL)	FlowPlate® A6	Ehrfeld Mikrotechnik GmbH
	316SS tubing		IDEX corporation
Sensors			
P1, P2	Flush diaphragm pressure transmitter (0-100 bars) 316TI/ 316L	Type S-11	WIKA
T1, T2, T3, T4	K-type thermocouple o.d. 1.5 mm with 310SS sheath installed in a 316SS Tee (1/8” ID) using a 1/16” to 1/8” reducer	Thermocouple: RS Pro 228-7445 Tee: SS-200-3 Reducer: SS-100-R-2BT	RS Group plc (thermocouple) Swagelok (Union Tee)
MFM	Coriolis Mass Flow Meter (mini CORI-FLOW)	M14-RGD-11-0-S	Bronkhorst®

Figure S18. Photographs of the mesofluidic setup (a), with emphasis on the Ehrfled Mikrotechnik FlowPlate® A6 reactor (b) and the collection and neutralization system (c).

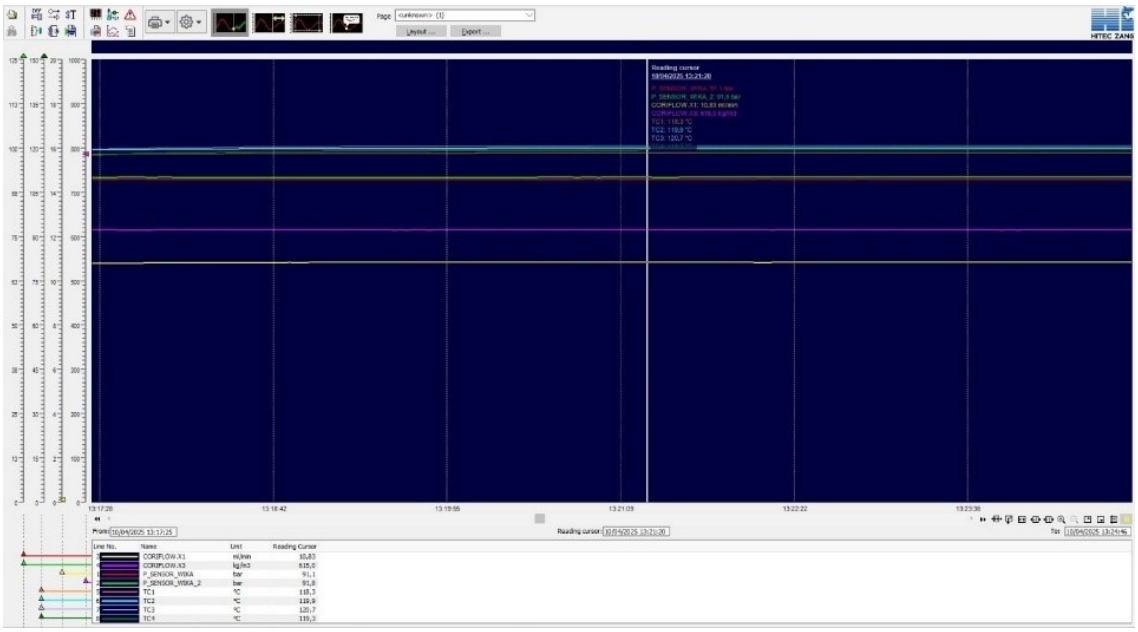

Figure S19. Process parameters monitoring (temperature, pressure and mass flow with Hitec Zang LabVison).

3.2.2.2 Startup procedure

The system is supposed to be stored under solvent like iPrOH.

Pressurize the system at 90 bars with solvent and then heat-up to 120 °C. After verification of the tightness of the gas line as well as the position of the valves v_1, v_2, v_3, heat the ammonia cylinder to approximately 30 °C (the tank temperature needs to be above ambient temperature, to avoid cavitation in the pump suction line), open the ammonia gas cylinder valve and fill one piston of the pump P_1 (the piston should contain a mixture of solvent, argon and ammonia). Empty P_1 (the pressure in the pump should increase until to reach 90 bars). The line before P_1 should be only filled with liquid ammonia and therefore P_1 can be use in double piston continuous flow mode. Pump ammonia in the system until the density measured with the MFM corresponds to the pure liquid ammonia. Then, start P_2 to deliver the **1b** feed in the reactor. After stabilization of the system, wait 4-5 residence times before collection.

3.2.2.3 Shutdown/cleaning procedure

Shutdown and cleaning are critical to avoid clogging. If product **2b** overreacts to **2c** and/or oligomerizes, HCl is released and forms amine hydrochloride salts; salt buildup can clog the system. To prevent this, do not turn off the pumps until cleaning is complete. Switch the ammonia line to MeOH without interruption. Once the MFM (via density) confirms the line is delivering only MeOH, switch the **1b** dosing line to solvent (typically EtOH). For extended shutdowns, include a water rinse and store the system filled with EtOH.

3.2.2.4 Results

All experiments were carried out with the setup described in section S3.2.2.1. Sample collection, quench and preparation followed the same protocol as in S3.2.1.2. The conversion and the selectivity were calculated by GC-FID %area comparison (GC-FID method 1, Table S10)

Table S10. Mesofluidic ammonolyis of **1b** toward **2b** with neat, liquified NH_3.

Entry	Temp (°C)	Q_{1b} (mL·min^{-1})	Q_{NH3} (mL·min^{-1})	NH_3 (equiv.)	Res. time (min)	Conv. **1b** (%)	Select. **2b** (%)
a	120	8.00	26.80	30	0.75	54	80
b	120	6.00	20.00	30	1.00	66	78
c	120	5.85	19.62	30	1.50	87	76
d	120	5.03	16.87	30	1.75	93	76
e	120	4.40	14.75	30	2.00	96	*
f	120	7.89	17.64	20	1.50	96	76
g	120	6.76	15.11	20	1.75	98	76
h	120	5.19	13.19	20	2.00	99	*

*white solid precipitated which distorted the quantification and led to clogging issue after some time.

3.2.2.5 Process metrics

Process metrics were calculated according to ref.[S2]

E factor: 6.6 (based on optimal reaction conditions: 20 NH_3 equiv, 4M epichlorohydrin (**1b**) solution, 75 %yield product **2b**).

$$E = \frac{\sum waste}{\sum product} \rightarrow E = \frac{m(NH3excess) + m(MeOH) + m(sideproduct)}{m(2b)}$$

Table S11. Molar masses and density used for the calculation of the E factor

Compounds	Molar mass (g·mol^{-1})	Density (g·cm^{-3})
NH_3	17.031	-
1b	92.52	-
2b	109.55	-
MeOH	-	0.792

Output: 3.2 kg·day^{-1} (based on optimal reaction conditions mentioned above Table S10, entry g)

STY (Space Time Yield): 83.6 kg·day^{-1}·L^{-1} ($V_{reactor}$= 38.3 mL)

4. Oxazolidinone synthesis

4.1 Preliminary catalyst screening

Organocatalysts were screened with a range of organic (super)bases: amidines (DBU, DBN), guanidines (TBD, MeTBD), phosphazenes (BEMP, P_1-t-Bu) and proton sponge (DMAN) (Scheme S1). The results are summarized in Figure S20.

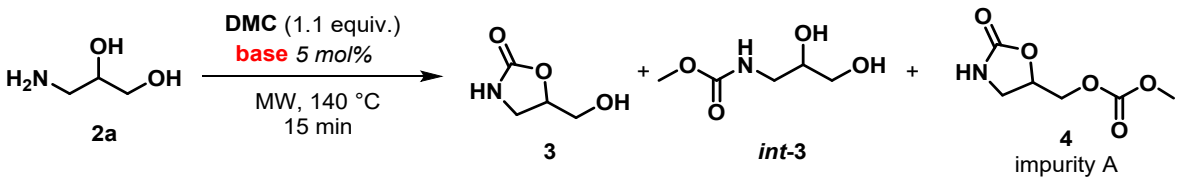

Scheme S1. Batch catalyst screening for the carbamatation of amino glycerol **2a** toward oxazolidinone **3**.

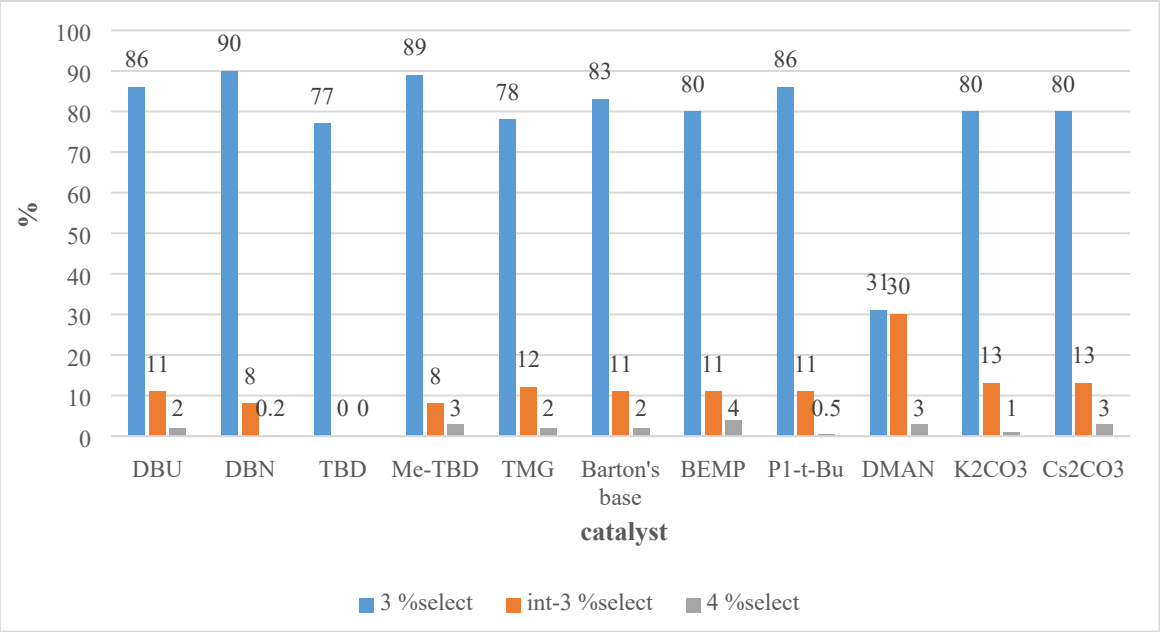

Figure S20. Selectivity results of the catalyst screening for the carbamatation of amino glycerol **2a** toward oxazolidinone **3**.

4.2 Design of Experiment (DoE)

Design of experiments (DoE) was performed with Sartorius MODDE® 13 (v13.0.2) software. The selected factors were temperature (100 - 140 °C), **DMC** equivalents (1.2 - 3.0), and catalyst loading (0 - 5 mol%). The responses were conversion of **2a** and selectivity to product **3**, intermediate ***int*-3**, and major side product **4** (Scheme S2). Reactions were conducted in a microwave reactor to enable rapid heating and operation under pressure, as **DMC** boils at 90 °C and MeOH is released during the reaction. Crude reaction mixtures were quenched with NH_4Cl and analyzed by GC-FID (method 2).

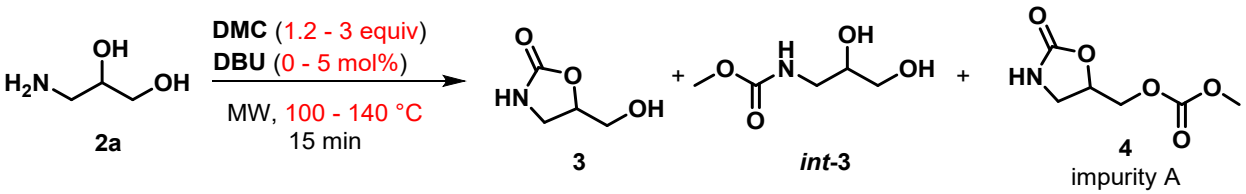

Scheme S2. DoE for the carbamatation of amino glycerol **2a** toward oxazolidinone **3**.

It appeared the conversion of **2a** was always complete. Therefore, it was not relevant to display this response.

A quadratic model *D-Optimal* was selected for the DoE, with 13 design runs and 2 centre points (15 points overall). Figure S21 below displays the summary of Fit (R2, Q2, Model validity and Reproducibility), the Coefficients (correlation between factors and responses) as well as the comparison between observed and predicted points.

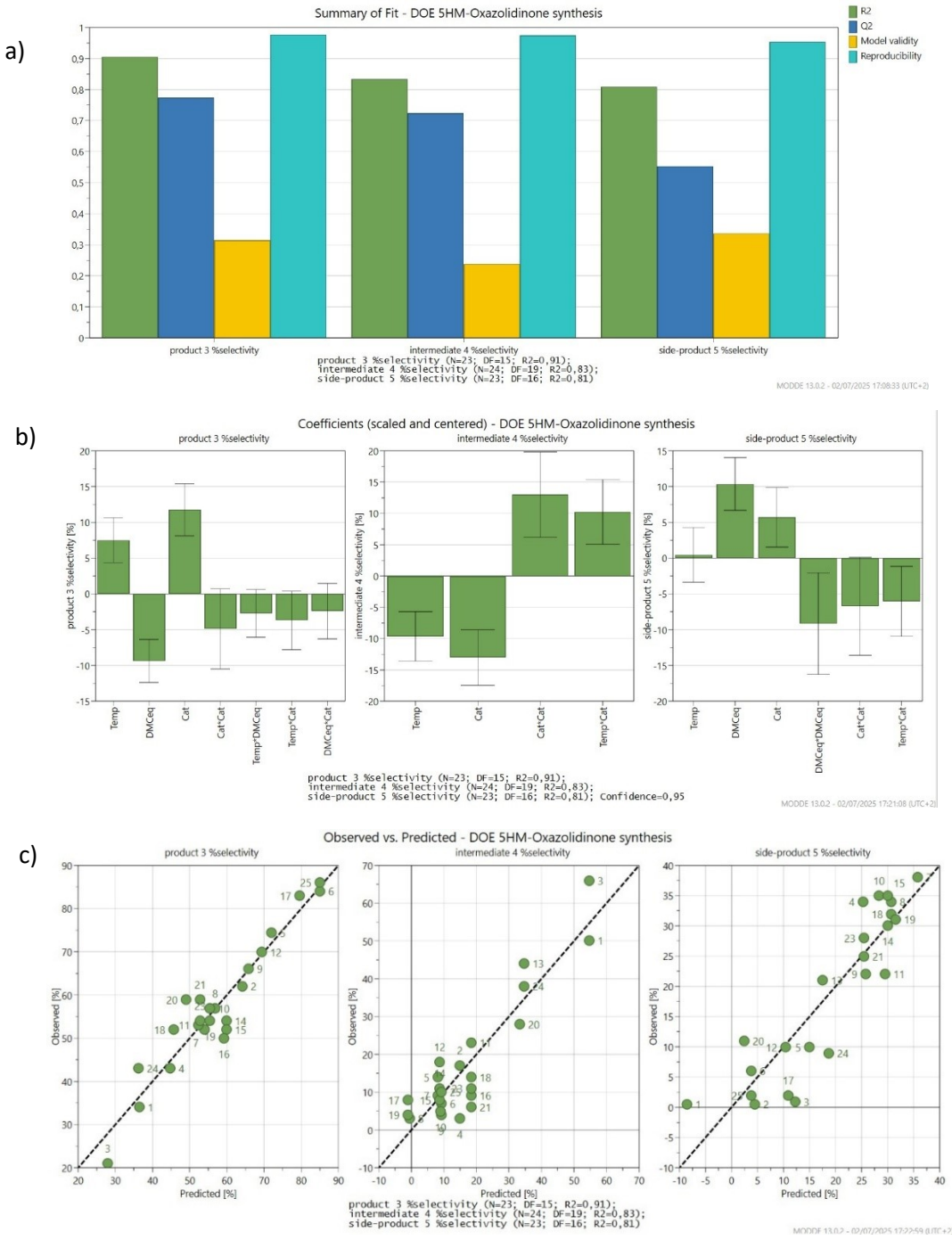

Figure S21. A) Summary of Fit (R2, Q2, Model validity and Reproducibility) b) The coefficients (correlation between factors and responses) c) observed vs predicted points.

The 4D contour representations of the selectivity toward compounds **3**, ***int-3*** and **4** are shown in Figure S22 below.

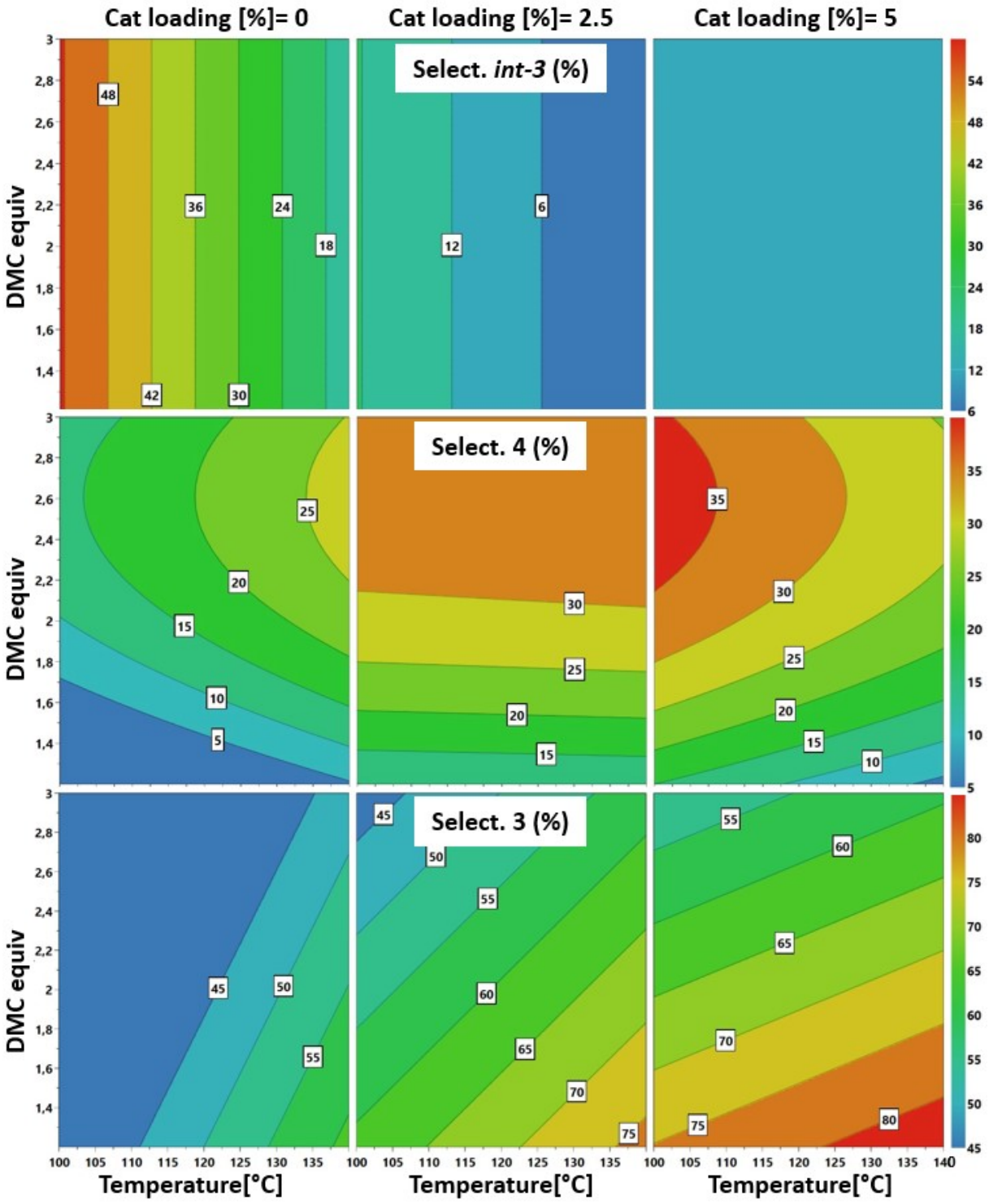

Figure S22. 4D display of the DoE results, emphasizing the selectivity toward compounds **3**, ***int-3*** and **4**, respectively.

The optimal condition window which maximized the yield of product **3** while minimizing the leftover of intermediate ***int*-3** and the formation of side-product **4** corresponded to the maximum temperature (140 °C), minimal **DMC** equivalent (1.2 equiv.) and maximum catalyst loading (5 mol%). Following that trend, the amount of **DMC** equivalents can be reduced to 1.1 or 1.0. Increasing the catalyst loading potentially may give improved results, however it would reduce the sustainability of the process.

4.3 Control experiments (batch)

a. Payne rearrangement

Compound ***iso*-3** (Scheme S3a) was dissolved in DMSO-d6 with 10 mol% DBU and heated to 100 °C; ^{1}H NMR monitoring showed no significant conversion after 3 h. The DoE indicated that formation of side product **4** is favoured at 100 °C with a large excess of **DMC** and maximum catalyst loading. Under analogous conditions, the Payne rearrangement between oxazolidinone **3** and cyclic carbonate ***iso*-3** appears unlikely.

b. Conversion of intermediate *int-3*

To ensure compound ***int*-3** was indeed a reaction intermediate toward the formation of **3**, it was synthesized from **2a** and made reacted with 5 mol% DBU at 140 °C for 15 min. Complete conversion and selectivity toward **3** were obtained (Scheme S3b).

c. Formation of side product 4

To product **3**, 1.1 equivalent **DMC** and 5 mol% DBU were added. The reaction mixture was heated at 100 °C for 15 min in a microwave reactor (Scheme S3c).

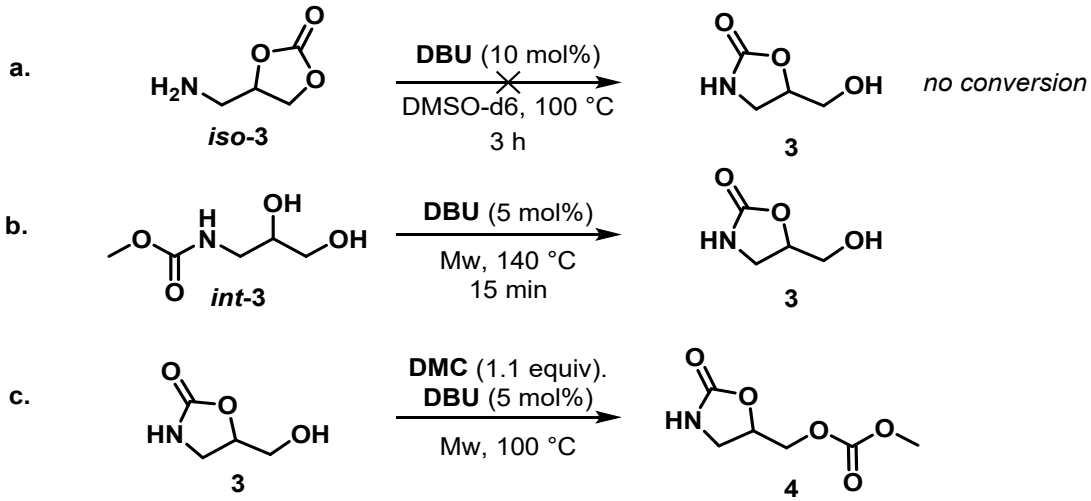

Scheme S3. Control experiments

4.4 Preparation of reference compounds for the control experiments

4.4.1 Preparation of intermediate ***int*-3**

The preparation of ***int*-3** is summarized in Scheme S4. 3-amino-1,2-propanediol (**2a**; 0.5 g, 5.5 mmol, 1 equiv.) and $NaHCO_3$ (23 mg, 0.28 mmol, 0.05 equiv.) were loaded and cooled at 0 °C in a 10 mL round-bottom flask. Then, methyl chloroformate (0.45 mL, 5.8 mmol, 1.05 equiv.) was added dropwise at 0 °C. The reaction was allowed to warm up to room temperature and left 1 h under vigorous stirring. After concentration under reduced pressure, compound ***int-3*** was obtained as a colorless, viscous liquid (90% yield).

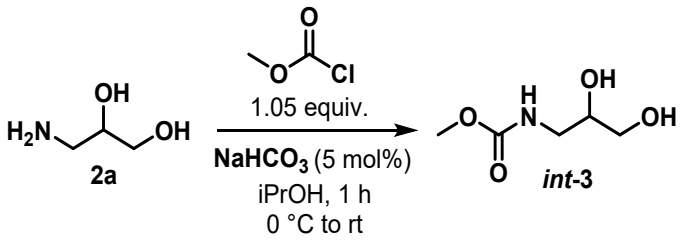

Scheme S4. Preparation of intermediate ***int*-3**.

4.4.2 Preparation of 1-amino-3-chloro-2-propanediol (**2b**)

The preparation of **2b** is summarized in Scheme S5. To a solution of benzaldehyde (6.8 mL, 66.99 mmol, 1.05 equiv.) in EtOH (20 mL) in a 25 mL round-bottom flask were added 7.68 mL of a 32 wt.-% aqueous NH_3 solution (2 equiv.). Then, **1b** (5 mL, 63.8 mmol, 1 equiv.) was added dropwise. The mixture was left at room temperature for 8 h under vigorous stirring. The reaction medium was then concentrated under reduced pressure to give a yellowish oil. After column purification (Hexane/AcOEt 4:1, isocratic), compound **7** was obtained in 85% yield. This procedure was inspired from ref.[S3]

Compound 7 (3.6 g, 18.2 mmol, 1 equiv.) was dissolved in 10 mL DCM. 5 mL of 3 M HCl and 10 mL H_2O were added. The biphasic medium was kept at room temperature under vigorous stirring for 30 min. After settling, the aqueous phase was separated and the organic phase was washed 2 times with brine. The aqueous phases were gathered and concentrated under reduced pressure. 5 mL of iPrOH were added to make **2b·HCl** precipitate. After drying under high vacuum, a white powder was obtained (40 %yield).

Sample for GC analysis were prepared by addition of isopropanol and $NaHCO_3$ to **2b·HCl** for few minutes under vigorous mixing, to release the free base **2b**. After centrifugation, the organic liquid phase was injected in GC.

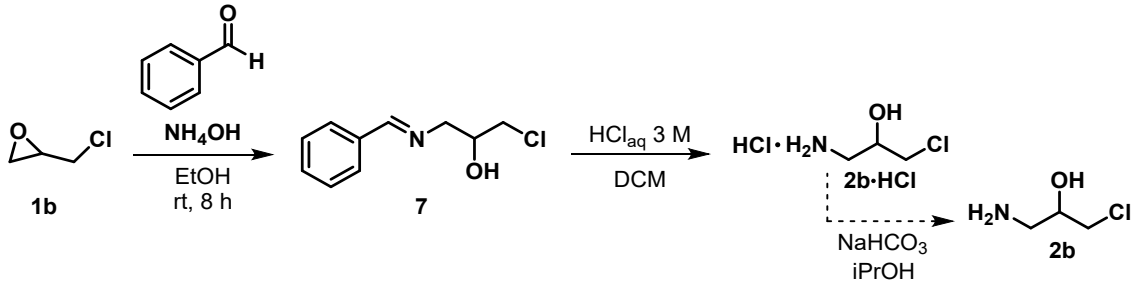

Scheme S5. Preparation of 1-amino-3-chloro-2-propanediol (**2b**)

4.4.3 Preparation of 4-(aminomethyl)-1,3-dioxolan-2-one (***iso*-3**)

The preparation of ***iso*-3** is summarized in Scheme S6.

In a 25 mL round-bottom flask, **2a** (0.590 g, 6.5 mmol, 1 equiv.) and **Boc_2O** (1.43 g, 6.5 mmol, 1 equiv.) were diluted in 8 mL EtOH. The reaction was kept at room temperature for 45 min under stirring. The crude reaction mixture was then concentrated under reduced pressure, and compound **8** was recovered as a white solid (quantitative).

In the next step, compound **8** (0.590 g, 3.1 mmol, 1 equiv.), **DMC** (0.52 mL, 6.2 mmol, 2 equiv.) and **DBU** (14 mg, 0.093 mmol, 0.03 equiv.) were loaded in a sealed vial and heated at 140 °C for 15 min in a microwave reactor. The crude reaction mixture was then concentrated under reduced pressure to give a solid (88% crude yield). The resulting solid was purified by column chromatography (AcOEt/Hex 1:1, isocratic), to afford 260 mg of **9** as a white solid (19% isolated yield).

Then, Boc-protected **9** (0.448 g, 2.1 mmol, 1 equiv.) was dissolved in 2 mL DCM at 0 °C. Amberlyst®15 (0.0136 g) was added. The medium was warmed up to room temperature and left under stirring for 6 h. The reaction was monitored with GC; when no traces of **9** were detected anymore, the Amberlyst®15 beads were washed with a 2 M solution of ammonia in methanol. The organic phase was concentrated under reduced pressure to give ***iso*-3** as a colourless, viscous oil (30% yield). This procedure is inspired from ref.[S4]

Alternatively, Boc-protected **9** (68 mg, 0.31 mmol, 1 equiv.) was dissolved in DCM (2 mL). Then, 1 mL of cold 6 M HCl in isopropanol was added slowly. The medium was left under stirring at room temperature for 1 h, until a white solid precipitated. The solvent was removed under reduced pressure to recover a white solid, which was subsequently washed with DCM. Hydrochloride ***iso*-3·HCl** was dried under high vacuum (70% yield).

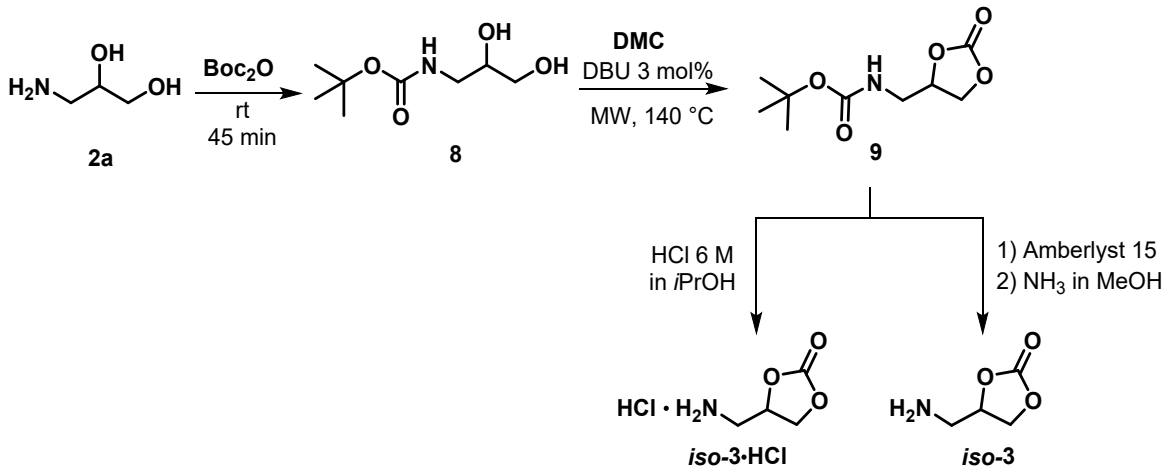

Scheme S6. Synthesis of compound ***iso*-3** and its hydrochloride salt ***iso*-3·HCl**

4.5 Microfluidic scale experiments

4.5.1 Microfluidic setup

The microfluidic setup was constituted of three main units connected in series (Figure S23):

a. **Unit 1.** DMC (containing the dissolved catalyst) was delivered with a CHEMYX syringe pump. To limit pressure-drop due to high viscosity, amino-glycerol **2a** was pumped with a CHEMYX syringe pump fitted with a heating jacket; the delivery line was heated electrically to 50 °C using resistive wires. Both feeds were preheated to reaction temperature in 0.5 mL stainless-steel loops, then mixed in an arrow-head PEEK static mixer before entering the first stainless-steel coil reactor (V = 0.5-9.8 mL). Downstream, a cooling loop, thermocouple, pressure sensor, and in-line IR probe were installed. A 250-psi cartridge BPR maintained system pressure.
b. **Unit 2**. The second module was a continuous-flow evaporator to distil the MeOH from the crude. The Unit-1 effluent was pumped with an Asia syringe pump and preheated in a PFA coil. A preheated N_2 stream was injected via a needle into the PFA tubing (connection via a PEEK tee), establishing a pseudo-annular flow. After gas injection, MeOH was evaporated in a heated 1/8" PFA coil. The evaporator coil outlet entered a phase separation column: the hot gas exited at the top, while the viscous, concentrated liquid was collected at the bottom. The entire evaporator module was housed in a GC oven for uniform heating.
c. **Unit 3.** The concentrated viscous stream from the bottom of the column was pumped into a second stainless-steel coil reactor using a Vapourtec® SF-10 peristaltic pump. A 250-psi cartridge BPR pressurized this reactor.

Parts and auxiliaries are listed in Table S12.

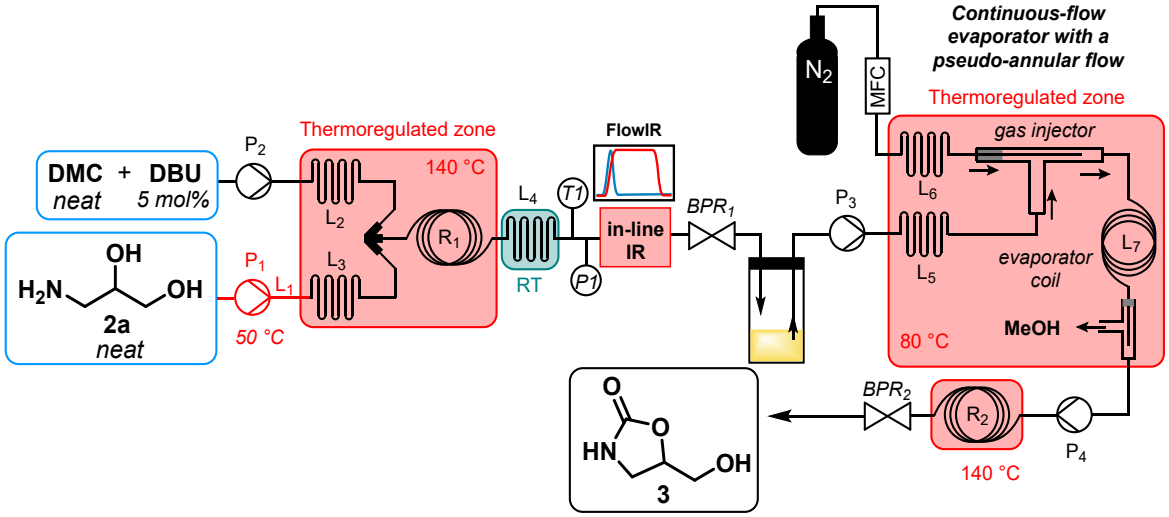

Figure S23. Complete scheme of the microfluidic setup for the carbamatation of amino glycerol **2a** toward the formation of oxazolidinone **3**.

Table S12. List of parts of the continuous microfluidic setup for the synthesis of **3**.

Symbol	Name, description	Reference number / product name	Manufacturer
Pumps			
P_1	Syringe pump (20 mL SS syringe equipped with a heating jacket)	Fusion 200X	CHEMYX
P_2	Syringe pump (20 mL SS syringe)	Fusion 200X	CHEMYX
P_3	Continuous syringe pump; equipped with Asia Red Syringes (2.5 mL, 5mL)	Asia Syringe Pump	Syrris Ltd.
P_4	Peristaltic pump	SF-10	VAPOURTEC
Back pressure regulators and check valves			
BPR_1, BPR_2	Back pressure regulator, spring-loaded, 250 psi	P-764	IDEX corporation
Tubing, pre-heating loop, reactor			
L_1	Pre-heating line, 1/16” 316SS tubing wrapped with resistive wire connected with an electric power supply	U-190 (SS tubing)	IDEX corporation
L_2, L_3	1/16” 316SS tubing, V = 0.5 mL	U-190	IDEX corporation
L_4	1/16” 316SS tubing, V = 0.4 mL	U-190	IDEX corporation
L_5	1/16” PFA tubing (I.D.= 0.75 mm, 2m)	1502XL	IDEX corporation
L_6	1/8” 316SS tubing (I.D.= 1.52 mm, 5m)	1921L	IDEX corporation
L_7	1/8” PFA tubing (I.D.= 1.52 mm, 1m)	1921L	IDEX corporation
R_1	Reactor, 1/16” SS tubing coil, i.d = 0.75 mm, V = 2 mL	U-190	IDEX corporation
R_2	Reactor, 1/16” SS tubing coil, i.d = 0.75 mm, V= 1 mL	U-190	IDEX corporation
Mixers			

Mixer	High pressure static mixing arrow-head	U-466	IDEX corporation
Sensors			
P	Chemically resistant pressure transducer (0-50 bars) [S1]	-	Developed internally
T	K-type thermocouple o.d. 0.5 mm, with 310SS sheath installed in a PEEK Tee	Thermocouple: 444-1275 Tee: P-716	RS Group plc (thermocouple) IDEX (Union Tee)
IR-probe	In-line IR system equipped with a Micro Flow Cell (Diamond probe)	ReactIR 702L	METTLER TOLEDO

4.5.2 Preliminary optimization with in-line IR

All experiments were carried out with the setup described in section S4.1.4. Samples were collected over one residence time and quenched with NH_4Cl and by cooling (the efficacy of the thermal quench was validated beforehand: the same sample was analyzed after 1 h and led to identical results). Samples were diluted in isopropanol before GC analysis with duplicates. The conversion and the selectivity were calculated by GC-FID %area comparison (GC-FID method 2, Figure S24 and Table S13).

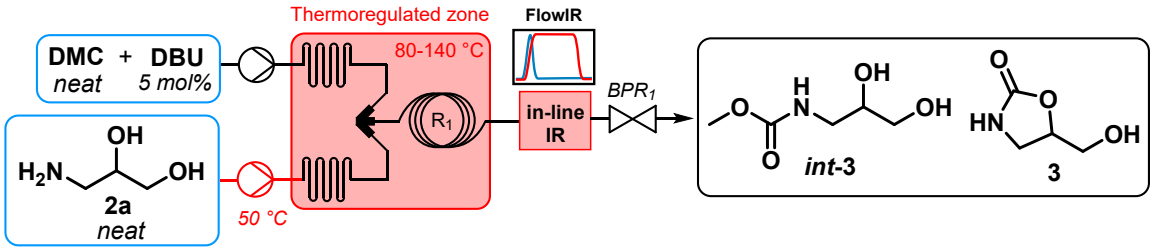

Figure S24. Simplified diagram of the microfluidic setup for the first flow optimization with in-line IR monitoring.

Table S13. Reaction conditions for the temperature gradient experiment.

$Q_{DMC/DBU}$ (mL·min^{-1})	Q_{AGL} (mL·min^{-1})	Res. time (min)	DMC (equiv.)	DBU loading (mol%)	Pressure (bar)
0.27	0.229	4.01	1	5	18

After stabilization of the system at 80 °C, a temperature gradient with plateau at 100 °C, 120 °C and 140 °C was applied. The crude outlet was continuously monitored by the in-line IR. To follow the evolution of intermediate ***int*-3** and product **3**, trends of several bands related to these two compounds were monitored. Clear band shifts were spotted on the stacked IR spectra (Figures S25-26). For instance, a C=O band at 1734 cm^{-1} from product **3** significantly increased, while C=O band at 1699 cm^{-1} from intermediate ***int*-3** virtually disappeared. The conversion of ***int*-3** was even more visible by following the band at 1540 cm^{-1}. Surprisingly, the best trends were obtained by plotting variation in the band at 1489 cm^{-1} (formation of product **3**) and variation in the band height at 1153 cm^{-1} (consumption of ***int*-3**) as shown on Figure S27.

Next, the impact of the residence time was studied, with a simplified microfluidic setup (Figure S28 and Table S14).

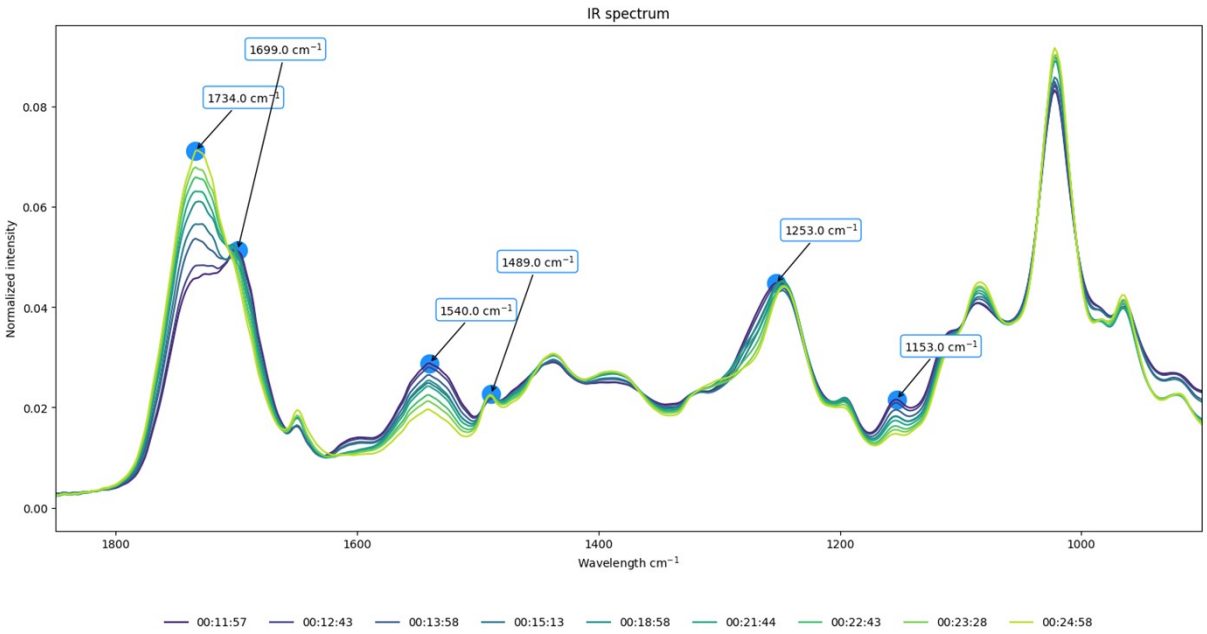

Figure S25. Stacking of the IR spectra (region of interest: from 900 cm^{-1} to 1850 cm^{-1}) over time.

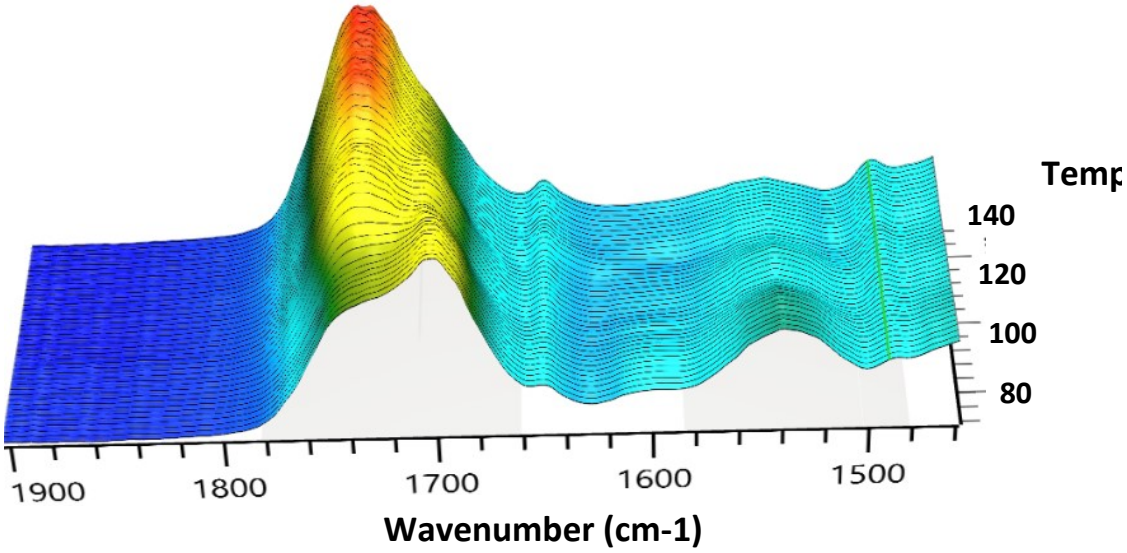

Figure S26. Surface IR spectra (region of interest: from 1460 cm^{-1} to 1900 cm^{-1}) over time.

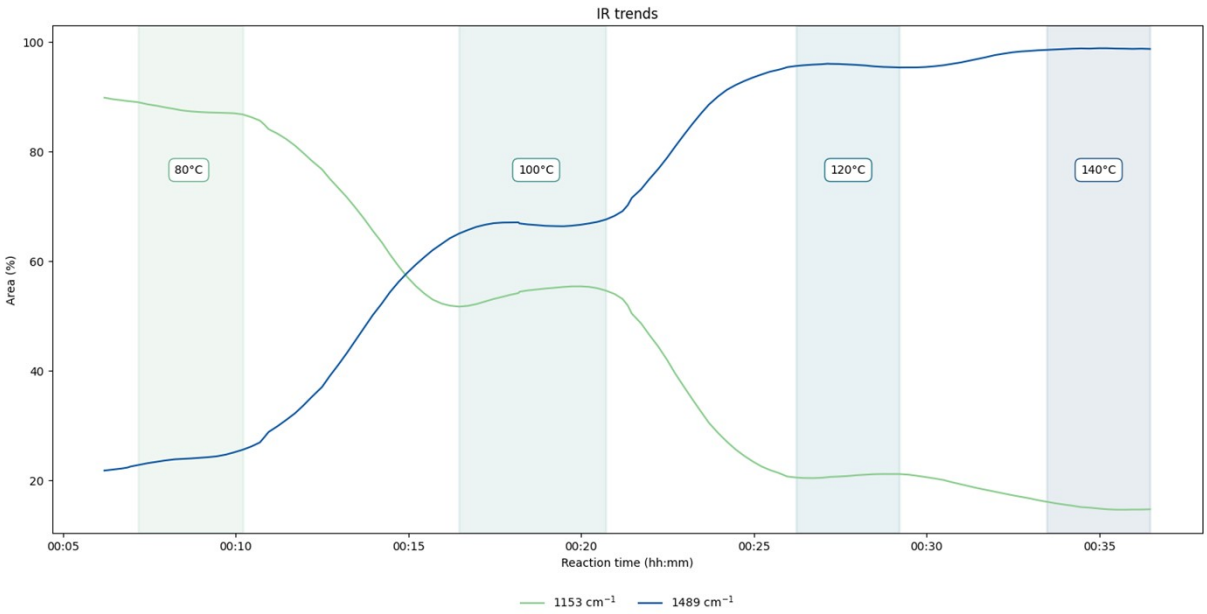

Figure S27. IR trends with the monitoring of intermediate ***int*-3** (1153 cm^{-1}) and oxazolidinone **3** (1489 cm^{-1}) over time following the temperature gradient.

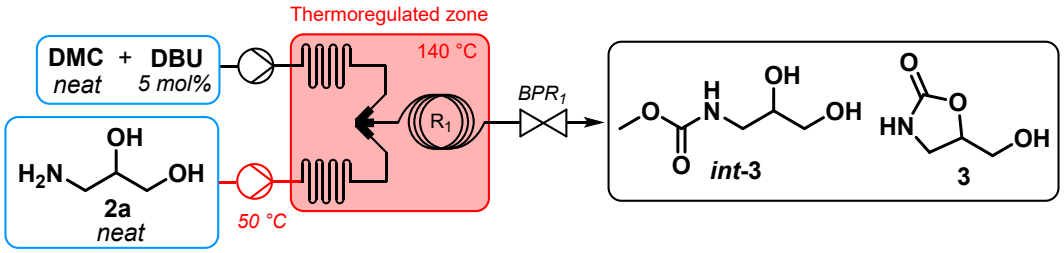

Figure S28. Simplified scheme of the microfluidic setup for residence time optimization.

Table S14. Results of the residence time optimization in continuous flow.

Entry	Res Time (min)	2a (%conv.)	3 (%select.)	4 (%select.)
a	0.25	45	21	24
b	0.50	68	36	29
c	1.00	82	47	29

4.5.3 Implementation of a continuous-flow evaporator

4.5.3.1 Design of the continuous flow evaporator

The idea for construction of this evaporator prototype emerged to enable continuous, small-scale removal of volatile components of liquid mixtures in a relatively simple way. The evaporation process can also enable achieving better conversions in the case of equilibrium reactions, if one of the products is volatile and can be removed.

The state-of-the-art solution for small scale continuous evaporation is based on spray formation and evaporation.[S5] This design uses relatively high flow rate of carrier gas to generate the spray, crating large surface enhancing the evaporation process. The main drawbacks of this device are its requirement for high flow rate of gas compared to liquid flow rate: 10 $L_N \cdot min^{-1}$ of carrier gas for 1 $mL \cdot min^{-1}$ liquid flow. This design is also highly sensitive to the carrier gas flow rate, liquid flow rate and liquid viscosity, due to requirement of fine liquid spray formation. Hence, it was not well suited for our research needs.

Our solution is also based on carrier-gas assisted evaporation, where in the ideal situation the carrier gas and the liquid exhibit annular flow regime, creating a liquid film on the internal wall of the evaporator tubing with the gas occupying the central part of the tube. The liquid film should provide high surface enhancing the evaporation process. However, performed experiments showed that the annular flow regime is not reliable, although very good results were obtained with the prototype as it is, in a broad range of tested conditions. For the small-scale laboratory use, all the heated components of the apparatus were placed inside of the old GC oven, keeping them at desired, elevated temperature. Furthermore, our device is easier to assemble and tune than the apparatus proposed by Deadman *et al* – it does not require the use of glass column and assembly of three co-axial tubes with adequate reducing unions and tees. The diagram of our apparatus is presented below (Figure S29), followed by photograph of the prototype (Figure S30).

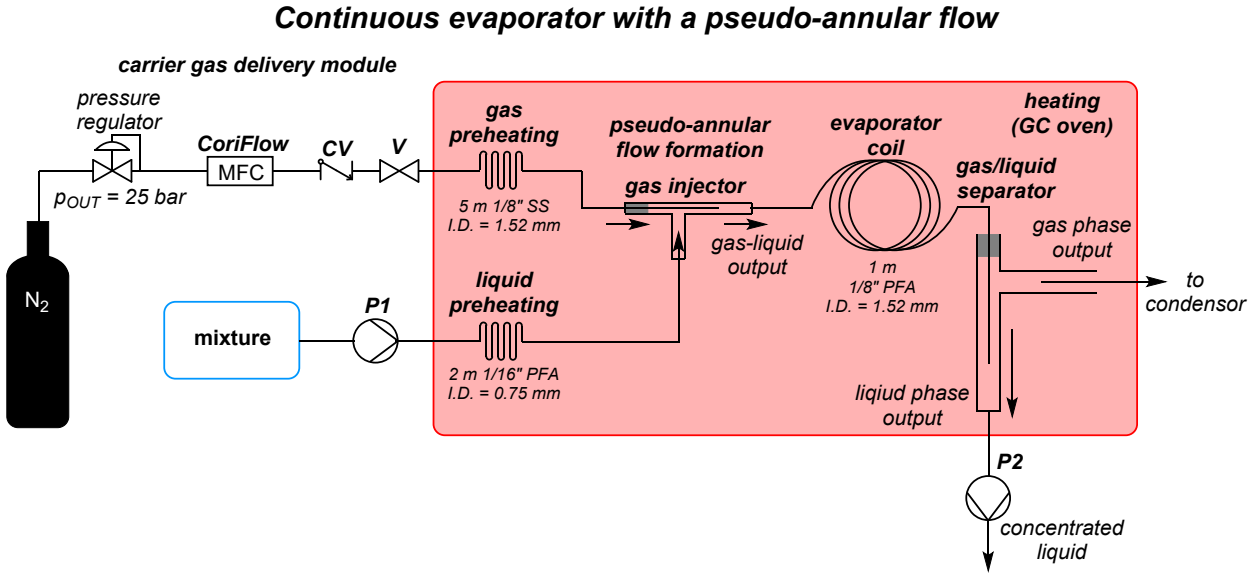

Figure S29. Diagram of the prototype continuous evaporator.

Figure S30. Photograph of the assembled prototype continuous evaporator apparatus.

The gas injector (Figure S31) was prototyped using fluidic parts (IDEX) and a syringe needle (23 G / 0.6 mm, 80 mm, B Braun) with the sharp tip cut off (perpendicular cut done with a mini-drill and a metal cutting disc). The needle is sealed in the PEEK tee connector (bore diameter 1.25 mm) by placing a 2 cm fragment of 1/16" PFA tubing (I.D. 0.03") on the needle and using flangeless ferrule to connect it with the tee. The position of the needle tip can be adjusted by loosening, moving and re-tightening the fluidic connector. The tip of the needle was placed inside of the evaporator coil tubing, which was connected at the opposite end of the PEEK tee. The gas supply is preheated by passing through stainless steel coil and then connected to the needle using IDEX Luer adapter.

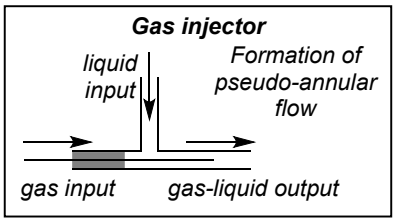

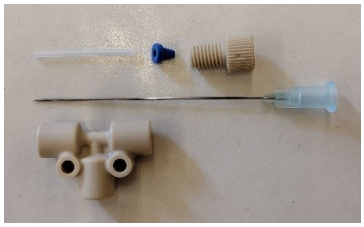

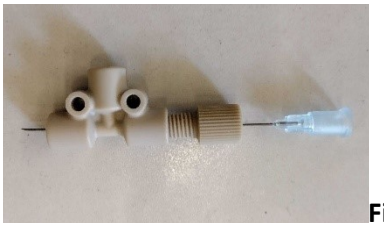

Figure S31. Diagram of the gas injector and photographs of the assembly process.

The gas-liquid separator (Figure S32) consists in 10 cm 1/2” PFA tube, a 1/2" tee (Swagelok), bored-through reducing union 1/8" to 1/2”, 1/8” SS tube introducing the gas liquid mixture, side 1/2” tube directing the gas phase to the condenser and 1/2” to 1/8” reducing union allowing to connect concentrated liquid output tubing. The liquid/gas mixture entry tube is placed slightly below the middle length of the 1/2” column.

All parts utilized for the assembly of this evaporator are listed below in Table S15.

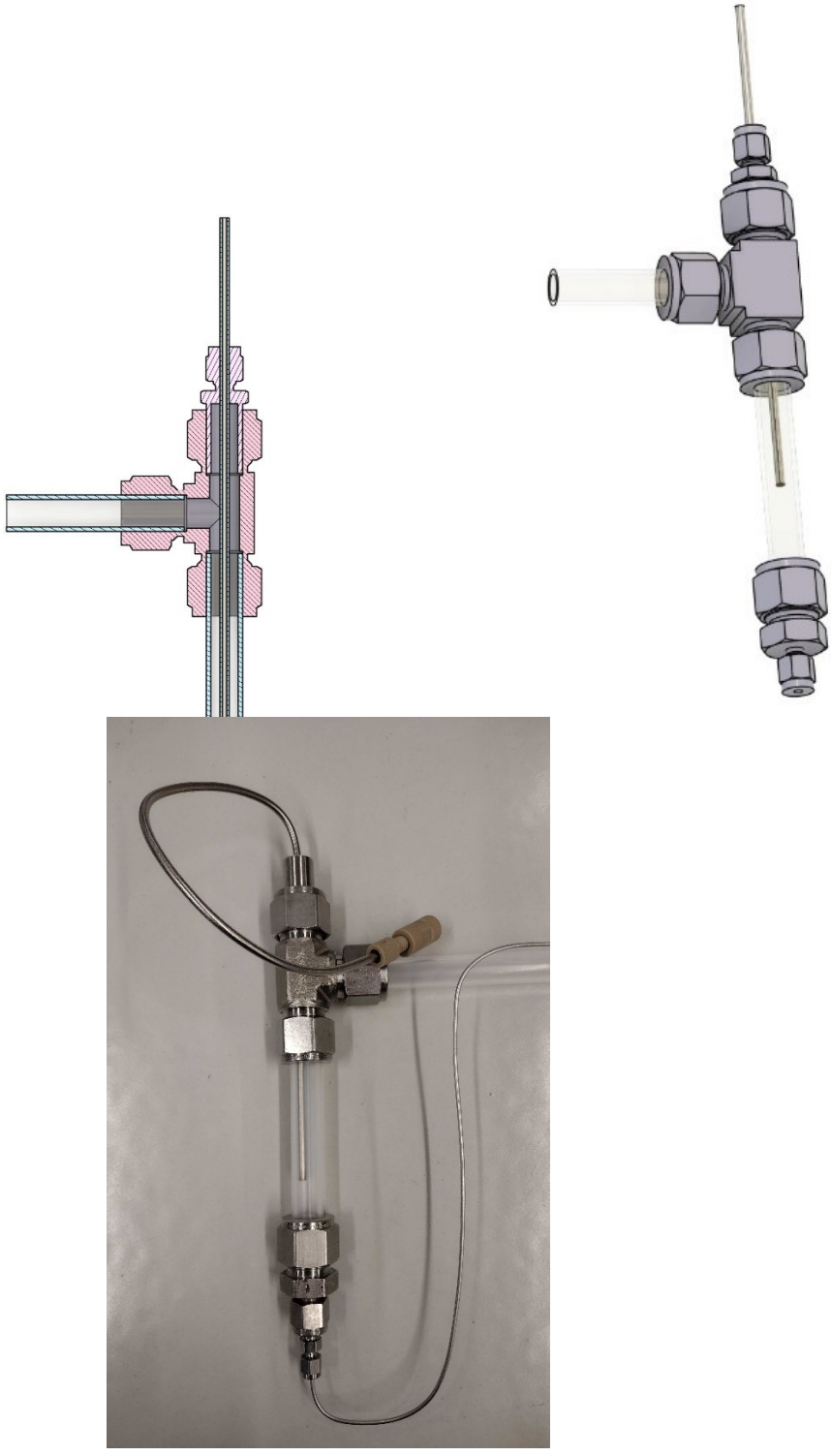

Figure S32. Drawings of the gas/liquid separator and photograph of assembled prototype.

Table S15. List of components used for the continuous flow evaporator apparatus.

Symbol	Name, description	Reference number / product name	Manufacturer
MFC	MiniCoriFlow M12, mass flow meter	M12-RGD-11-0-S	Bronkhorst
CV	Check Valve Inlet Non-Metallic	CV-3320	IDEX Corptoration
V	Shut Off Valve Assembly PEEK 0.020”	P-732A	IDEX Corporation
P1	Generic pump or direct feed from upstream system	-	-
P2	Syrris Asia or Vapourtec SF10 (peristaltic)	-	Syrris; Vapourtec Ltd
Gas injector	a. PEEK Low Pressure Tee Body 1/8" PEEK 0.050” thru hole b. 1/4-28 Female to Male Luer Fitting c. Flangeless Fitting, PEEK, 1/4-28 Flat-Bottom	a. P-713-01 b. XP-230 c. P-675	IDEX Corporation
Interconnecting tubing	PFA Tubing Natural 1/16" OD x 0.030" ID x 50ft	1514L	IDEX Corporation
Gas/liquid separator	a. Tee 1/2” b. Reducing union 1/8" to 1/2” (bored through) c. Reducing union 1/2" to 1/8” d. 1/2" PFA tubing e. 1/8” SS316 tubing	a. SS-810-3 b. SS-400-R-8-BT c. SS-810-6-2 d. PFA-T8-062-100 e. JR-TSS260-M10	a.-d. Swagelok e. VICI JOUR

To perform initial tests, mixtures of high and low boiling point solvents were used: NMP with MeOH and glycerol with MeOH. In both cases, the volumetric ratio of components was 1:1. With liquid flow rate of 1 $mL \cdot min^{-1}$, carrier gas (N_2) flow rate of 250 $mL_N \cdot min^{-1}$ and temperature set to 80 °C, majority (>70%) of the volatile component can be removed. In the case of tests with glycerol, a Vapourtec SF10 peristaltic pump was used for the liquid withdrawal, with its suction line electrically heated using a resistive wire, allowing to reduce the liquid viscosity.

The gas flow rate and temperature can be adjusted according to requirements of process like thermal stability of compounds and the required fraction of the removed volatile component.

Table S16. Results of initial tests of the continuous flow evaporator prototype.

Entry	Temp. (°C)	Gas flow ($mL_N \cdot min^{-1}$)	Mixture	Removed MeOH* (%)
1	80	15	NMP/MeOH	30

2	80	31	NMP/MeOH	38
3	80	62	NMP/MeOH	50
4	80	125	NMP/MeOH	59
5	80	250	NMP/MeOH	72
6	60	250	NMP/MeOH	47
7	100	250	NMP/MeOH	83
8	100	500	NMP/MeOH	88
9	100	1000	NMP/MeOH	92
10	60	250	Glycerol/MeOH	54
11	80	250	Glycerol/MeOH	80
12	100	250	Glycerol/MeOH	90
13	100	500	Glycerol/MeOH	93

*The "Removed MeOH (%)" value was calculated based on the relative GC-FID areas, by comparing their value for the input mixture and for the concentrated liquid. Following formula was used:

$$Removed_{MeOH} = \frac{Reference_{MeOH} - Sample_{MeOH}}{Ref_{MeOH}} \cdot 100$$

4.5.3.2 Microfluidic results with the incorporation of the continuous evaporator

The crude from the first reactor R_1 contained mainly a mixture of product **3**, intermediate ***int*-3** and *in-situ* generated MeOH. The idea was to use the continuous-flow evaporator described in section *4.1.6.1* to remove MeOH from the medium (Figure S33) and then continue the reaction in a second reactor R_2 (Figure S34).

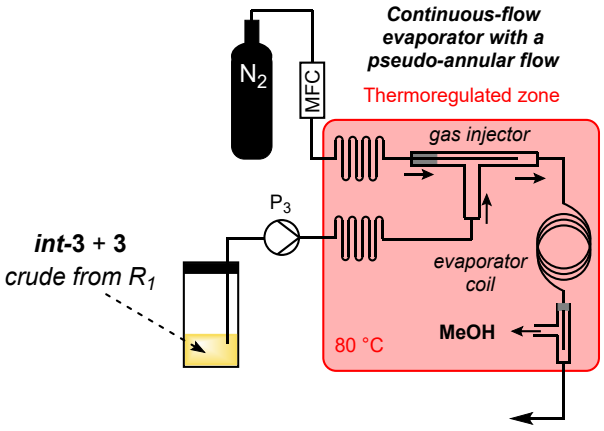

Figure S33. Simplified scheme of the microfluidic setup for MeOH distillation of the crude from R_1.

The evaporator's oven temperature was set to 80 °C (and not above) to avoid potential distillation of the product. The results are summarized in Table S17.

Table S17. Continuous flow evaporator set parameters.

Entry	QN_2 ($mL_N \cdot min^{-1}$)	Q_{pump3} ($mL \cdot min^{-1}$)	T_{oven} (°C)
a	250	0.5	80

Only a small amount of MeOH left after the process. It is noteworthy, that no significant conversion of **4** into product **3** was observed while removing MeOH at 80 °C (Tables S17 and S18, entries a,b).

Table S18. Results of the continuous flow evaporator

Entry	**Area%** (GC-FID)	**MeOH**	**3**
a	Crude from R_1	42	78
b	Concentrated crude after continuous distillation	7	81
c	Condensed vapor	100	0

The MeOH contained in the gas phase was condensed, recovered and analyzed by GC. Only MeOH was present in the condensed phase, meaning no product was lost during the evaporation process (Table S18, entry c).

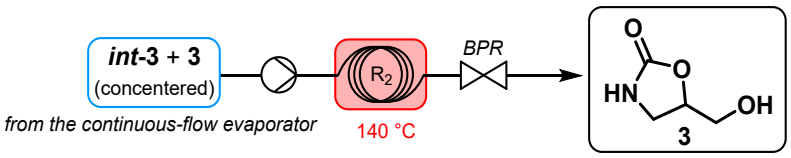

Figure S34. Simplified scheme of the setup for the second cyclization reaction optimization.

Surprisingly, the second cyclisation appeared to be much slower than the first one. Indeed, it took 2 min to convert 6% of ***int*-3** into product **3** (Table S19) while most of the solvent was removed before.

Table S19. Results of the second cyclization reaction optimization.

Entry	**Residence Time** (min)	**3 (%)**	***int*-3 (%)**
a	1	86.8	6.0
b	2	89.6	4.1
c	3	98.8	1.2

4.6 Pilot-scale mesofluidic experiments

4.6.1 Preliminary scalability trials

A transfer to pilot-scale was attempted, following the preliminary trials in a lab-scale mesofluidic reactor. Due to initially biphasic nature of the reaction medium, efficient mixing is critical for converting **2a** and achieving good selectivity toward **3**. The required intense mixing can be achieved in reactors such as the Corning® Advanced-Flow™. An initial trial was performed in a G1 Low-Flow skid reactor equipped with 2.5 mL glass fluidic modules. Subsequently, a scale up to a standard pilot-scale Corning® AFR™ G1 unit (Figure S35) was performed. Representative results are summarized in Table S20. The results indicated that the equilibrium was already reached after 1 min of residence time.

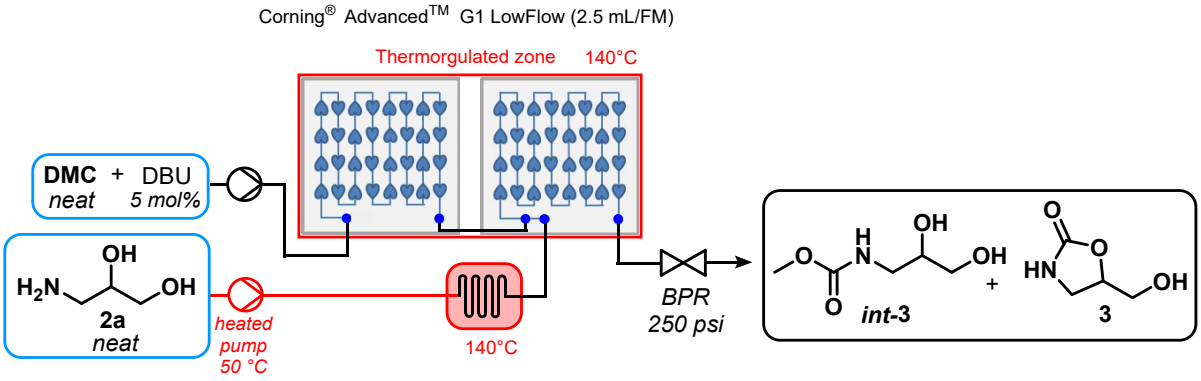

Figure S35. Scheme of the G1 Low Flow skid setup for residence time optimization.

Table S20. Result of the residence time optimization with G1 LowFlow reactor

Entry	Res. time (min)	Conv. **2a** (%)	Select. **3** (%)	Select. ***int*-3** (%)
a	1.00	98	73	19
b	1.25	99	73	20

4.6.2 Scalability trials: transfer to pilot-scale

4.6.2.1 Pilot-scale mesofluidic setup

As in the microfluidic setup, one dosing line delivered **DMC** with catalyst (feed 1) and the other delivered neat amino alcohol **2a** (feed 2). Neat **2a** was charged into a pressurized reservoir and delivered by a Teledyne® ISCO dual-piston pump. To facilitate the pumping, the transfer line leading to thermostated zone was preheated, allowing to decrease the viscosity of feed 2. Feed 1 was delivered by a KNAUER BlueShadow® 80P HPLC pump coupled to a Bronkhorst® CoriFlow™ mass-flow meter. Both lines were equipped with purge valves and flushing lines. The feeds entered setup composed in 5 Corning® Advanced-Flow™ G1 glass fluidic modules operated at 140 °C. The 2 upstream modules were used to preheat both feeds, while the 3 downstream modules were used for reaction (24 mL total internal volume). The effluent was cooled before passing through the in-line IR flow cell. An Equilibar® BPR maintained pressure of 9 bar. Thermocouples and pressure sensors were installed at key locations. After depressurization, a valve directed the stream either to crude collection vessel or to a CSTR. The CSTR was a 500 mL three-neck round-bottom flask open to atmosphere and equipped with an overhead mechanical stirrer, immersed in an oil bath at 140 °C. The CSTR was used in lieu of the microfluidic continuous-flow pseudo annular-flow evaporator. Three parallel channels of Syrris Asia syringe pumps continuously withdrew effluent from the CSTR, with a cooling loop placed between

the CSTR and the pumps' inlets. The flowchart of the mesofluidic setup is depicted in Figure S36. Parts and auxiliaries are listed in Table S21. Photographs of the setup are provided in Figure S37.

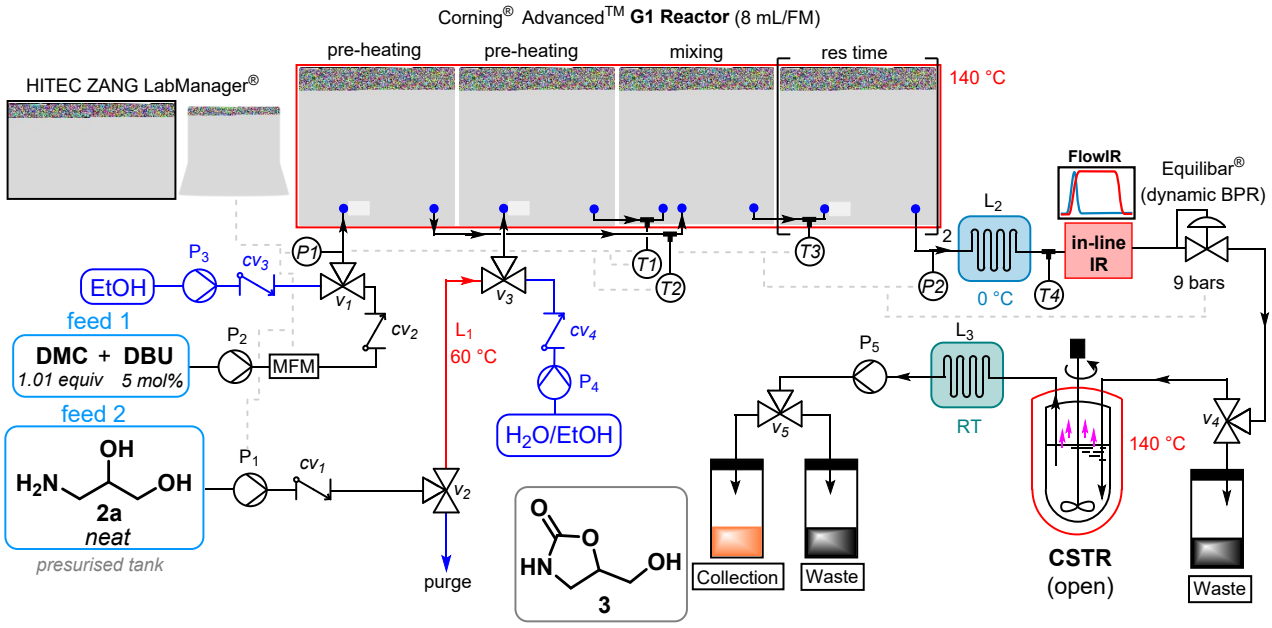

Figure S36. Detailed flowchart of the mesofluidic setup) for the pilot-scale carbamatation of **2a** toward oxazolidinone **3**, featuring a downstream CSTR.

Table S21. List of parts of the continuous mesofluidic system for the synthesis of **3**

Symbol	Name, description	Reference number / product name	Manufacturer
Pumps			
P_1	Dual piston (500 mL/each) ISCO Pump, electric valves	SyriXus E500	Teledyne
P_2	HPLC-type pump (plunger) 500 mL Titanium head	BlueShadow® 80P	KNAUER GmbH
P_3	HPLC-type pump (SS head)	ReaXus M1 Class	Teledyne
P_4	HPLC-type pump (plunger) 10 mL stainless steel head	Azura P4. 1S	KNAUER GmbH
P_5	3x continuous syringe pump; equipped with Asia Red Syringes (2.5 mL, 5mL)	Asia Syringe Pump	Syrris Ltd.
Back pressure regulators, check valves and valves			
BPR_1	Equilibar® Back Pressure Regulator coupled with a Bronkhorst El-Press Pressure Controller	BPR: H3P1SNN8-NSBP1500T100S4KKB-G Pressure Controller: M23211621B; PCS-DV-B-100-PG	Pressure Control Solution (BPR) Bronkhorst (Pressure Controller)
cv_1, cv_2, cv_3	Poppet Check Valve 316SS (1/8" ID)	SS-4C-1	Swagelok
cv_4	Check-valve, spring loaded	CV-300NF	IDEX corporation

v_1, v_2, v_3	3-ways ball valve 316SS, L flow path, (1/8” ID)	SS-41GXHLS2	Swagelok
v_4, v_5	4-way valve PEEK Bulkhead “L” flow	V-101-L	IDEX corporation
Tubing, pre-heating loop, reactor			
L_1	Pre-heating line, 1/8” 316SS tubing wrapped with resistive wire connected with an electric power supply	U-803 (SS tubing)	IDEX corporation In-house made
FM	Glass plates (8 mL/flow module)	G1 reactor	Corning® Advanced-Flow™
CSTR	500 mL three-neck glass round bottom flask equipped with a mechanical overhead stirrer	-	-
	316SS tubing		IDEX corporation
	1/4" and 1/8” PFA tubing		
Sensors			
P1	Flush diaphragm pressure transmitter (0-100 bars) 316TI/ 316L	Type S-11	WIKA
P2	Chemically resistant pressure transducer (0-50 bars) connected via a PEEK Tee [S1]	Tee: P-716	Developed internally (pressure transducer) IDEX Corporation (tee)
T1, T2, T3	K-type thermocouple o.d. 0.5 mm, with 310SS sheath installed in a PEEK Tee	Thermocouple: 444-1275 Tee: P-716	RS Group plc(thermocouple) IDEX (tee)
T4	K-type thermocouple with 310SS sheath 1.5 mm diameter installed in a 316SS Tee (1/4” ID) using 1/16” – 1/4" reducing adapter	Thermocouple: RS Pro 228-7445 Tee: SS-400-3 Reducer: SS-100-R-4BT	RS Group plc (thermocouple) Swagelok (tee, reducing adapter)
MFM	Coriolis Mass Flow Meter (mini CORI-FLOW)	M14-RGD-11-0-S	Bronkhorst®
IR-probe	In-line IR system equipped with a Micro Flow Cell (Diamond probe)	ReactIR 702L	METTLER TOLEDO
Thermostats			
Thermostat (G1 reactor)	Chiller	Integral IN 2560 PW	LAUDA
Thermo fluid	Silicon oil	HL-60	-
Thermostat (cooling L2)	Ice bath	-	-
Thermostat (CSTR)	Heating plate with an oil bath	-	HEIDOLPH

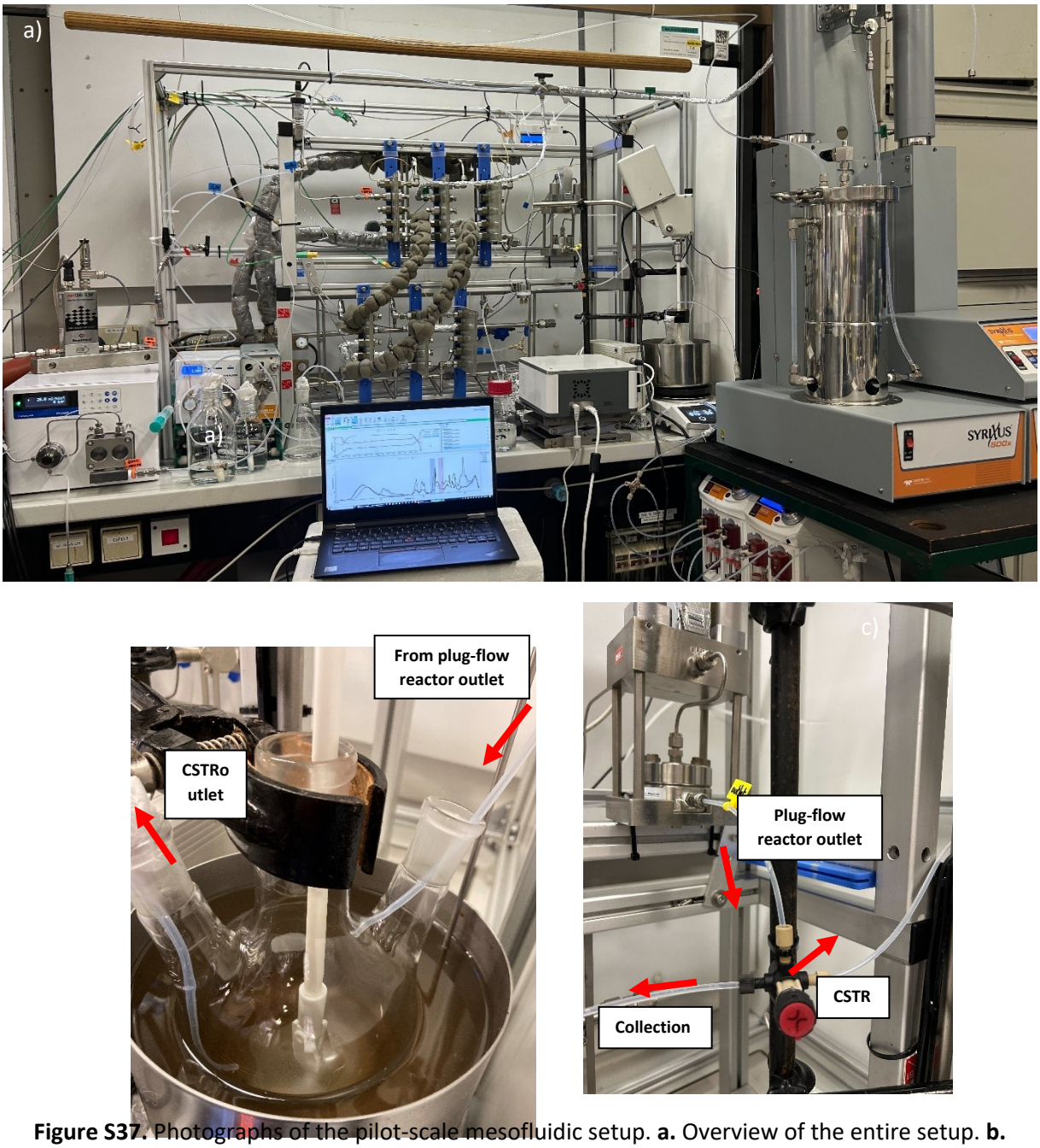

Figure S37. Photographs of the pilot-scale mesofluidic setup. **a.** Overview of the entire setup. **b.** Downstream CSTR and **c.** Sampling valve *v4.*

4.6.2.2 Pilot-scale mesofluidic experiments

The setup as described in Section 4.1.8.2. was used. The collection, quench and analysis procedure were identical to Section 4.1.5. Preliminary trials excluded the downstream CSTR (Figure S38 and Table S22). Additional trials featured the addition of a downstream CSTR to shift the equilibrium connecting intermediate ***int*-3** and product **3** (Figure S39 and Table S23).

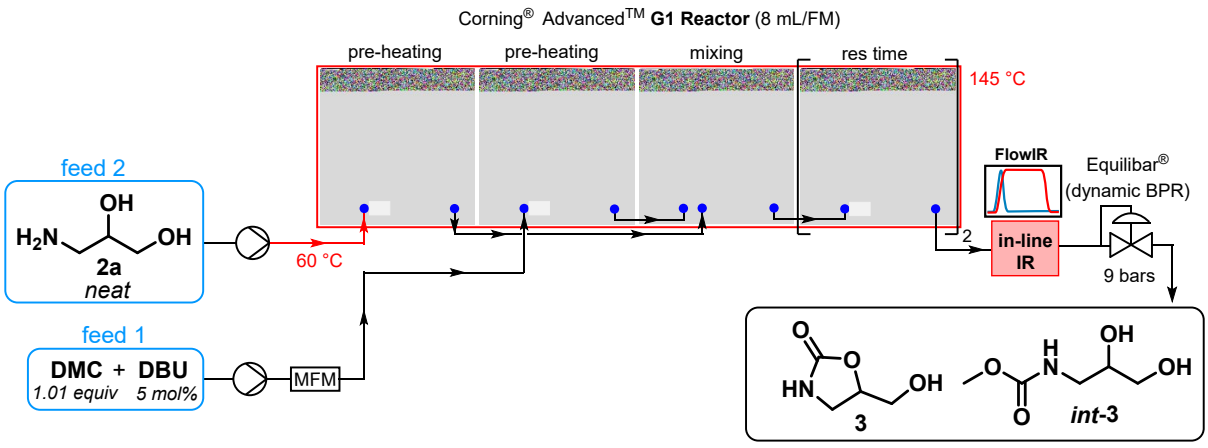

Figure S38. Simplified flowchart of the mesofluidic setup for the carbamatation of **2a** toward oxazolidinone **3** (see Table 22).

Table S22. Result of the residence time optimization with G1 reactor

Entry	Q_{feed1} (mL·min^{-1})	Q_{feed2} (mL·min^{-1})	Res. time (min)	Conv. **2a** (%)	Select. **3** (%)	Select. ***int*-3** (%)
a	11.30	9.50	1.25	99	69	24
b	14.12	11.88	1.00	98	66	25
c	18.83	15.84	0.75	98	66	26

The higher residence times implied lower flow rates, which resulted in total flow rates below the Corning G1 reactor minimal specifications (Q_{tot} min > 30 mL·min^{-1}). Operating the reactor below that threshold does not guarantee efficient mass transfer.

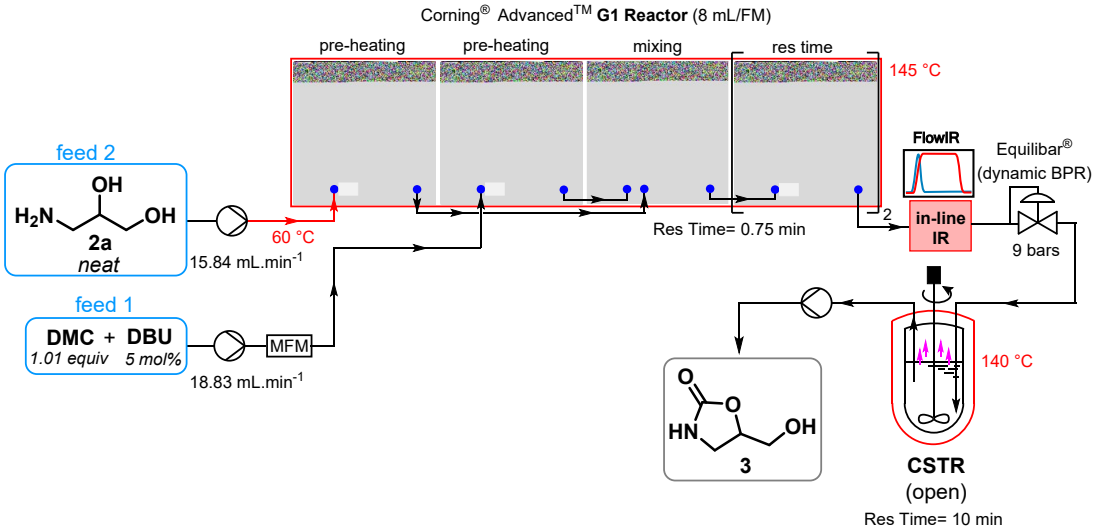

Figure S39. Simplified flowchart of the mesofluidic setup for the carbamatation of **2a** toward oxazolidinone **3**, featuring a downstream CSTR (see Table 23).

The density of the feed 1 measured with the Mass Flow Meter was: d_{feed1}= 1.067 g·cm^{-3} (24.2°C).

Table S23. Result of the residence time optimization with G1 rector + CSTR

Entry	Collection	Res. time	Conv.	Select.	Select.

	location	(min)	**2a** (%)	**3** (%)	***int*-3** (%)
a	After plug flow reactor	0.75	>99	61	34
b	After open CSTR	~ 10*	>99	95	<1

***Residence time (CSTR).** The reported residence time is approximate because continuous MeOH distillation changes the reactor volume. Accordingly, the flow rate of pump 5 was calculated as: $Q_{\text{pump5}} = Q_{\text{tot}} - Q_{\text{MeOH,evap}}$ where Q_{tot} is the total flow from the plug-flow reactor and $Q_{\text{MeOH,evap}}$ is the volumetric rate of MeOH evaporated over the same interval.

Phase behavior and mixing. After combining the two feeds, a colorless biphasic (L/L) medium was observed; it became homogeneous rapidly (after ~1-2 rows of static mixers in the first module).

CSTR performance. With a single CSTR, the residence-time distribution is expected to be broad. However, in this process a partial MeOH removal is sufficient to convert the residual ~30% of intermediate **4**, so the chosen design was suitable.

4.6.2.3 In-line IR reaction monitoring

The effluent of the plug-flow reactor (Corning® Advanced™ G1 Glass Reactor) was continuously analyzed by in-line IR. A characteristic band of the product **3** (1735 cm^{-1}) and of the intermediate **4** (1540 cm^{-1}) were monitored (Figure S40). After a stabilization phase, a steady state was reached. To highlight the stability of the system, a 23 min run was carried out.

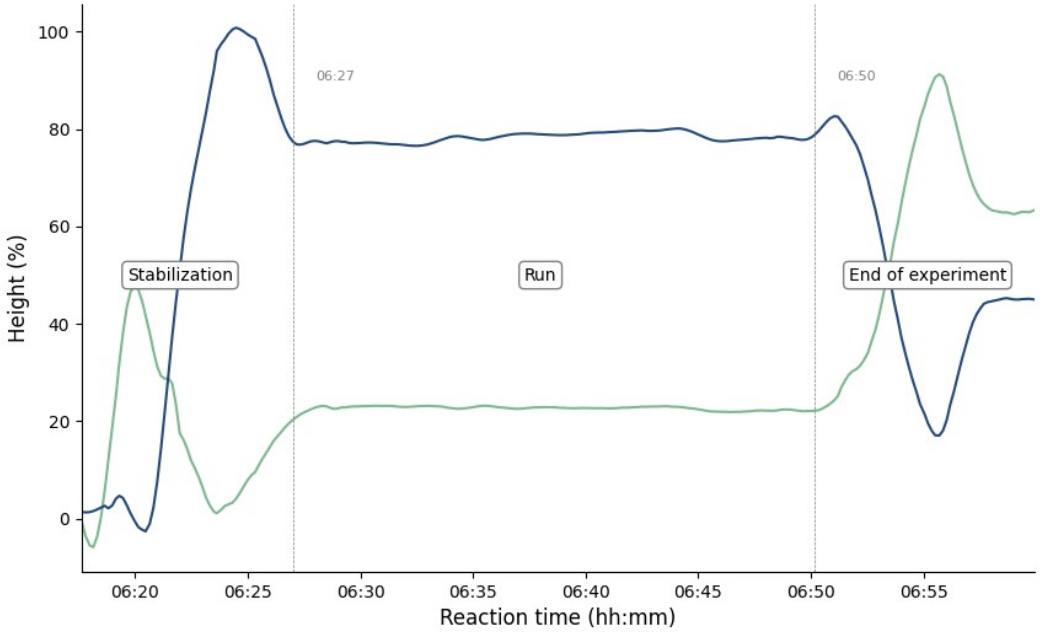

Figure S40. IR trends of the bands related the oxazolidinone product **3** (1735 cm^{-1}) and to the intermediate **4** (1540 cm^{-1}) over time during the mesofluidic experiment (Table 21. line a.)

4.6.2.4 Typical GC chromatograms of reactor effluents

Typical GC chromatograms of reactor effluents are presented in Figures S41 (before the CSTR) and S42 (after the CSTR).

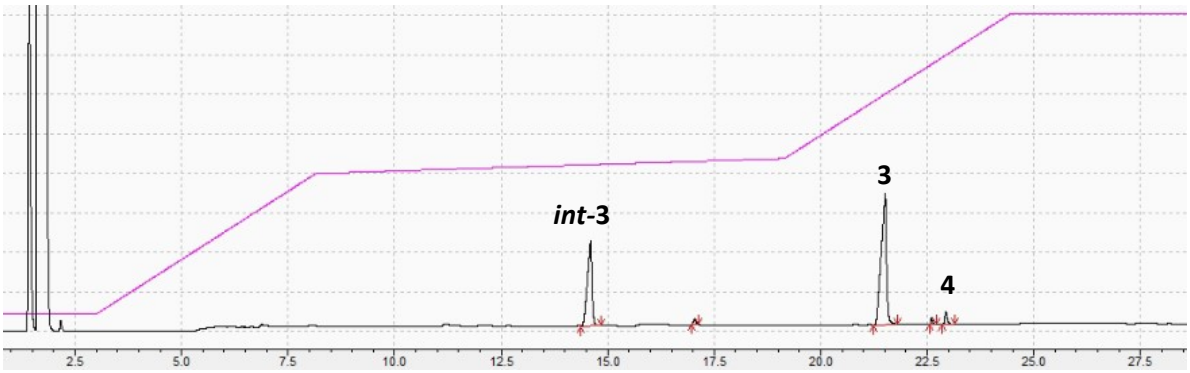

Figure S41. GC-FID chromatogram of the crude from the outlet of plug-flow reactor (Table S23, entry 1)

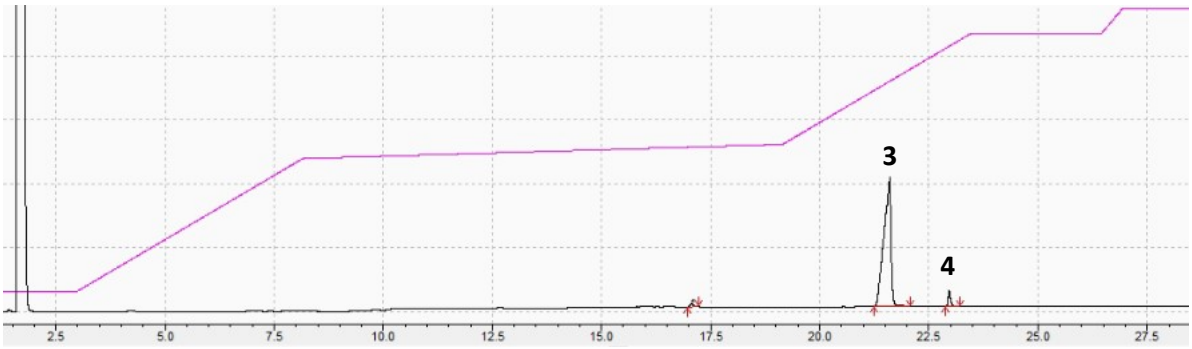

Figure S42. GC-FID chromatogram of the crude from the outlet of CSTR (table S21. line b)

4.6.2.5 Process metrics

Process metrics were calculated according to ref.[S2]

$$E = \frac{\sum waste}{\sum product} \rightarrow E = \frac{m(MeOH - byproduct) + m(sideproduct) + m(catalyst)}{m(product\ 3)}$$

Output: 32 kg·day^{-1}

STY (Space Time Yield): 101 kg·day^{-1}·L^{-1}

5. Characterization of compounds

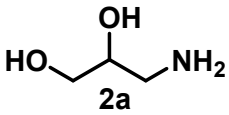

2a

$C_3H_9NO_2$

MW = 91.11

3-amino-2-propandiol (2a). ^{1}H NMR (DMSO-d6, 400 MHz): δ = 3.36-3.32 (m, 1H), 3.30-3.26 (m, 2H), 2.60-2.56 (dd, *J* = 12, 4 Hz, 1H), 2.45-2.40 (dd, *J* = 12, 4 Hz, 1H) ppm. ^{13}C NMR (DMSO-d6, 101 MHz) δ = 72.9, 64.0, 45.1 ppm. The NMR data matched the commercial reference (in D_2O).[S6]

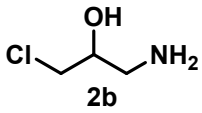

2b

C_3H_8ClNO

MW = 109.55

1-amino-3-chloropropan-2-ol (2b). Compound **2b** was too unstable to be isolated. Crude samples were analyzed by GC-FID and GC-MS. A reference sample was prepared by the neutralization of **2b·HCl** (commercial or prepared through another route, see section S4.4). Both samples (crude mixture of reference sample) had identical retention time and MS fragmentation patterns.

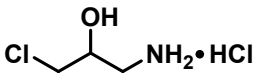

2b•HCl

C_3H_8ClNO

MW = 109,55

1-amino-3-chloropropan-2-ol hydrochloride (2b·HCl). ^{1}H NMR (D_2O, 400 MHz): δ = 4.22-4.16 (dtd, 1H), 3.76-3.66 (qd, 2H), 3.31-3.27 (dd, *J* = 16, 4 Hz, 1H), 3.13-3.07 (dd, *J* = 12, 8 Hz, 1H) ppm. ^{13}C NMR (D_2O, 101 MHz) δ = 67.2, 46.1, 42.1 ppm. The NMR data matched those reported in the literature (in D_2O).[S7]

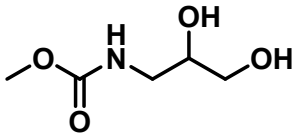

***int*-3**

$C_5H_{11}NO_4$

MW = 149.15

Methyl *N*-(2,3-dihydroxypropyl) carbamate (*int*-3). ^{1}H NMR (DMSO-d_3, 400 MHz): δ = 7.96-7.93 (t, *J* = 4 Hz, 1H), 4.70-4.69 (d, *J* = 4 Hz, 1H), 5.54-4.51 (t, *J* = 4 Hz, 1H), 3.50 (s, 3H), 3.48-3.42 (m, 1H), 3.29-3.26 (t, *J* = 4 Hz, 2H), 3.10-3.04 (m, 1H), 2.94-2.86 (m, 1H) ppm. ^{13}C NMR (DMSO-d_6, 101 MHz) δ = 157.2, 70.8, 64.0, 51.6, 43.1 ppm. LC-MS (ESI+): m/z calcd. for $C_5H_{11}NO_4$: 149.15 [M+H]+; found 150. LC-MS (ESI+): m/z. for $C_6H_9NO_5$: found 150 [M+H]+; (ESI-): 194 $[M+FA-H]^-$ (FA = formic acid).

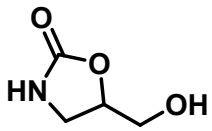

3

$C_4H_7NO_3$

MW = 117.10

5-(Hydroxymethyl)oxazolidin-2-one (3). ^{1}H NMR (CD_3OD, 400 MHz): δ = 4.68-4.62 (m, 1H), 3.72-3.68 (dd, *J* = 12, 4 Hz, 1H), 3.61-3.56 (m, 2H), 3.41-3.37 (dd, *J* = 8, 8 Hz, 1H) ppm. ^{13}C NMR (CD_3OD, 101 MHz) δ = 162.4, 78.6, 63.5, 42.9 ppm. The NMR data matched those reported in the literature (in DMSO-d6). [S8] LC-MS (ESI+): m/z. for $C_6H_9NO_5$: found 118 $[M+H]^+$.

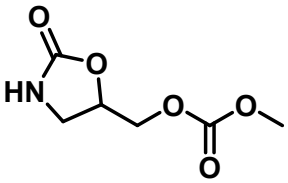

4 (impurity A)

$C_6H_9NO_5$

MW = 175.14

Methyl ((2-oxooxazolidin-5-yl)methyl) carbonate (4). ^{1}H NMR (solvent, 400 MHz): δ = 7.52-7.49 (t, 1H), 4.84-4.78 (m, 1H), 4.54-4.50 (t, J= 8Hz, 1H) 4.23-4.20 (dd, J_1= 4Hz, J_2= 8Hz, 1H), 3.55 (s, 3H), 3.35-3.31 (m, 2H) ppm. ^{13}C NMR (DMSO-d6, 101 MHz) δ =157.3, 154.8, 75.5, 66.9, 51.7, 42.3 ppm. The NMR data matched those reported in the literature.[S9] LC-MS

(ESI+): m/z. for $C_6H_9NO_5$: 176 [M+H]+; (ESI-): found 220 $[M+FA-H]^-$ (FA = formic acid).

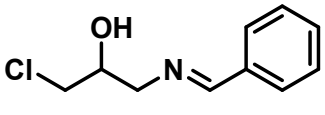

7
$C_{10}H_{12}ClNO$
MW = 197.66

1-(benzylidenamino)-3-chloro-propan-2-ol (7). ^1H NMR ($CDCl_3$, 400 MHz): δ = 8.36 (s, 1H), 7.75-7.71 (m, 2H), 7.46-7.40 (m, 3H), 4.17-4.11 (m, 1H), 3.86-3.75 (m, 2H), 3.68-3.63 (m, 2H) ppm. ^{13}C NMR ($CDCl_3$, 101 MHz) δ = 163.9, 135.8, 131.3, 128.8, 128.4, 71.1, 63.2, 47.2 ppm. The NMR data matched those reported in the literature.[S10]

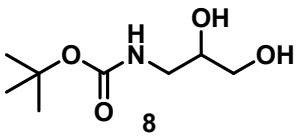

8
$C_8H_{17}NO_4$
MW = 191,23

tert-Butyl-N-(2,3-dihydroxypropyl)carbamate (8). ^1H NMR (in DMSO-d6, 400 MHz): δ = 6.59-6.56 (t, J = 4 Hz, 1H), 4.62-4.60 (d, J = 8 Hz, 1H), 4.47-4.44 (t, J = 4 Hz, 1H), 3.47-3.40 (m, 1H), 3.28-3.25 (m, 2H), 3.06-3.00 (m, 1H), 2.87-2.81 (m, 1H), 1.37 (s, 9H) ppm. ^{13}C NMR (in DMSO-D_6, 101 MHz) δ = 155.8, 77.6, 70.7, 63.8, 48.5, 28.3 ppm. The NMR data matched those reported in the literature (in CDCl3).[S11] LC-MS (ESI-): m/z. for $C_6H_9NO_5$: found 236 $[M+FA-H]^-$ (FA = formic acid; LC-MS analysis performed under alkaline method using ammonia and formic acid, pH ~ 9.5).

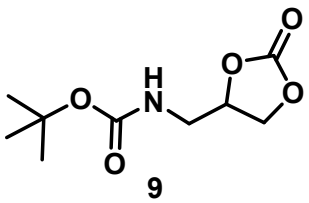

9
$C_9H_{15}NO_5$
MW = 217.22

tert-butyl N-[(2-oxo-1,3-dioxolan-4-yl)methyl]carbamate (9). ^1H NMR (in DMSO-d_6, 400 MHz): δ = 7.22-7.19 (t, J= 4Hz, 1H), 4.82-4.76 (m, 1H), 4.53-4.49 (t, J= 8Hz, 1H), 4.23-4.20 (dd, 2H), 1.38 (s, 9H) ppm. ^{13}C NMR (in DMSO-D_6, 101 MHz) δ = 156.0, 154.7, 78.2, 75.5, 66.9, 41.8, 28.1 ppm. The NMR data matched those reported in the literature (in $CDCl_3$).[S12] LC-MS (ESI+): m/z. for $C_6H_9NO_5$: 235 $[M+NH_4]$+; (ESI-): found 262 $[M+FA-H]^-$ (FA = formic acid; LC-MS analysis performed under alkaline method using ammonia and formic acid, pH ~ 9.5).

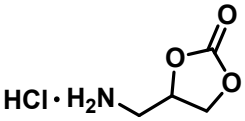

iso-3·HCl
C4H8ClNO3
MW = 117.10

4-(aminomethyl)-1,3-dioxolan-2-one hydrochloride (*iso*-3·HCl). ^1H NMR (in D_2O, 400 MHz): δ = 5.27-5.20 (m, 1H), 4.83-4.79 (m, 1H), 4.42-4.38 (dd, *J* = 12, 8 Hz, 1H), 3.48 (s, 1H), 3.47 (d, 1H) ppm. ^{13}C NMR (in D_2O, 101 MHz) δ = 156.4, 74.0, 67.6, 41.3 ppm. LC-MS (ESI+): m/z. for $C_4H_8ClNO_3$: 118.10 [M+H]+; found 118 $[M+H]^+$.

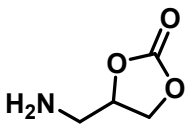

***iso*-3**
$C_4H_7NO_3$
MW = 117.10

4-(aminomethyl)-1,3-dioxolan-2-one (*iso*-3). ^1H NMR (in DMSO-d_6, 400 MHz): δ = 3.48-3.42 (m, 1H), 3.28 (d, 2H), 3.12-3.04 (m, 1H), 3.94-385 (m, 1H) ppm. LC-MS (ESI+): m/z. for $C_4H_7NO_3$: found 118 $[M+H]^+$.

1,3-

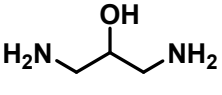

2c
$C_3H_{10}N_2O$
MW = 90.13

Compound **2c** is **diaminopropan-2-ol (2c).** commercially available. The NMR data matched those of a reference

commercial sample.

6. Copies of NMR spectra

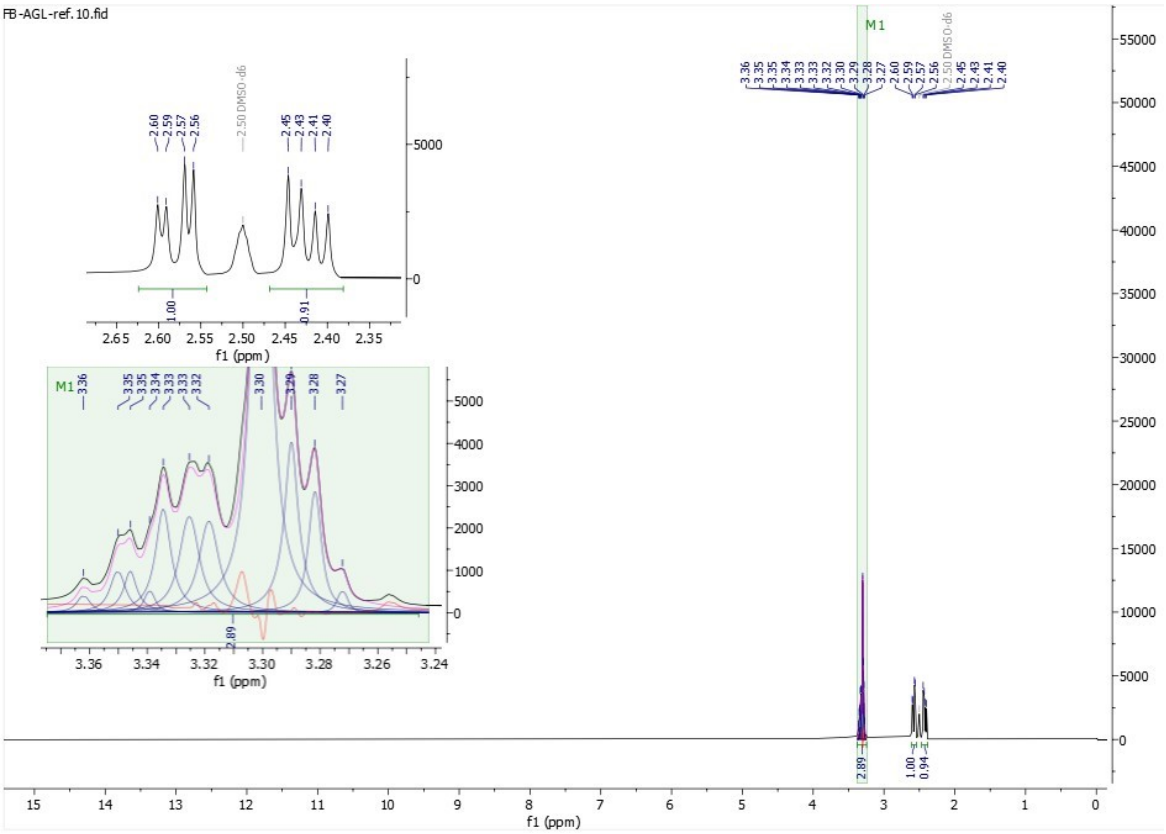

Figure S43. ^{1}H NMR spectrum (400 MHz, DMSO-d_6) of **2a**.

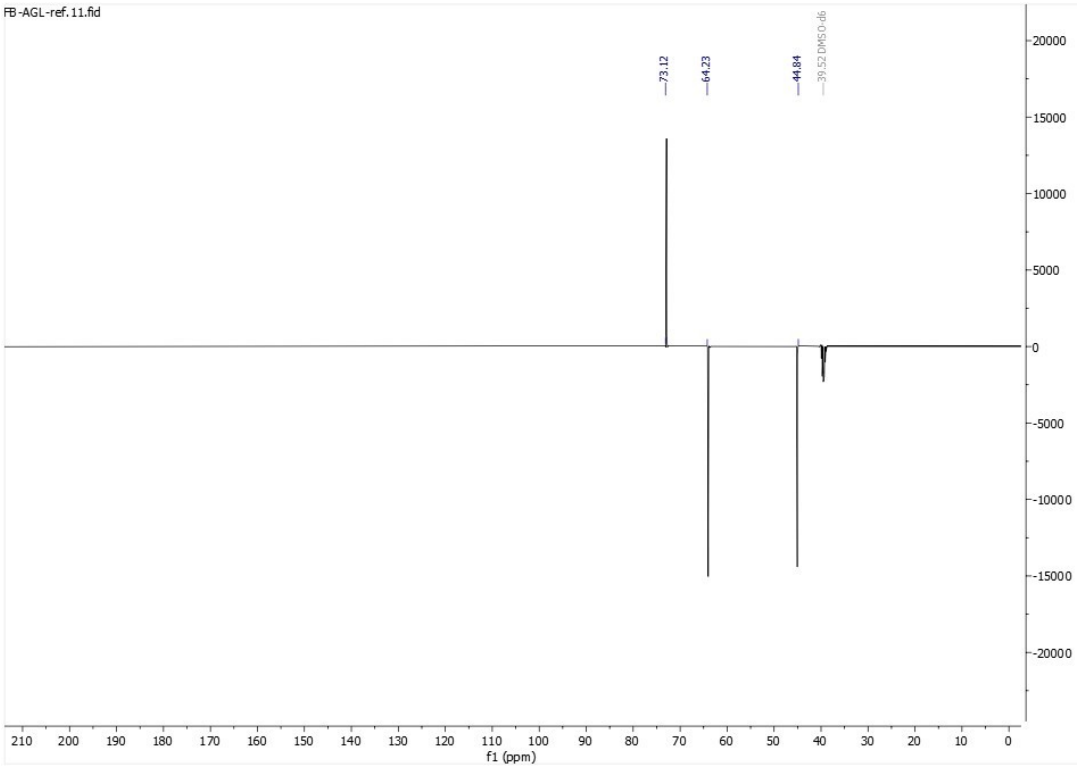

Figure S44. ^{13}C NMR spectrum (101 MHz, DMSO-d_6) of **2a**.

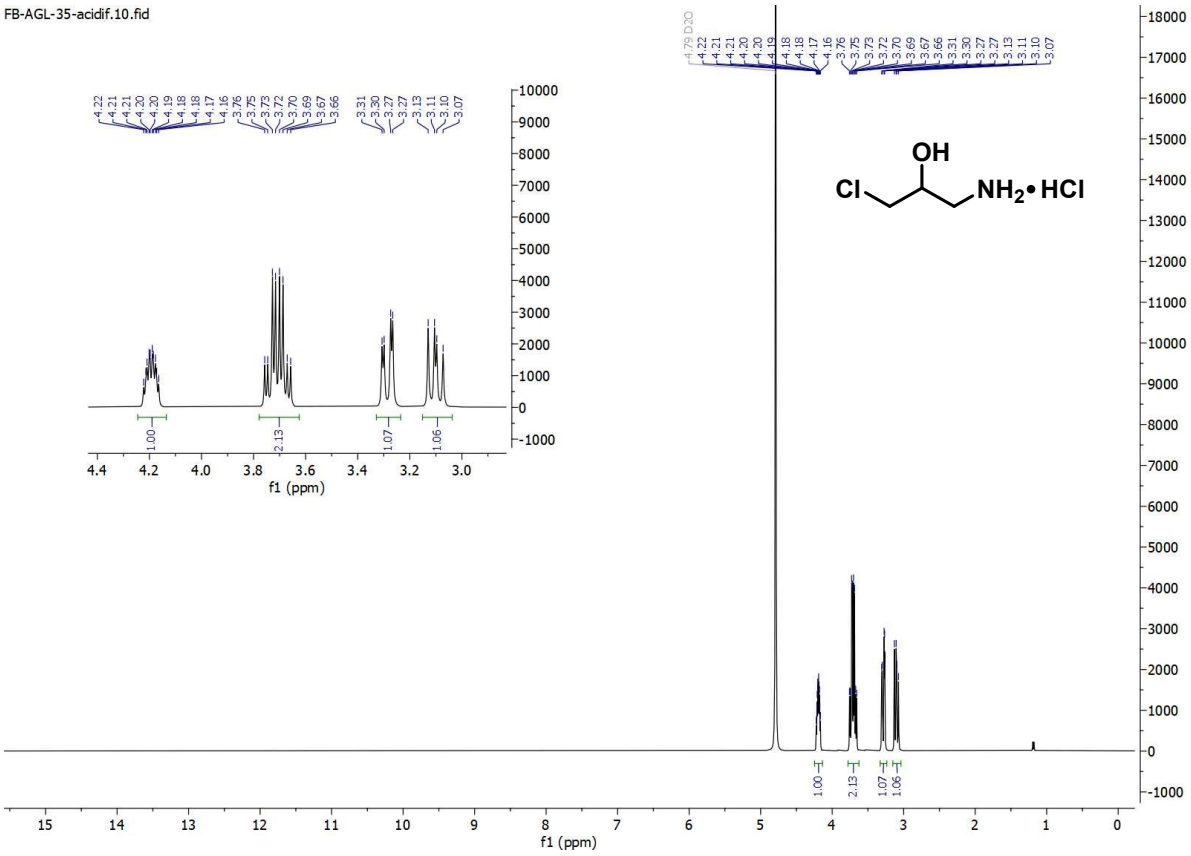

Figure S45. ^{1}H NMR spectrum (400 MHz, D_2O) of **2b·HCl**.

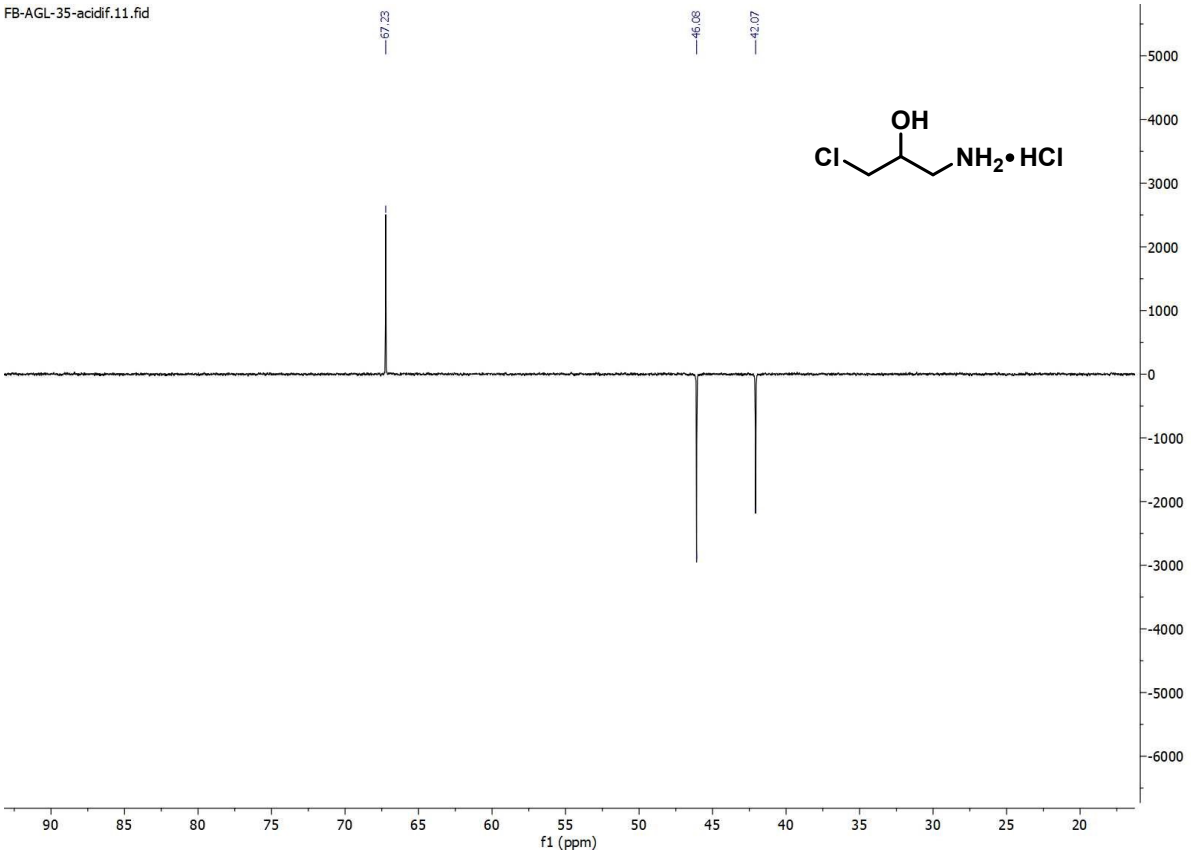

Figure S46. ^{13}C NMR spectrum (101 MHz, D_2O) of **2b·HCl** .

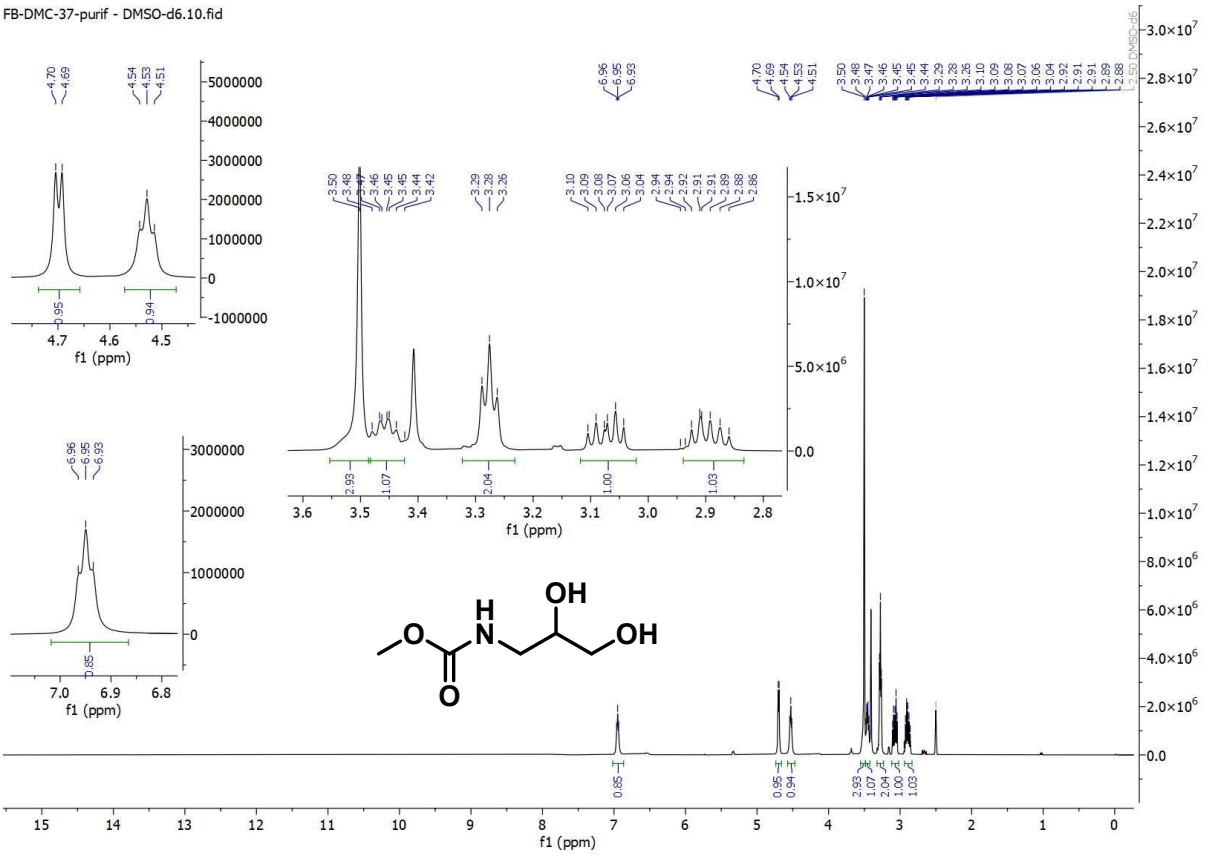

Figure S47. ^{1}H NMR spectrum (400 MHz, DMSO-D_6) of ***int*-3**.

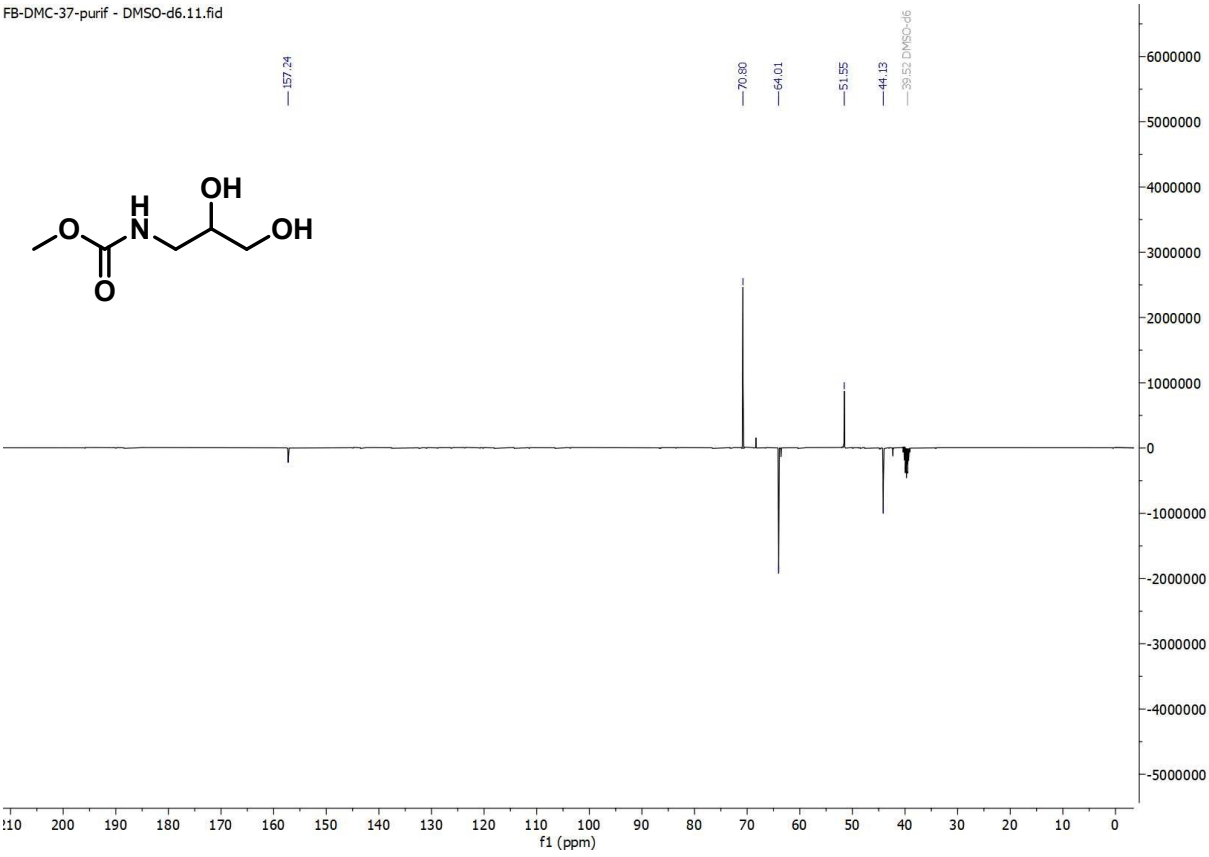

Figure S48. ^{13}C NMR spectrum (101 MHz, DMSO-D_6) of ***int*-3**.

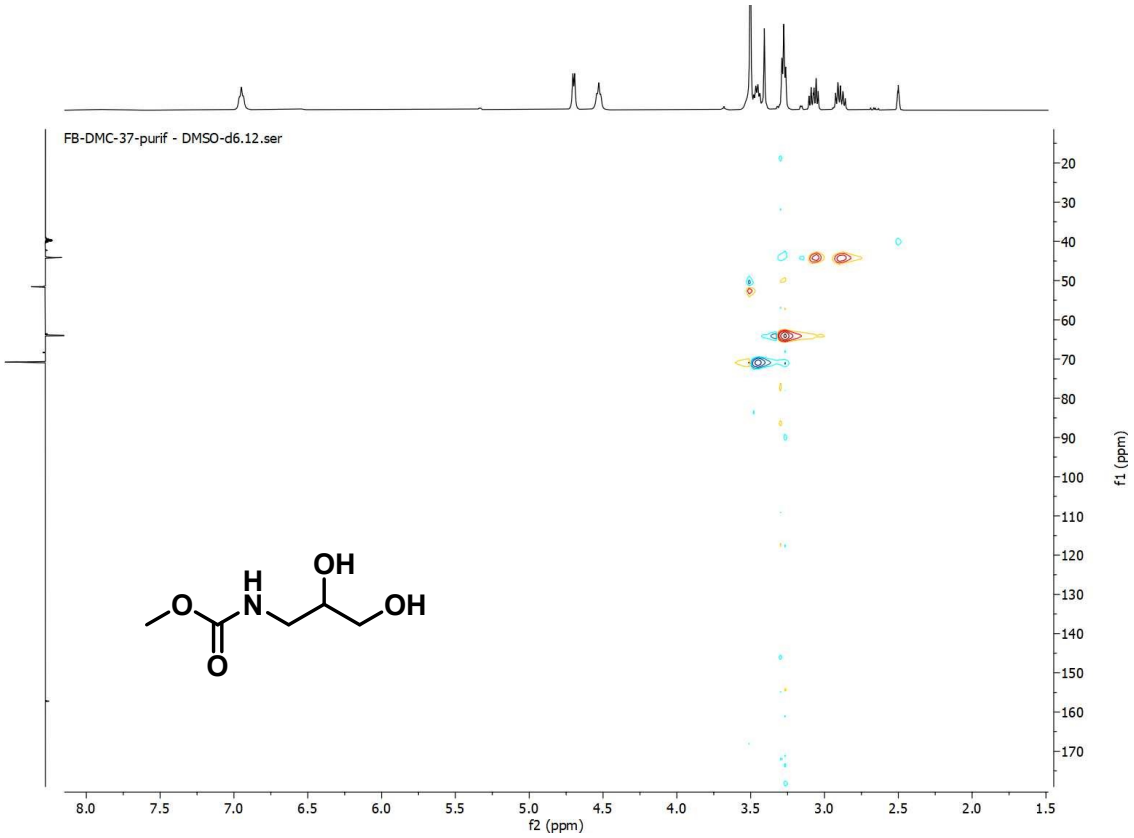

Figure S49. HSQC NMR spectrum (DMSO-D_6) of ***int*-3**.

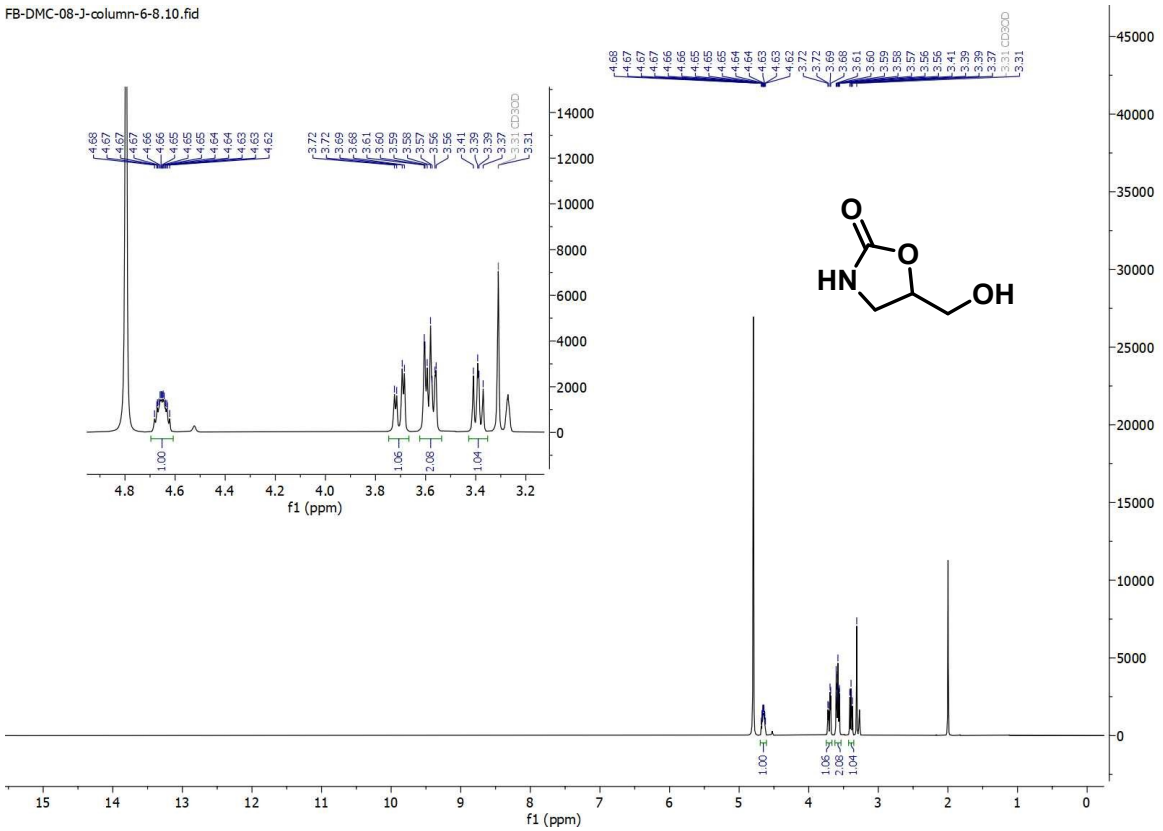

Figure S50. ^{1}H NMR spectrum (400 MHz, CD_3OD) of **3**.

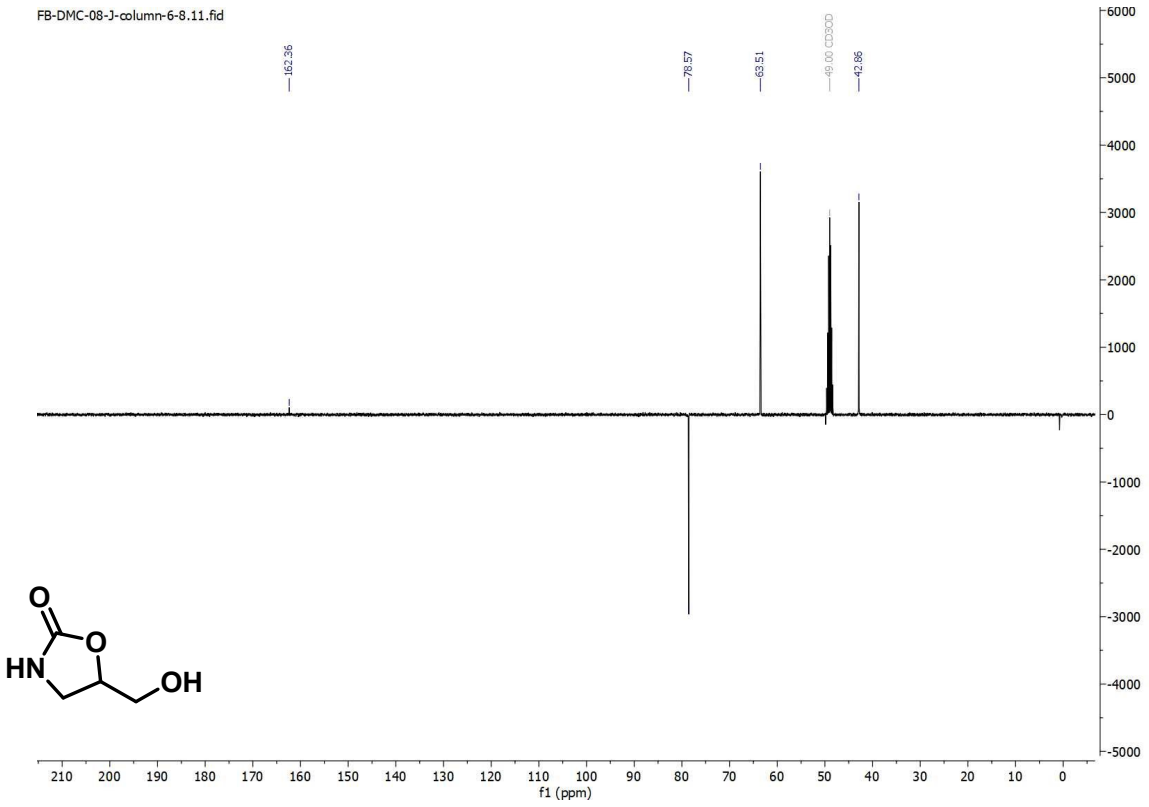

Figure S51 ^{13}C NMR spectrum (101 MHz, CD_3OD) of **3**.

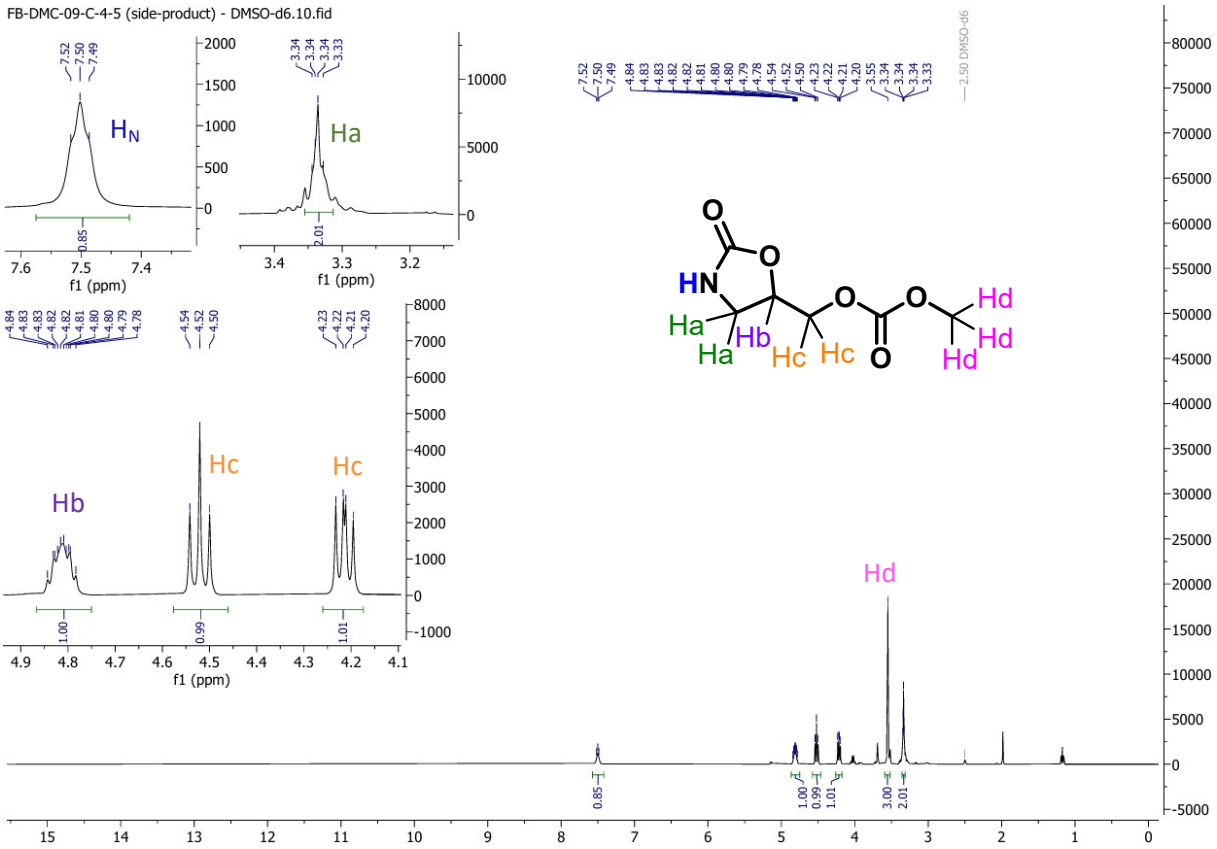

Figure S52. ^{1}H NMR spectrum (400 MHz, DMSO-D_6) of **4**.

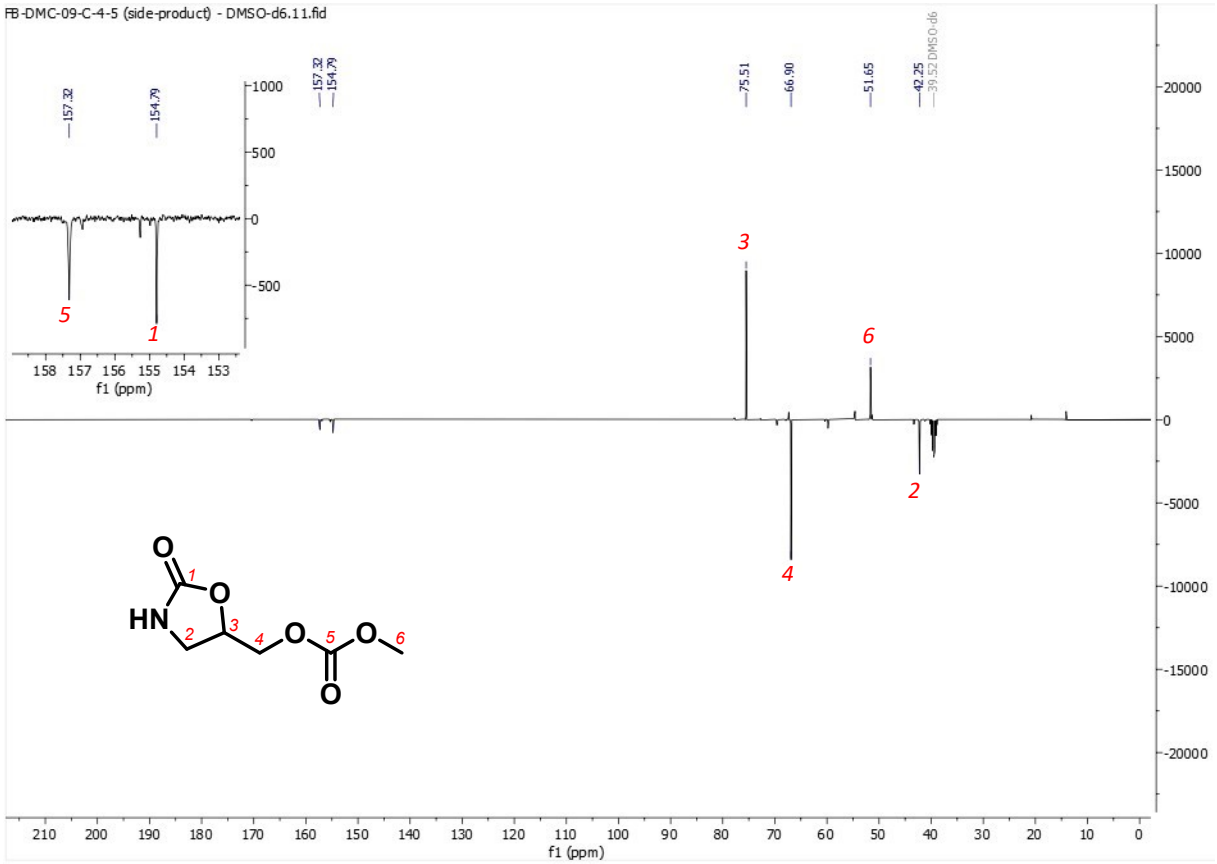

Figure S53. ^{13}C NMR spectrum (101 MHz, DMSO-D_6) of **4**.

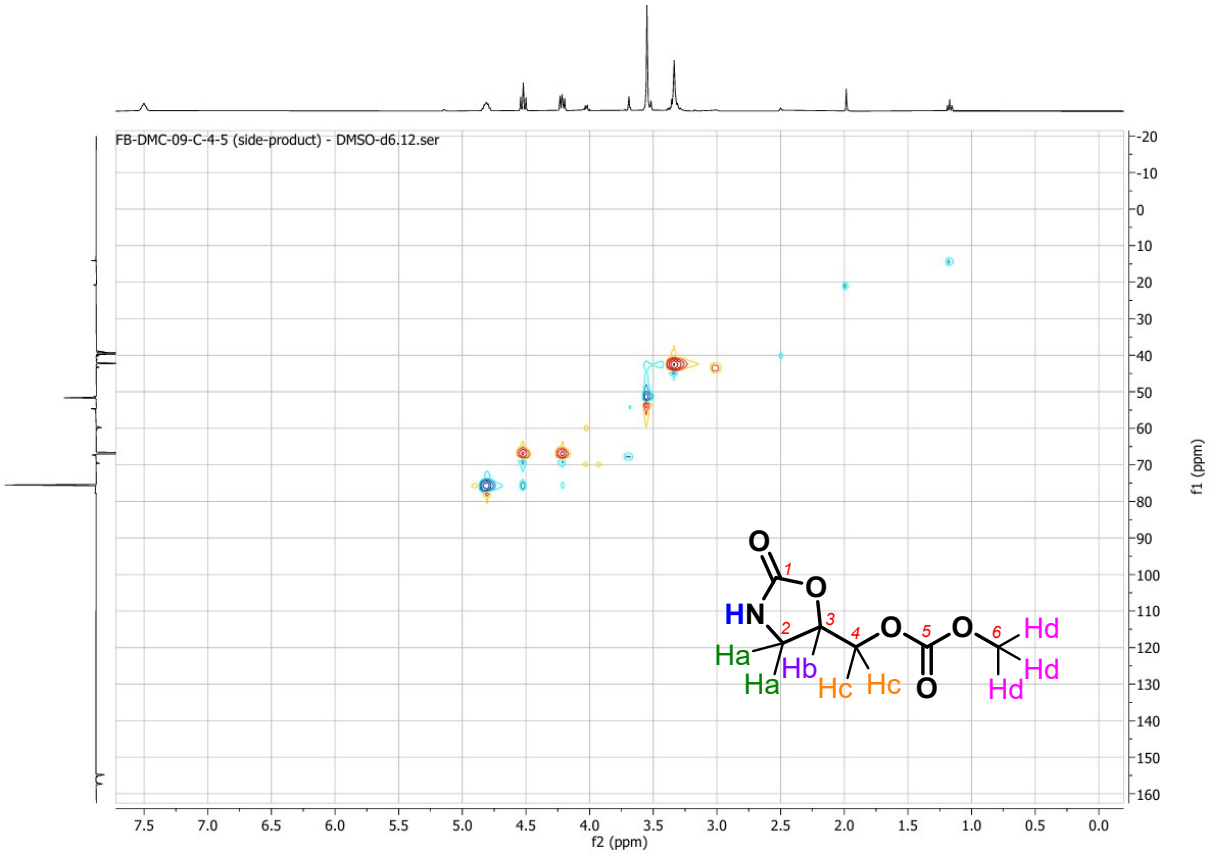

Figure S54. HSQC NMR spectrum (DMSO-D_6) of **4**.

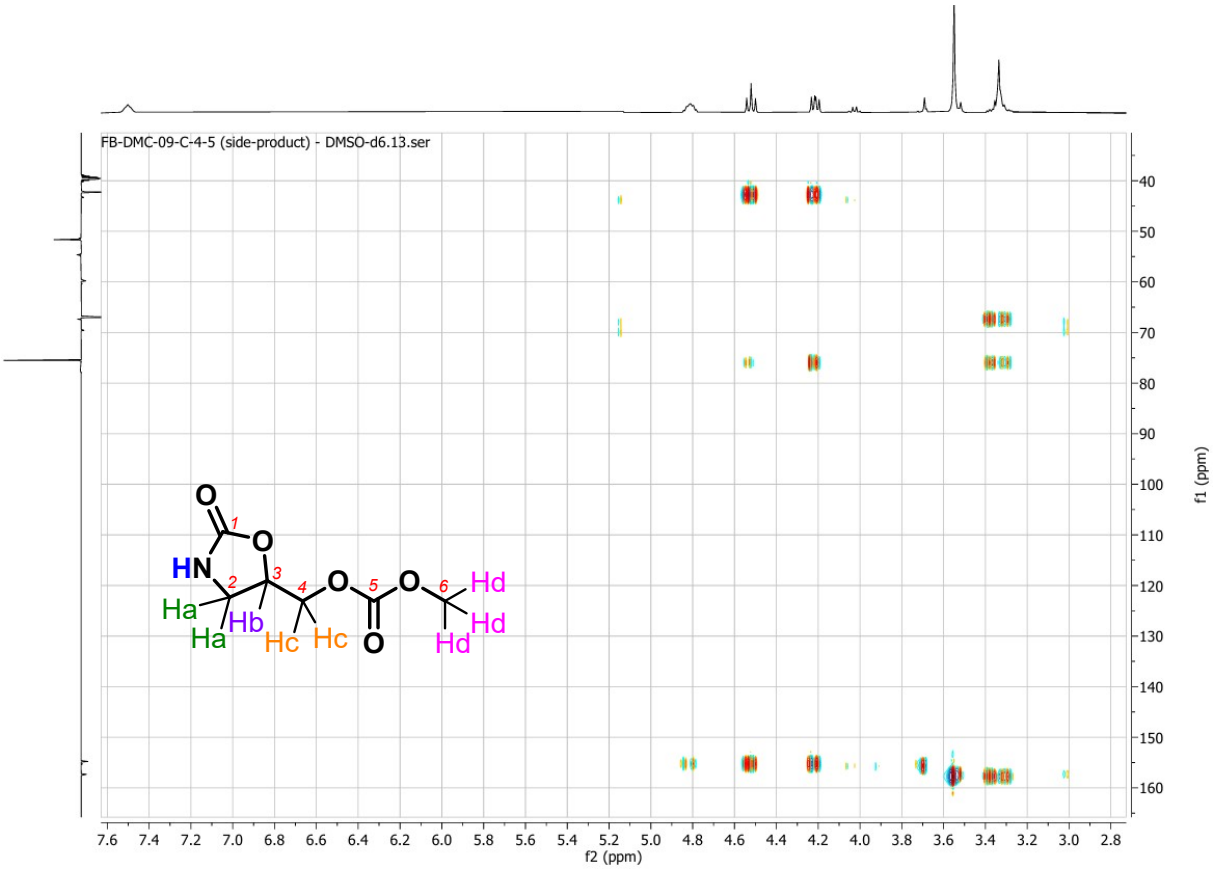

Figure S55. HMBC NMR spectrum (DMSO-D_6) of **4**.

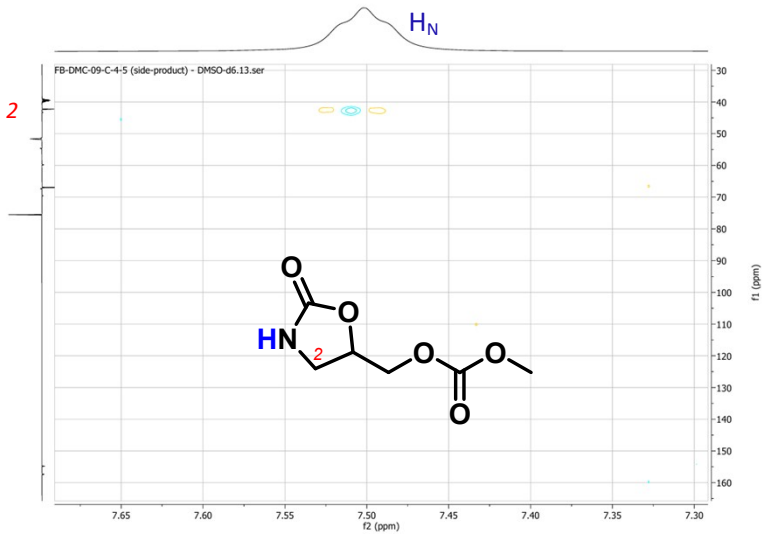

Figure S56. HMBC NMR spectrum (DMSO-D_6) (zoom) of **4**.

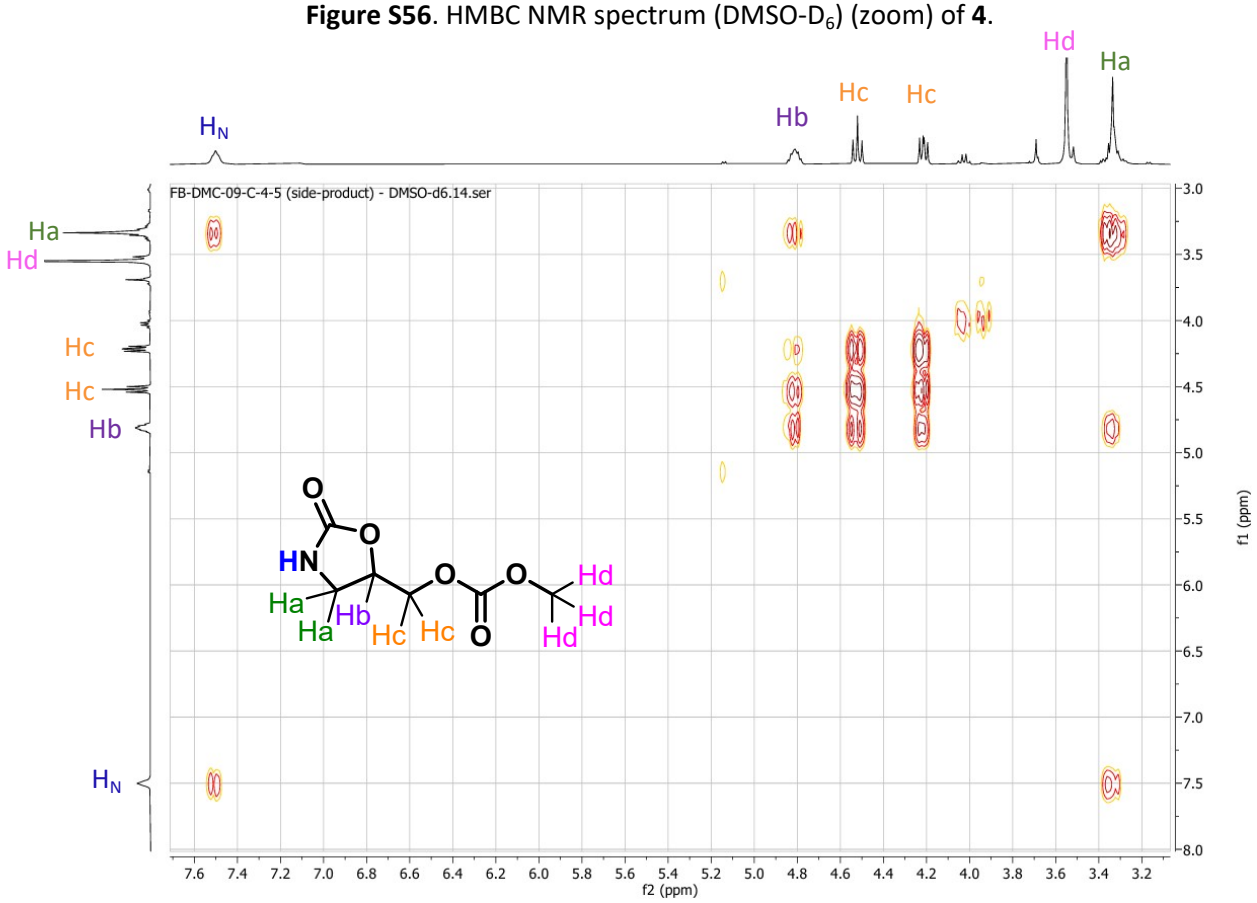

Figure S57. COSY NMR spectrum (DMSO-D_6) of **4**.

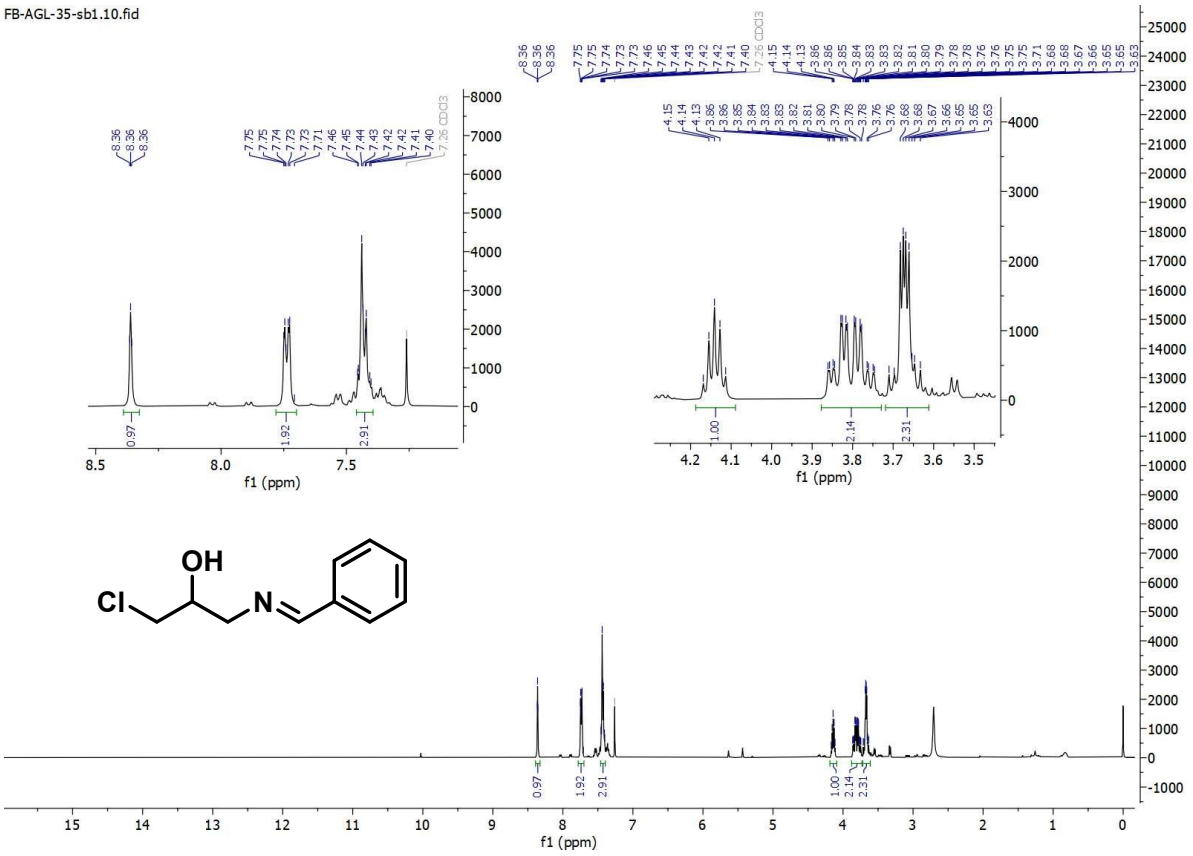

Figure S58. ^{1}H NMR spectrum (400 MHz, $CDCl_3$) of **7**.

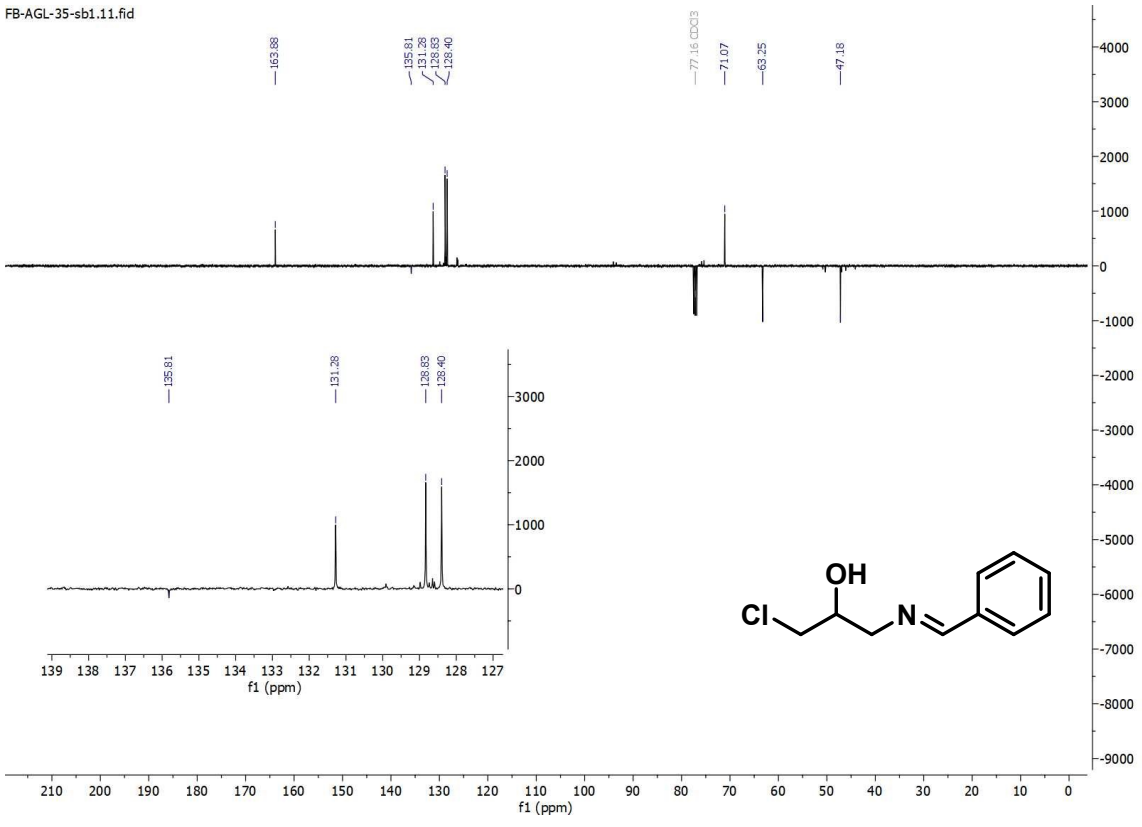

Figure S59. ^{13}C NMR spectrum (101 MHz, $CDCl_3$.) of **7**.

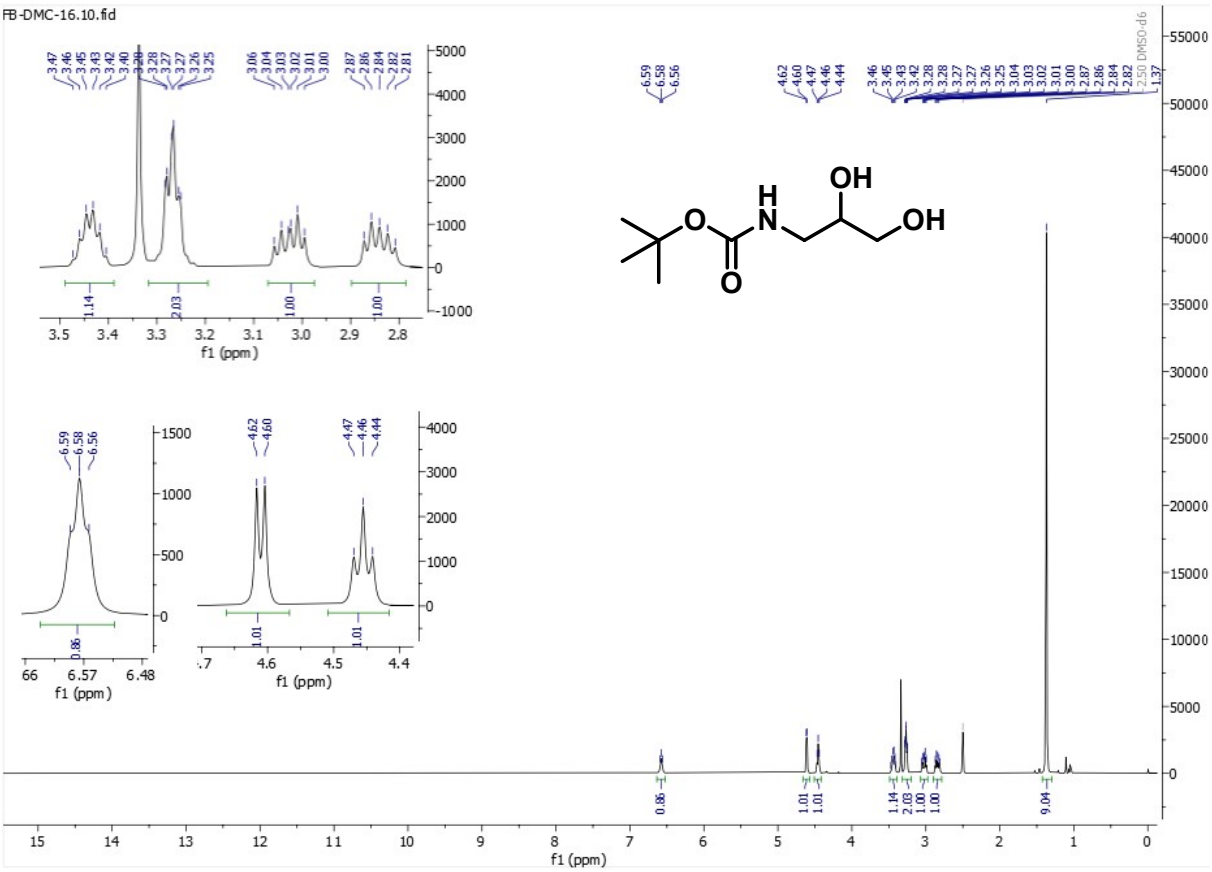

Figure S60. ^{1}H NMR spectrum (400 MHz, DMSO-d_6) of **8**.

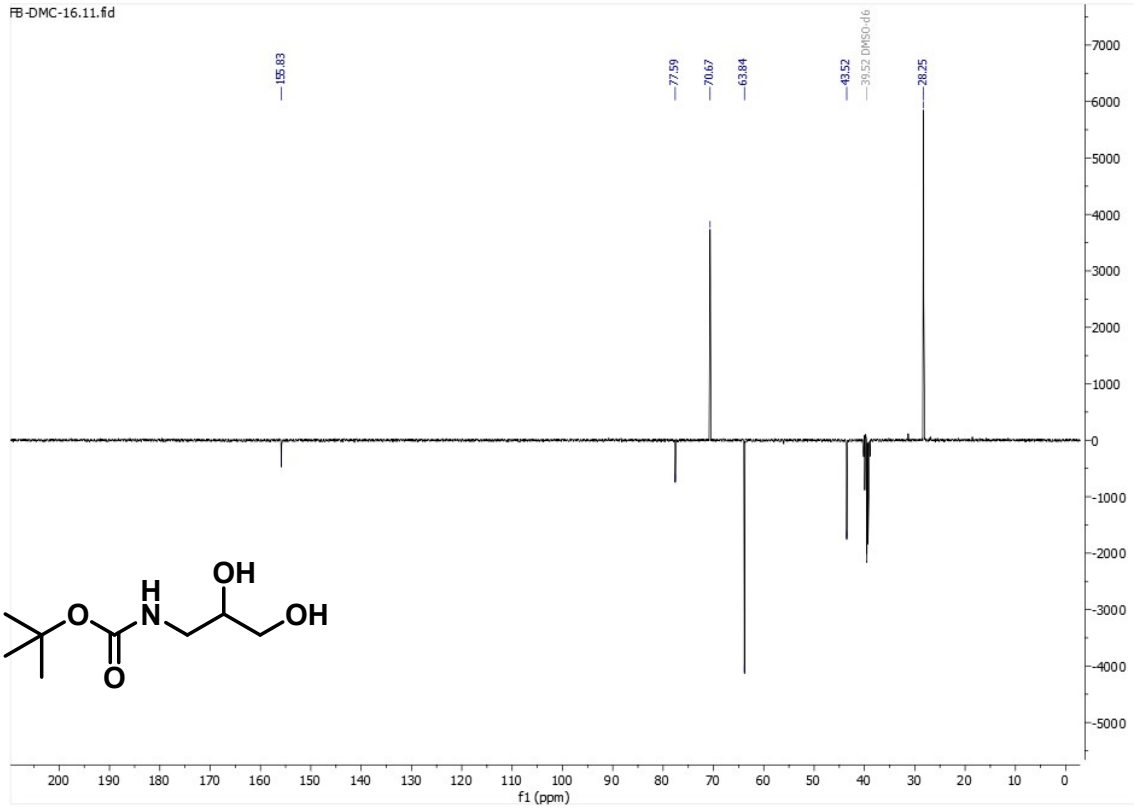

Figure S61. ^{13}C NMR spectrum (101 MHz, DMSO-d_6) of **8**.

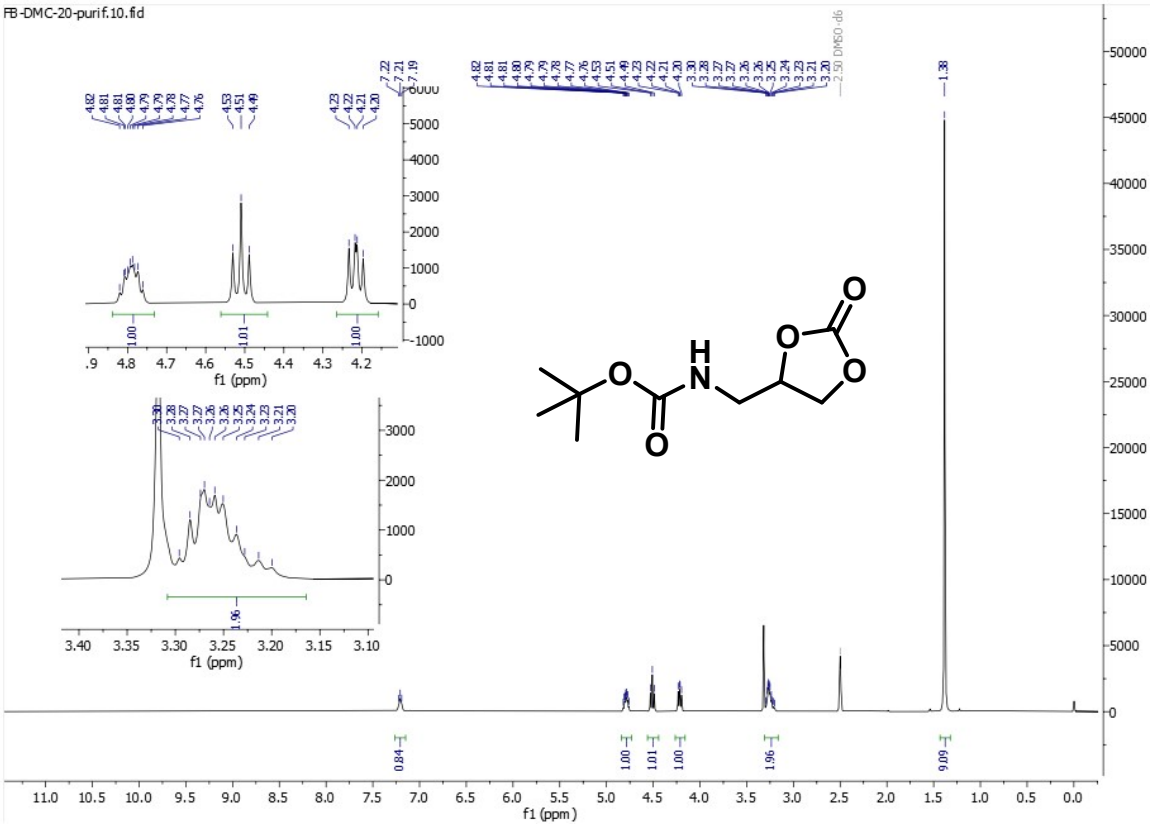

Figure S62. ^{1}H NMR spectrum (400 MHz, DMSO-d_6) of **9**.

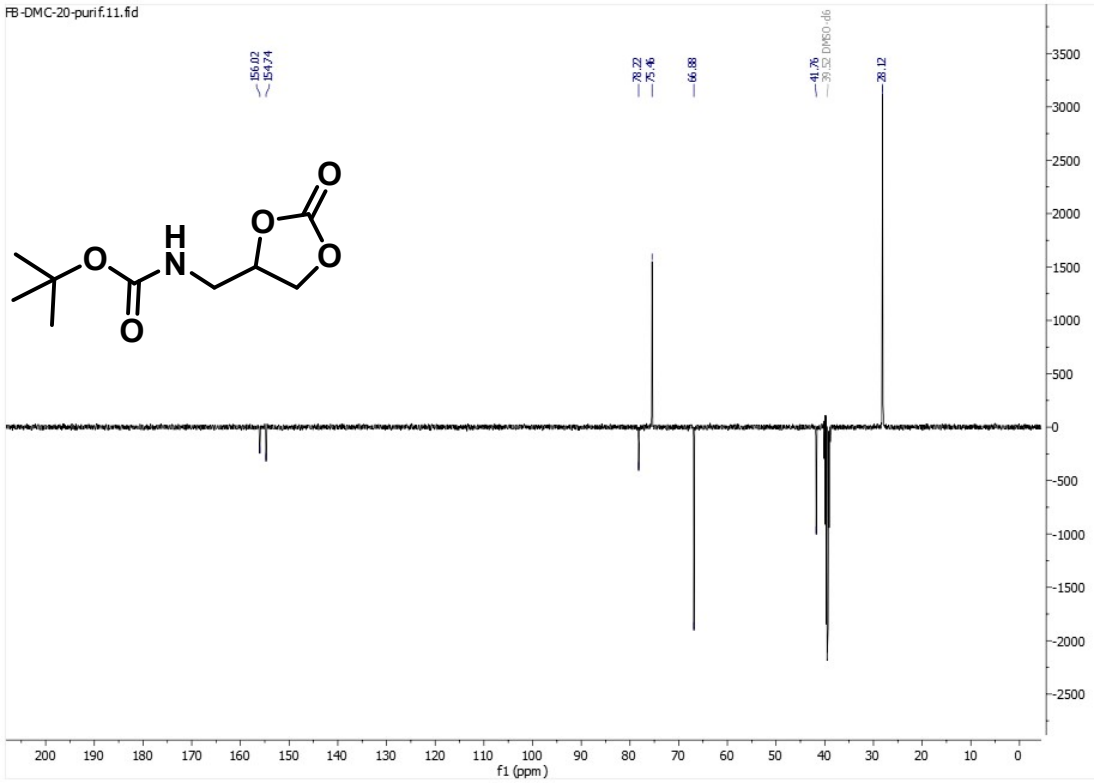

Figure S63. ^{13}C NMR spectrum (101 MHz, DMSO-d_6) of **9**.

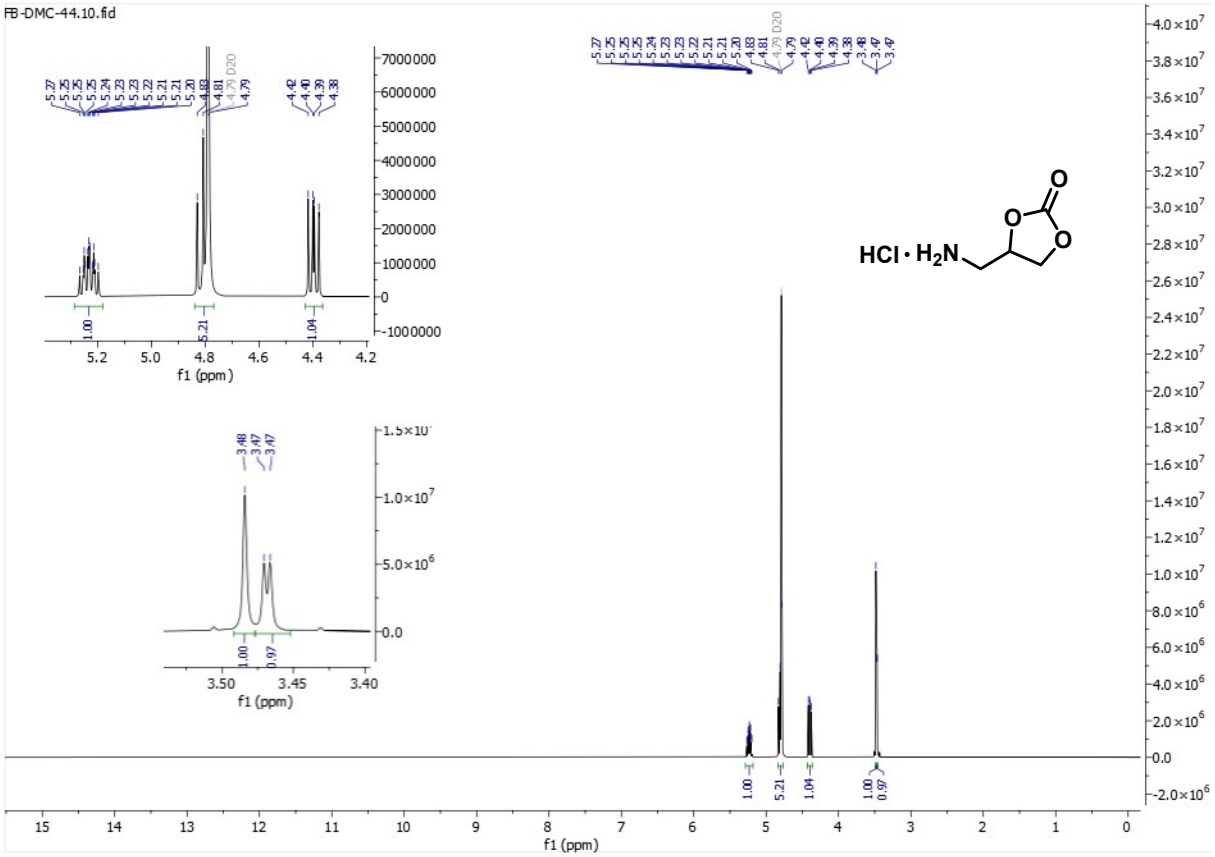

Figure S64. ^{1}H NMR spectrum (400 MHz, D_2O) of ***iso*-3·HCl**.

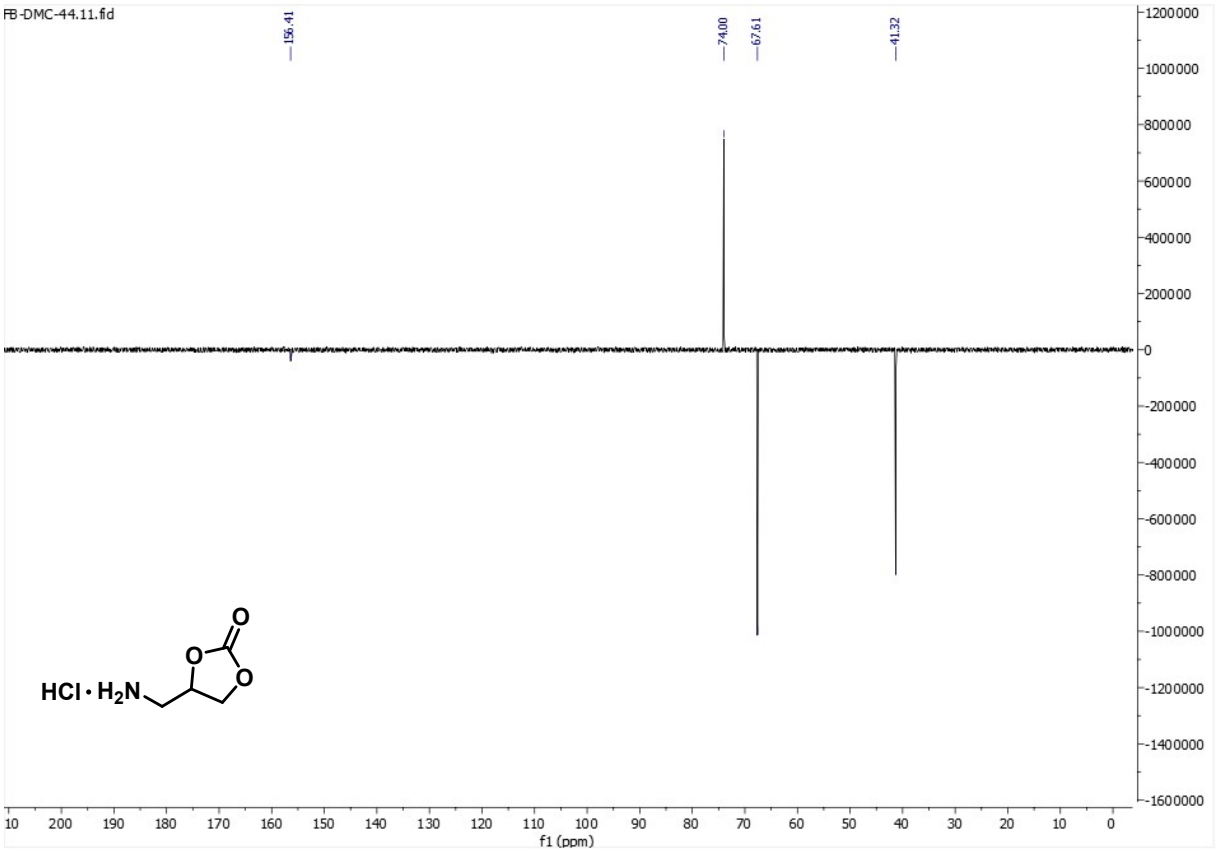

Figure S65. ^{13}C NMR spectrum (101 MHz, D_2O) of ***iso*-3·HCl**.

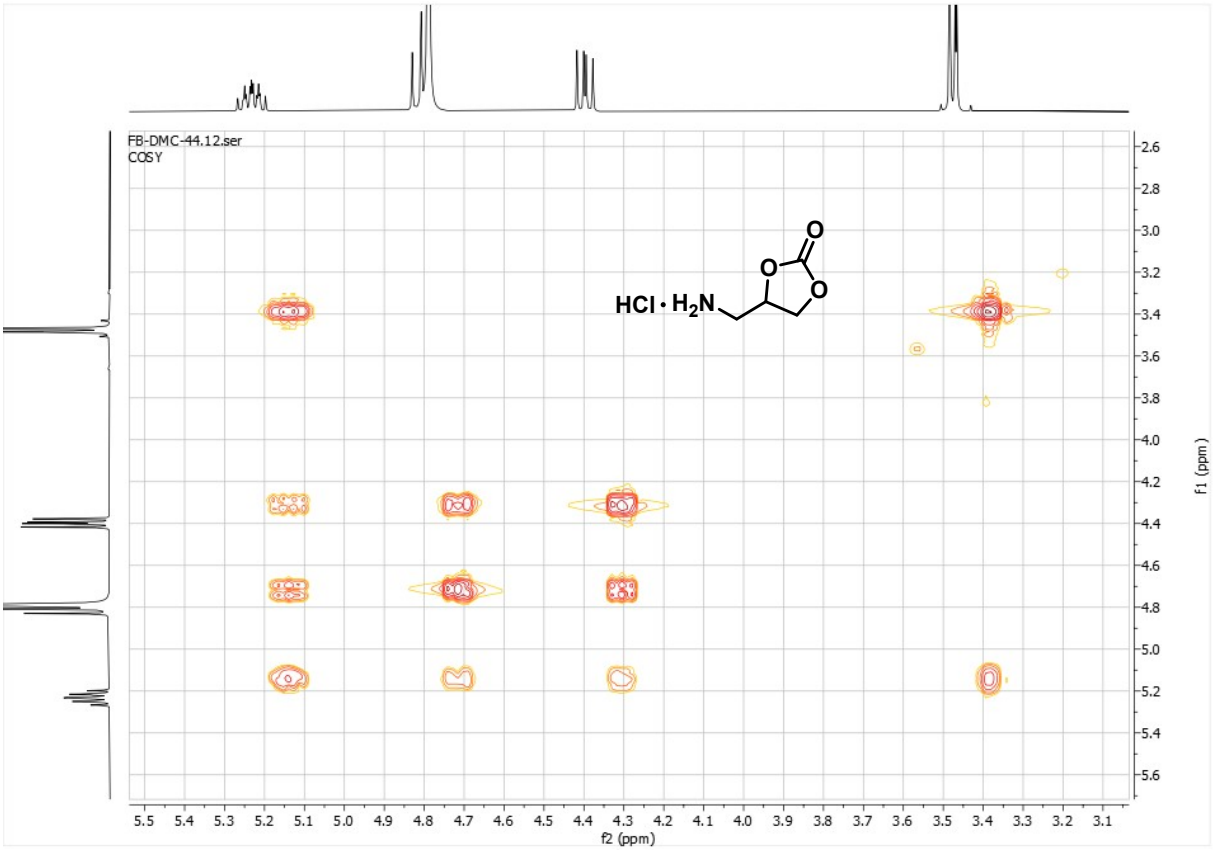

Figure S66. COSY NMR spectrum (400 MHz, D_2O) of ***iso*-3·HCl**.

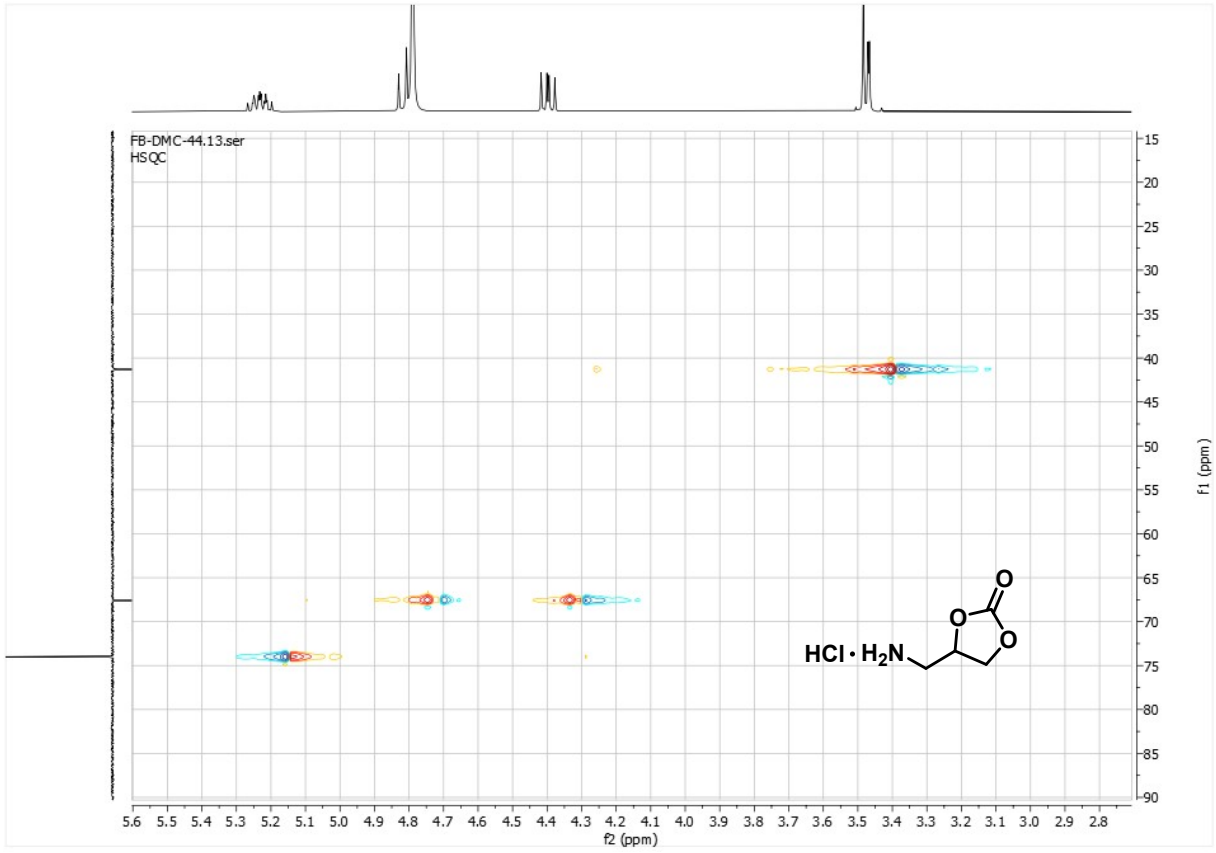

Figure S67. HSQC NMR spectrum (400 MHz, D_2O) of ***iso*-3·HCl**.

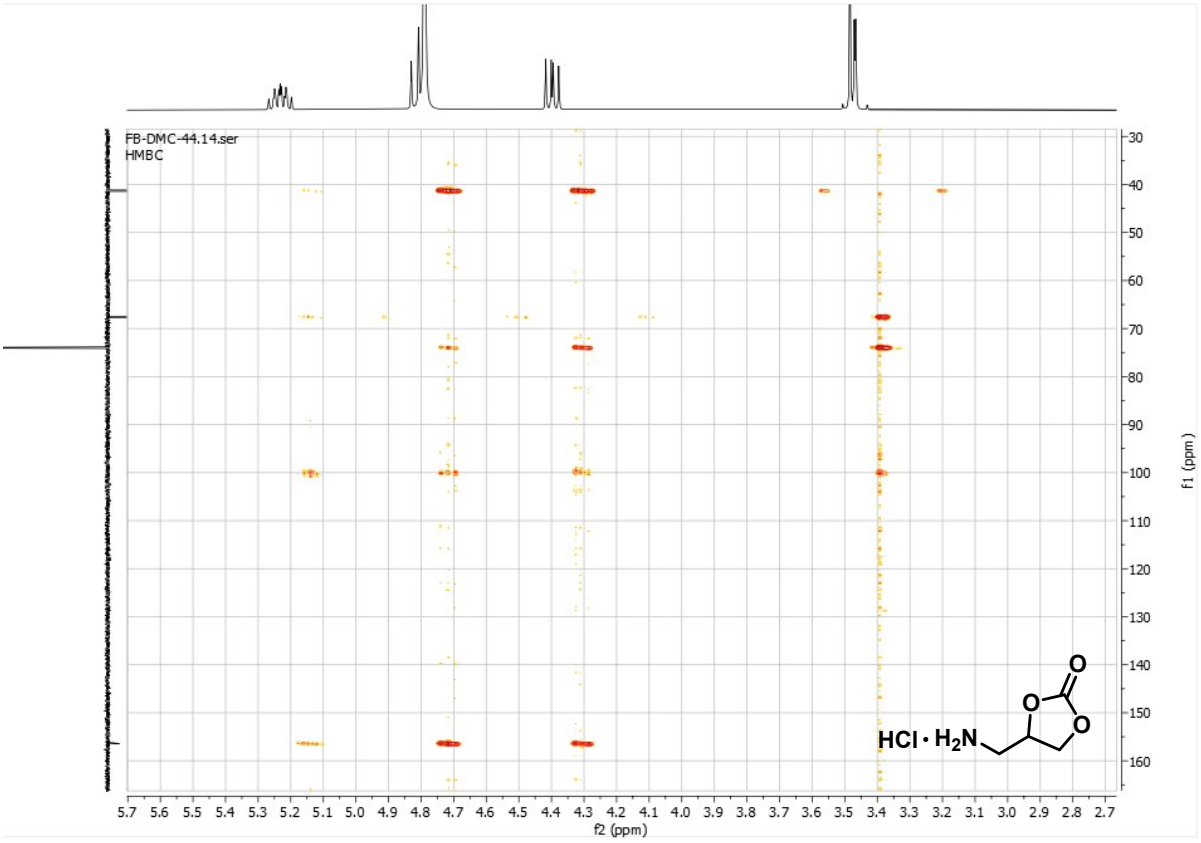

Figure S68. HMBC NMR spectrum (400 MHz, D_2O) of ***iso*-3·HCl**.

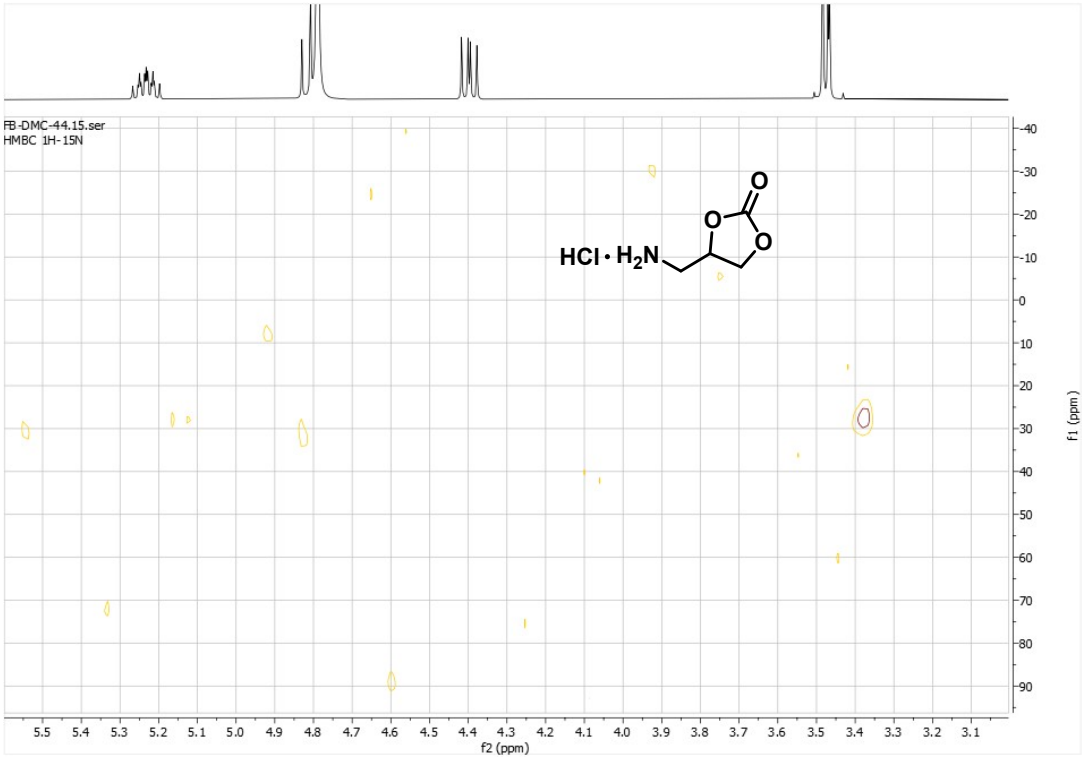

Figure S69. ^{1}H-^{15}N NMR spectrum (400 MHz, D_2O) of ***iso*-3·HCl**.

7. References

S1. H. Hellwig, L. Bovy, K. Van Hecke, C. P. Vlaar, R. J. Romañach, Md. Noor-E-Alam, A. S. Myerson, T. Stelzer and J.-C. M. Monbaliu, *Angew. Chem. Int. Ed*., 2025, **64**, e202501660 (description in the supporting information)

S2. R. A. Sheldon., *ACS Sustainable Chem. Eng.*, 2018, ***6***, 32-48.

S3. W. R. Perrault, et al, *Org. Process Res. Dev.,* 2003, **7**, 533-546.

S4. Y.-S. Liu, C. Zhao, D. E. Bergbreiter and D. Romo, *J. Org. Chem.,* 1998, **63**, 3471-3473.

S5. B. J. Deadman, C. Battilocchio, E. Sliwinski and S. V. Ley, Green Chem., 2013, **15**, 2050–2055.

S6. A. Sivo, I. Montanari, M. C. Ince and G. Vilé, *Green Chem.*, 2023, **26** (13), 7911−7918.

S7. J. J. Lim and D. C. Leitch, *Org. Process Res. Dev.*, 2018, **22**, 641−649.

S8. M. Pallavicini, C. Bolchi, R. Di Pumpo,a L. Fumagalli, B. Moroni, E. Valotia and F. Demartin, *Tetrahedron: Asymm.*, 2004, **15**, 1659–1665.

S9. J. T. Je, and K. S. Kim, An electrolyte for secondary battery, comprising a novel compound or an isomer thereof, WO Pat., WO2024232742, 2024.

S10. R. Jorda, L. Havlícek, M. Perina, V. Vojácková, T. Pospísil, S. Djukic, J. Škerlová, J. Gruz, N. Renesovᡠ, P. Klener, P. Řezácovᡠ, M. Strnad and V. Krystof, *J. Med. Chem.*, 2022, **65**, 8881−8896.

S11. M. R. Maddani and K. R. Prabhu, *Synlett*., 2011, **6**, 821–825.

S12. C. J. Whiteoak, N. Kielland, V. Laserna, E. C. Escudero-Adan, E. Martin and A. W. Kleij, *J. Am. Chem. Soc*., 2013, **135**, 1228−1231.